INVESTIGATING SLOPE STABILITY IN AN OPEN PIT MINE – A CASE STUDY OF THE PHYLLITES WESTERN WALL AT SENTINEL PIT

Ephraim Simataa

Master of Science in Mining Engineering

A research report submitted to the Faculty of Engineering and the Built Environment, University of the Witwatersrand, Johannesburg, in partial fulfilment of the requirements for the degree of Master of Science in Engineering.

Johannesburg, 2019

DECLARATION

I declare that this research report is my own unaided work. It is being submitted to the Degree of Master of Science to the University of the Witwatersrand, Johannesburg. It has not been submitted before for any degree or examination to any other University.

………………………………….

Ephraim Simataa

September 2019

ABSTRACT

Slope stability is critical for final wall in open pit mining operations. Not only is slope failure costly to manage, it might also be accompanied by loss of lives. Factor of safety is very critical during the slope design phase, however, the execution of the design is as important as the design phase itself. Among the many factors affecting stability of highwalls, geology, groundwater and blasting are at the top of the list. This research takes a kinematic stability analysis approach and investigates the possible failure mechanisms in the phyllites rock mass. The data collected from the structural geological mapping along with the window mapping classifies the rock as fair to good rock. The induced failures causing reduced catchment berms and consequently longer bench heights are largely influenced by the prevailing geological conditions, presence of groundwater seeping through the highwall and quality of blasting being conducted.

Amongst the factors influencing slope stability, blasting is the only controllable one. Therefore, adjustments to the blast designs need to be made as mining progresses keeping in mind that rock is not homogeneous. Wall control blasting techniques should be continuously adjusted depending on the Rock Mass Rating or blastability index of the rock mass in that area. Hydrogeological testing of boreholes including Packer testing was conducted in order to estimate the hydraulic conductivity. Adjustments to blast designs were made taking due cognizance of the geological conditions as well as presence of ground water.

Adjustments to the wall control blasting techniques need to be made as mining progresses through the different rock mass zones.

A few blasts on the lower levels (mining benches below 1112RL) were conducted which saw an improvement in the quality of the highwall. Further adjustments to blast designs need to be made as the pit gets deeper and as geological conditions vary.

DEDICATION

This research is dedicated to wife and my children *"Musebezi wo kiwamina bana baka babasikapepwa kale"*

ACKNOWLEDGEMENTS

I return all the glory to God Almighty. Simply put, I am nothing without Him.

Many thanks to Professor Rudrajit Mitra for the mentorship and guidance during the research project. I am grateful to Ms. Anzolette Saville and the entire Faculty of Engineering and Built Environment at the University of the Witwatersrand.

Much gratitude goes to the Kalumbila Minerals Limited management, particularly Mr. Junior Keyser and Mr. Colin duPlessis for allowing me to conduct the research on their Mine site. I would like to address my sincere gratitude to Mr. Gregory More O'Ferrall, Mr. Mutale Chisanga, Mr. Nsipa Simbile and Mr. Benson Nsonde for the support rendered during my research.

To the BME management, Mr. Wayde DeBruin, Mr. Deon Pieterse and Mr. Albie Visser for the confidence, work flexibility and financial support during my studies.

A special thank you to Arnold and Joyce Simataa for always believing in me and convincing me that I can do anything I commit my mind to. Further gratitude goes to my siblings, Paul, Melody, Prudence and Abigail, you guys are my happiness. Further gratitude goes to Jermaine Mulusa for the support rendered. I am grateful to all my family and friends too numerous to mention for having walked with me even when I wasn't the easiest to deal with. Peace and grace to you all.

Special thanks go to Kudakwashe Chichera and my children. All this hard work is for you my dear ones.

Finally, I would like to express my deepest gratitude to all those who provided insight and expertise that greatly assisted this research, too numerous to mention, nonetheless, I am extremely grateful.

TABLE OF CONTENTS

LIST OF FIGURES

LIST OF TABLES

LIST OF ABBREVIATIONS

2D: Two dimensional

3D: Three dimensional

C: Cohesion

FOS: Factor of safety

GSI: Geological strength Index

kPa: kilo Pascal

GPa: Giga Pascal

H-B: Hoek-Brown criterion

FE: Finite Element

LE: Limit equilibrium

M-C: Mohr-Coulomb criterion

MPa: Mega Pascal

NM: Numerical modelling

NA: Not applicable

POF: Probability of failure

UCS_i: Uniaxial Compressive Stress for intact rock

LOM: Life of Mine

RQD: Rock Quality Designation

RMR: Rock Mass Rating

MRMR: Mining Rock Mass Rating

BME: Bulk Mining Explosives

IRMR: In-situ Rock Mass Rating

IRS: Intact Rock Strength

JS: Joint Spacing

JC: Joint Condition

Kg: kilogram

m: metre

mm: millimetre

ms: millisecond

mamsl: metres above mining sea level

mbgl: metres below ground level

Cu: Copper

Mtpa: Million Tons Per Annum

t: tonnes

CHAPTER ONE

1.0 INTRODUCTION

The research project was conducted at the Sentinel copper operation which is 100% owned by Kalumbila Minerals Limited (KML), a First Quantum subsidiary and falls under the Trident Project. The Trident project is located approximately 150 km from Solwezi district along the T5 main road to Mwinilunga in the Northwestern province of Zambia. The Trident Project comprises of Sentinel Mine, Enterprise Mine and Intrepid Pit. Figure 1 shows the location of the project geographically. Sentinel Mine is a low-grade, open pit mine whose ore contains only 0.51% of copper. A grade of 0.5% Cu requires a high throughput of about 55 Mtpa to achieve the production target of 280 – 300,000t Cu per annum set by the company. In 2018, 223,656t of copper was produced with a projection of approximately 230,000t copper production in 2019. Sentinel Mine has a strip ratio of 2.2: 1 and cut-off grade of 0.2% Cu.

Slope design is one of the critical components of a surface mining operation especially for a large scale open-pit mine. It is critical to design final walls that will remain stable for the Life of Mine (LOM) while extracting as much ore as safely and economically as possible. There is direct correlation between slope geometry and wall stability, and economically recoverable ore that can be exposed. There is an increased risk of slope instability where slope angles are steepened to expose the maximum mineable reserve. For any mining operation, it is important to strike that fine balance between the mineable reserve at an angle that makes mining that reserve safe and economic. For any operation, the risk that is acceptable to a company should be determined/defined by the design engineers before commencement of mining. In cases where this risk is not determined due to fear of being too conservative, industry acceptable criteria are used, predominantly due to lack of geotechnical data to better identify or determine the risk being accepted. Therefore, at Sentinel Mine, final walls are designed on a factor of safety of 1.5 whereas temporary walls are designed on a Factor of Safety of 1.2. Nonetheless, execution of design is as important as the slope design phase itself.

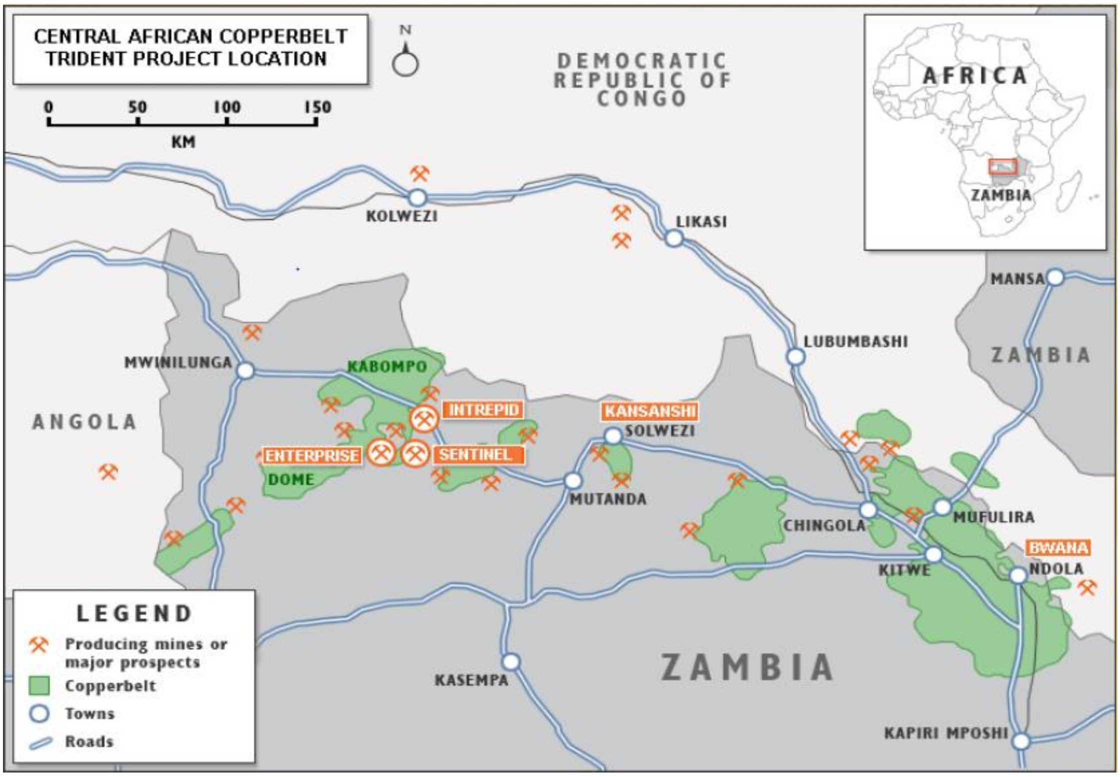

Figure 1: Geographical location of the Trident Project (The Trident Project, 2014)

Sentinel Mine's western highwall is experiencing instability in the form of toppling and wedge failures. This study will focus on the slope stability and factors influencing the stability of the Western highwall. Mining commenced in 2013 with the installation of In-Pit Crushers (IPC); IPC3 is located in the western wall towards the northern side of the pit. Additional infrastructure on the western wall includes an overland conveyor from IPC3 to the processing plant, a prism monitoring cabin and an electrical substation which supplies power to the machinery in the open pit. All of this infrastructure could be adversely affected by wall instability (Figure 2). For this reason, the stability of this wall is very critical to this operation (Gray et al, 2015).

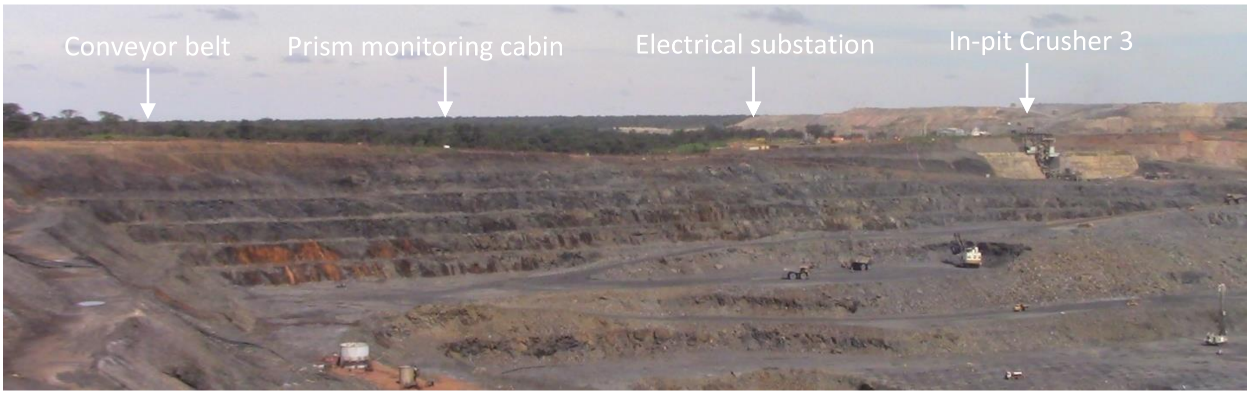

Figure 2: Western final wall and the infrastructure that lies above it

Slope stability evaluation requires the identification of potential modes of slope failure, rock mass strength, sufficient geological knowledge and rock mass deformation parameters which determine the slope behaviour and potential failure surfaces. Modes of failure of rock slopes are generally characterised as plane, rotation/circular, wedge and toppling failures according to Wyllie and Mah (2004). Hoek et al. (2000) further added that slope instability and failure are controlled largely by natural physical processes. Over the years, various research has been carried out on the prediction of mechanisms for slope failure, however, there is still no universally acceptable model for failure particularly in hard and strong rocks (Stacey, 2007). Understanding the natural physical processes that contribute largely to the deformation and failure of rock slopes is key to having stable highwalls. Figure 3 is a close up on a section of the western wall with localized failure occurring and consequently causing reduced catchment berm widths.

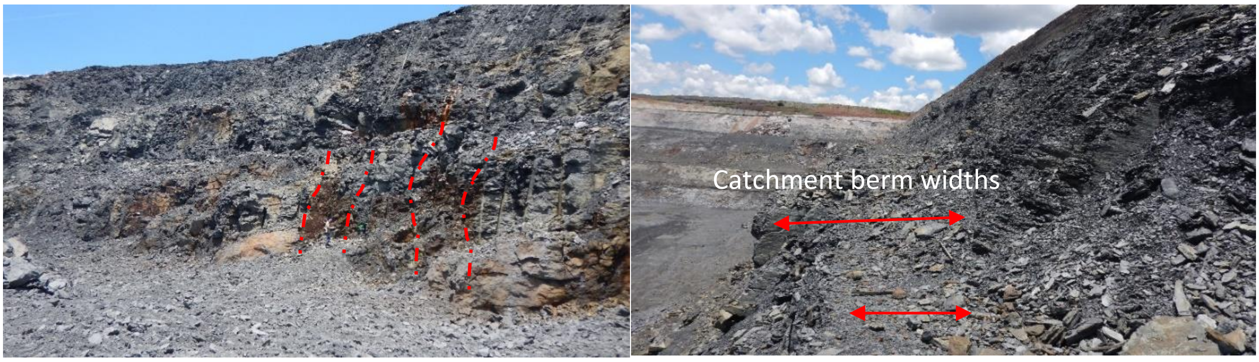

Figure 3: Close-up on a section of the western wall with localized failure and reduced catchment berm width.

1.1 Problem Statement

The western wall of Sentinel Mine is predominantly comprised of phyllite. Localised failures of benches have occurred, which have resulted in reduced catchment berm widths, including resulting in an excessively high bench height in one instance.

1.2 Research Objectives

This project aims at understanding the cause(s) of the highwall instability, sources of reduced catchment berm widths and identifying mitigating measures that will reduce or alleviate the wall instabilities. The objectives are:

- To investigate the causes of instabilities and reduced catchment berm widths; and
- To identify remedial actions to minimize the potential for these failures to occur.

1.3 Research Methodology

The methodology that will be used for this research will include the following research methods which are collection or acquisition of data, kinematic stability assessment and evaluation of the validity of the results.

1.4 Geotechnical and geological data

Geotechnical and geological data will be collected, a few parameters will be interpolated and others will be calculated, as specified below.

Geological and geotechnical data will be collected by:

- Logging – boreholes in this area have already been logged geotechnically and subjected to uniaxial compression modulus tests. Every joint is recorded and its dip, dip direction and joint properties are measured. This information will be consolidated and used for interpolating other parameters listed further in this subsection.
- Mapping – A measuring tape, clinorule, geological compass, geological hammer and logging sheet will be used for this. Every structure (fault, joint or bedding plane) that intersects the tape will have its dip and dip direction as well as all the joint properties (roughness, alteration, spacing and condition) recorded. Scanline surveys and window mapping will be conducted.

Below parameters will be measured and others computed.

- Uniaxial Compressive Strength (UCS)
- Fracture Frequency
- Rock Quality Designation (RQD)
- Barton's Q
- Bieniawski's RMR
- Laubscher's MRMR
- GSI

Parameters to be calculated are

- Slope angle
- Blastability Index

1.5 Ground water

Water that is stored in the earth's crust and percolates through the fissures, pores, joints or cavities can be a nuisance as well as cause instability to slopes. The western wall under investigation has a lot of water seeping through. This is evident from the weathering and iron staining of the joint surfaces. The research will quantify the groundwater flow and pressure through the western wall, the effect of this water on the stability of the slope, if any, and mitigation factors to be considered to improve stability. Hydrological testing will be conducted including packer testing, airlift pumping and recovery testing. The objective of the hydrogeological testing is to estimate the hydraulic conductivity of various intervals intersected at different boreholes.

1.6 Blasting practices (design and execution)

The following will be investigated under blasting practices.

- Adequacy of wall control blasting techniques
- Comparison of trim blast and presplit blast parameters against rules of thumb
- Blasting practices (design versus implementation) and how that is causing damage to the wall
- Sources of toes that end up occupying most of the catchment berm width
- Predicting wall damage using BME's Wallpro software.

1.7 Effects on Mining (Excavation and scaling)

The phrase "effects of mining" will be used to refer to the process of loading of the blasted muckpile. Large equipment is used to move the blasted muck pile. The following will be tested to see whether they affect stability:

- Effects of size of loading unit on stability. Will the size and weight of the loading unit bucket affect stability?
- Does the scaling of the walls weaken the rock mass?
- Does handling of toes as secondary blasting weaken the rock mass?

1.8 Facilities used

The facilities or tools used in this research have been provided by the mine upon availability. A measuring tape, clinorule, Clar/geological compass, geological hammer and logging sheet have been used for all the geotechnical and geological mapping. The tools used were arranged with respective Heads of Departments. A kinematic analysis was performed using DIPS software to investigate failure modes. An empirical stability analysis approach was utilized.

1.9 Research Report Structure

The research report is divided into five (5) chapters with the contents of each chapter briefly highlighted below:

Chapter 1 contains an introduction to the problem of slope stability, the problem statement, research objectives and research methodology.

Chapter 2 presents a review of causes and types of slope failures. Further specific reviews of work done by several authors on slope stability were also carried out.

Chapter 3 contains the data collected from the field using standard industry practices. It also presents the analysis of current practices that might affect slope stability.

Chapter 4 presents the proposed drill and blast design that promotes highwall stability.

Chapter 5 contains the conclusion drawn from the research and recommendations for further research.

CHAPTER TWO

2.0 LITERATURE REVIEW

Instability of rock mass slopes is largely affected by mining activity (Hustrulid *et al.*, 2000). The stability is however aggravated by various factors such as slope design, complex geology, discontinuities in the rock mass, presence of groundwater and mining operations including blasting (Read and Stacey, 2009). According to Sharma (2017), one of the important factors that is relatively less talked about or emphasized is the blasting induced stress, which over time can result in devastating outcomes when least expected. Stacey and Swart (2001) further added that the two controllable factors which have a significant contribution to slope stability are blasting and groundwater. Stability can be ensured or at least improved by improving the quality of blasting and by dewatering the slopes. Eberhardt (2003) argues that most of the rock slope stability problems are related to geological complexity, in situ stresses, anisotropy and inhomogeneity of the material as well as pore pressures and seismic loading.

Above all, Kliche (1999) argues that failure cannot be attributed to a single cause but rather, a combination of several factors indicated above which cause slope failure. Call (1982) agreed that no movement will occur to a rock mass unless there is a change in forces acting on it over time to eventually trigger the slope failure.

2.1 Slope design

During the slope design process, the main objective is to design a slope of acceptable height and inclination that will be economically mineable and remain stable for the duration of the mining project (Nicholas and Sims, 2000). A balance has to be drawn between optimal ore extraction and the stability of highwalls. The steeper the slope angle, the less the material to be mined and lower the slope stability. Mining companies are always caught up in the dilemma of designing slopes that are neither too shallow for economic concerns nor too steep for safety concerns (Wyllie and Mah, 2004).

For an open pit mine, the design of the slopes is a major challenge during every phase of the project and operation. It requires knowledge of the site geological structure and lithology and a thorough understanding of the geotechnical properties of the bench material. It also requires an understanding of the practical aspects of design implementation (Read and Stacey 2009). Nicholas and Sims (2000) explained that the risk surrounding large scale slope failures (from death of personnel to loss of equipment) coupled with the economic consequences of slight alterations of slope angles (as small as one degree) is what makes this process critical.

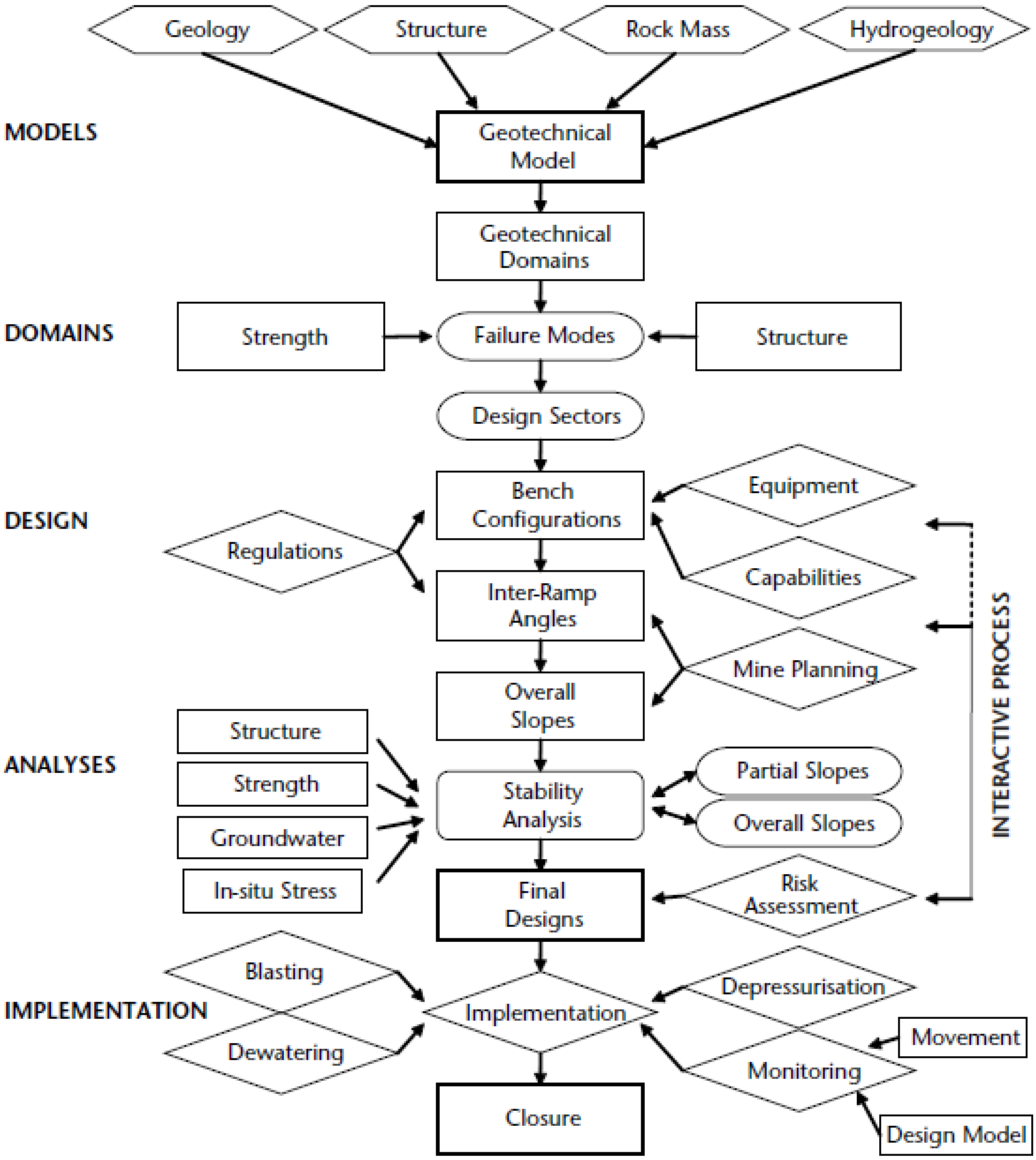

Figure 4: Slope design process (Read and Stacey, 2009)

Read and Stacey (2009) diagrammatically represent the design process (Figure 4) and split it into five (5) connected stages. The first stage involves collection of data for the geotechnical model using traditional or newly developed data collection methods available in the industry. These methods can range from direct or digital mapping and surface outcrop sampling to direct and indirect geophysical surveys, rotary augering and core drilling.

The second stage involves identification of the failure modes likely to be experienced based on the data collected. After this comes the interactive process which involve the design and analysis of the slopes.

According to Wyllie and Mah (2004), some of the basic slope factors to be considered include fixed criteria, such as bench height increment and minimum catchment berm width, which are based on the size of the mining equipment and regulatory requirements, and more subjective considerations, such as the overall design factor of safety and acceptable level of risk. Sjoberg (1996) also considers the overall slope angle as a function of bench and inter-ramp angles and widths which are governed by geomechanical properties of the slope. Figure 5 shows the typical slope geometry.

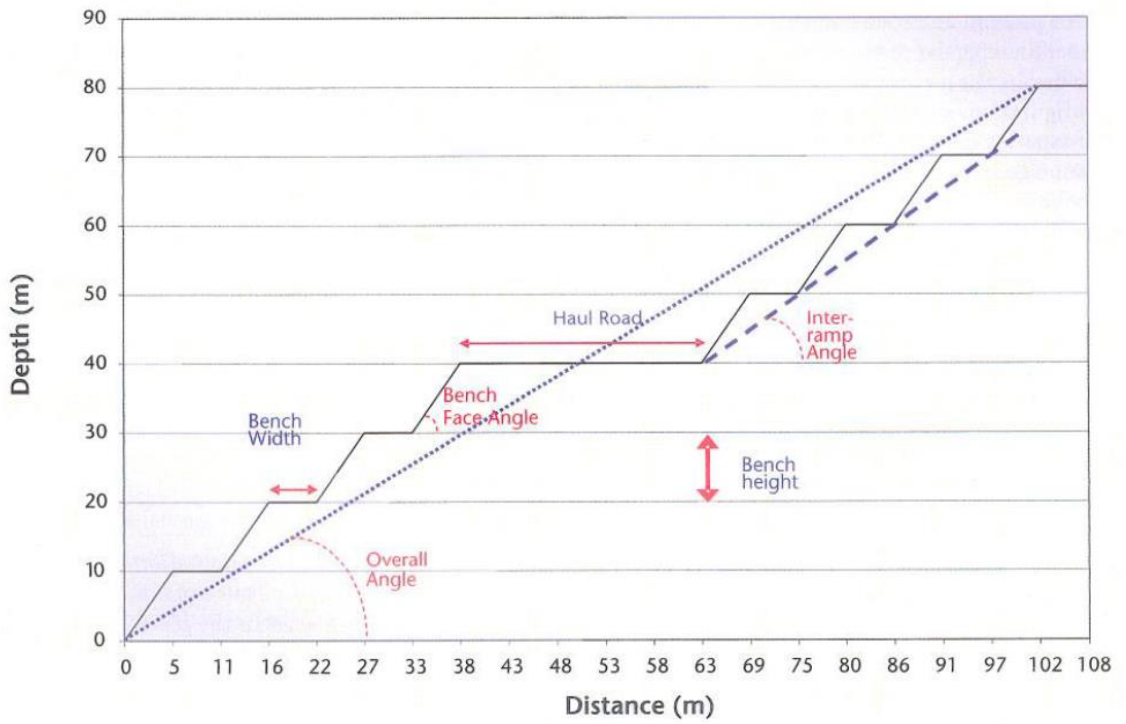

Figure 5: Open pit slope geometry showing some of the relevant design parameters (Williams, et al. 2009).

Abramson (2002) emphasizes on the use of a considerable range of strength parameters and different slope geometry using computer programs to test the stability. According to Read and Stacey (2009), the implementation stage, which also includes monitoring, is the last stage before closure of the mine in the slope design process. Wyllie and Mah (2004) reckon that failure may occur whenever stability conditions of the slope design are not met.

2.2 Geological structures

Wyllie and Mah (2004) refer to structural geology as discontinuities, which are naturally occurring breaks in the rock such as bedding planes, joints and faults along which failure tends to occur preferentially. The properties of discontinuities that affect stability are orientation, persistence, roughness and infilling. Nicholas and Sims (2000) also agree that major-structures (intermediate and regional structures) are the most important geologic structures along which failure is most likely expected. However, when analyzing the overall slope, all of the geological structures should be incorporated to allow one to predict any potential rock mass failure.

2.3 Slope Failure modes and mechanisms

Abramson (2002) reckons that failure originates from some single points and is propagated to the entire rock until the entire rock mass fails. This is as a result of the redistribution of the excess loading of the shear stress, on sections of rock where the strength is exceeded, to neighbouring zones. Eberhardt et al. (2004) simulated slope failure using models and suggested that in the absence of any triggering event, rock mass failure is attributed to brittle strength degradation and progressive failure resulting from time-dependent mechanisms. According to Sjoberg (1996), the failure mode of rock mass is of macroscopic description (visible to the naked eye). The shape and appearance of the resulting failure surface should visibly indicate failure mode. The failure mode encompasses the mechanisms, kinematics and kinetics of the failure. Wyllie and Mah (2004) classify rock slope failure into four primary modes:

1) Plane failure;
2) Wedge failure;
3) Rotational/circular failure; and
4) Toppling failure.

The four modes of failure above assume that the slope failure occurs on the identified surface which makes identification of the critical failure surface and the acting forces the basis of the limit equilibrium analysis of slope stability. Sjoberg (2000) and Stacey (2007) however suggest that there might be other possible failure modes which do not correspond with the established mechanisms particularly when high stress is a factor.

2.3.1 Plane Failure

Plane failure (Figure 6) involves the movement of a failing mass downward and outward along a gently undulating release surface or sliding of a failing mass on a single surface (Hoek and Bray, 1981; Kliche, 1999). Kliche (1999) further added that plane failure is likely to occur with pre-existing joints striking parallel to the slope, but dipping less than the slope angle and movement dictated by surface weakness. Failure is expected to occur along the path of least resistance due to the integration of sliding and separation along discontinuities and failure through small blocks of intact rock (Piteau and Martin, 1981).

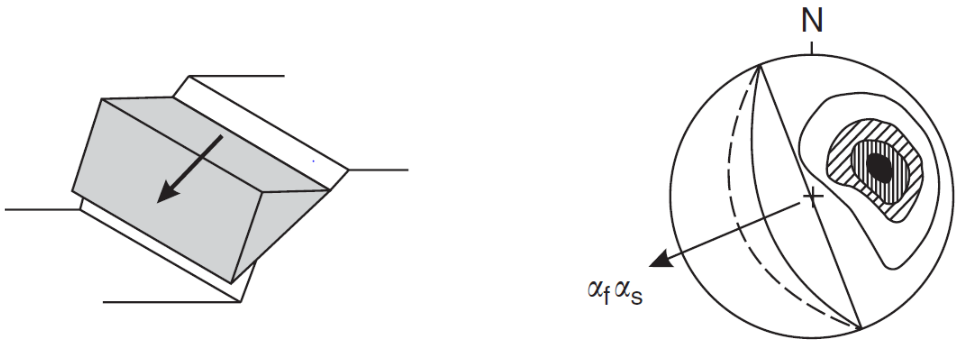

Figure 6: Plane failure in rock containing persistent joints dipping out of the slope face, and striking parallel to the face (Wyllie and Mah, 2004)

For plane failure to occur, the following conditions have to be satisfied (Hoek and Bray, 1981):

i. The strike of the plane of weakness must be within +/-20˚ of the strike of the crest of the slope;
ii. The toe of the failure plane must daylight between the toe and the crest of the slope; and
iii. The dip of the failure plane must be less than the dip of the slope face, and greater than the angle of internal friction of the failure plane.

Wyllie and Mah (2004) also added that apart from what Hoek and Bray established, the following should comprise part of the conditions for plane failure:

iv. The upper end of the sliding surface either intersects the upper slope, or terminates in a tension crack;
v. Release surfaces that provide negligible resistance to sliding must be present in the rock mass to define the lateral boundaries of the slide.

2.3.2 Wedge Failure

Wedge failure occurs when two intersecting discontinuities (represented by planes A and B in Figure 7) form a tetrahedral failure block which could slide out if the inclination of this line is considerably greater than the internal angle of friction along the discontinuities (Hoek and Bray, 1981: Kliche, 1999). According to Hudson and Harrison (1997), wedge failure can only occur under the following conditions:

i. The dip of the slope must exceed the dip of the line of intersection of the two discontinuity planes associated with the potentially unstable wedge;
ii. The line of intersection of the two discontinuity planes associated with the potentially unstable wedge must daylight on the slope plane; and
iii. The dip of the line of intersection of the two discontinuity planes associated with the potentially unstable wedge must be such that the strengths of the two planes are reached.

Hoek and Bray (1981) and Goodman and Kieffer (2000) both agree that wedge failure has the likelihood of being the most commonly experienced failure mechanism in rock slopes. It is experienced over a much wider range of geological and geometrical conditions than plane failures. Other authors who have previously extensively discussed wedge failure are Nathanail (1996), Low (1997) and Wittke (1990).

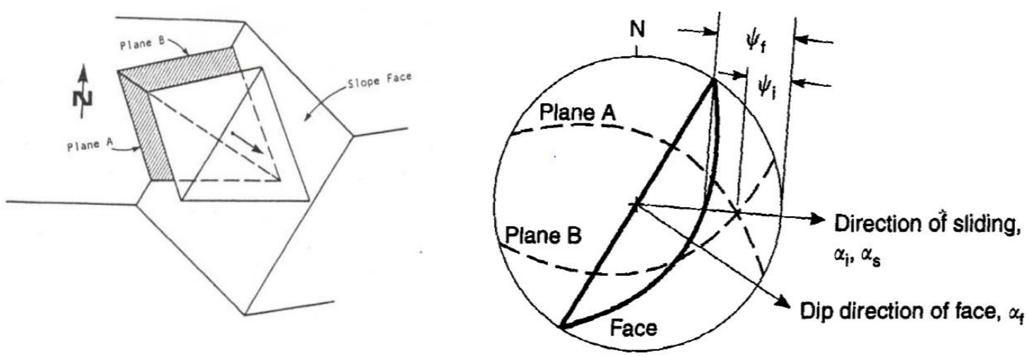

Figure 7: (a) Wedge failure mode (Piteau and Martin, 1981) (b) Kinematic analysis of wedge failure

Rock slopes which are intersected by at least two sets of discontinuities form unstable wedges which can fail by sliding (Hoek and Bray, 1981). Goodman (1989) and Low (1997) defined four different types of failure modes for a wedge:

i. Sliding along the line of intersection of both planes forming the block;
ii. Sliding along plane A only;
iii. Sliding along plane B only;
iv. A floating type of failure.

Stereonets are extensively used to assess the kinematic feasibility of wedge failure. As previously established, the criteria of failure is sliding. Sliding is likely to occur if the intersection point of planes A and B falls within the shaded region as shown in Figure 8. The actual factor of safety however cannot be determined from the stereonet but rather from the geometry of the wedge and the shear strength of each plane and water pressure (Wyllie and Mah, 2004). The factor of safety can be determined using the limit equilibrium method (Hoek and Bray, 1981).

Friction-only stability charts can also be used as a rapid stability check. Hoek and Bray (1981) detail how to calculate factor of safety using charts. Wyllie and Mah (2004) argued that based on friction only, a slope with factor of safety of less than 2.0 should be regarded as potentially unstable. Further examination of such slopes is required and must take into account wedge shape, dimensions, weight, water pressures, shear strengths, external forces, and bolting forces. Further analysis of wedge stability can be done using numerical modeling software such as SWEDGE (Rocscience, 2001) and ROCKPACK III (Watts, 2001).

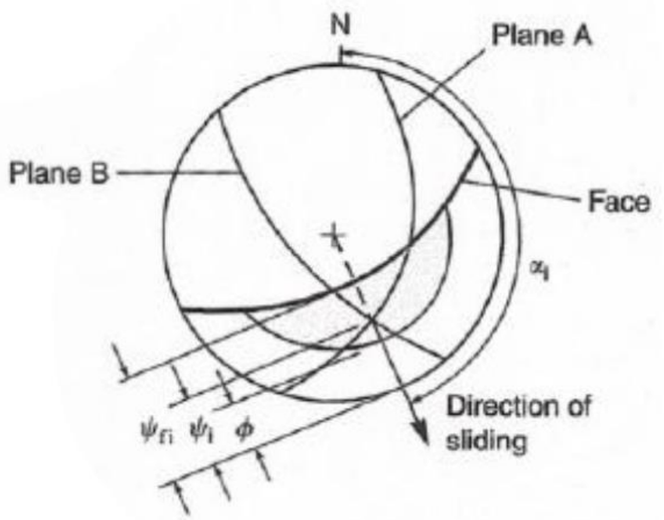

Figure 8: Wedge geometry for sliding mechanisms (Hoek and Bray, 1981)

2.3.3 Rotational/Circular Failure

This type of failure has been referred to as rotational shear failure by Coates (1977, 1981) and circular failure by Hoek and Bray (1981) and these are illustrated in Figures 9a and 9b respectively. This failure mode is experienced mostly in continuum slopes consisting of highly jointed or weak rock masses (Coates, 1981).

(a) (b)

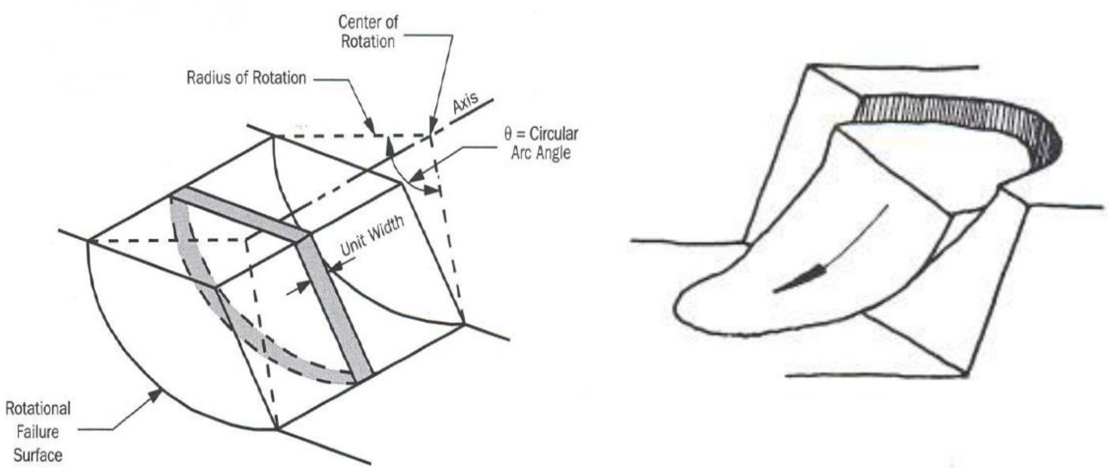

Figure 9: (a) Rotational failure mode according to Coates (1977, 1981) (b) Circular failure mode, according to Hoek and Bray (1981)

Circular shear failures are predominantly experienced in weak materials such as highly weathered or closely fractured rock (Hoek and Bray 1981). However, they can also occur in hard-rock slopes (Dahner-Lindqvist, 1992). Kliche (1999) also added that circular failure occurs mostly in homogenous materials such as fills, highly jointed rock slopes and constructed embankments and is aggravated by water intrusion. Hudson and Harrison (1997) explained the development of circular/curvelinear slips under different conditions as can be seen in Figure 10.

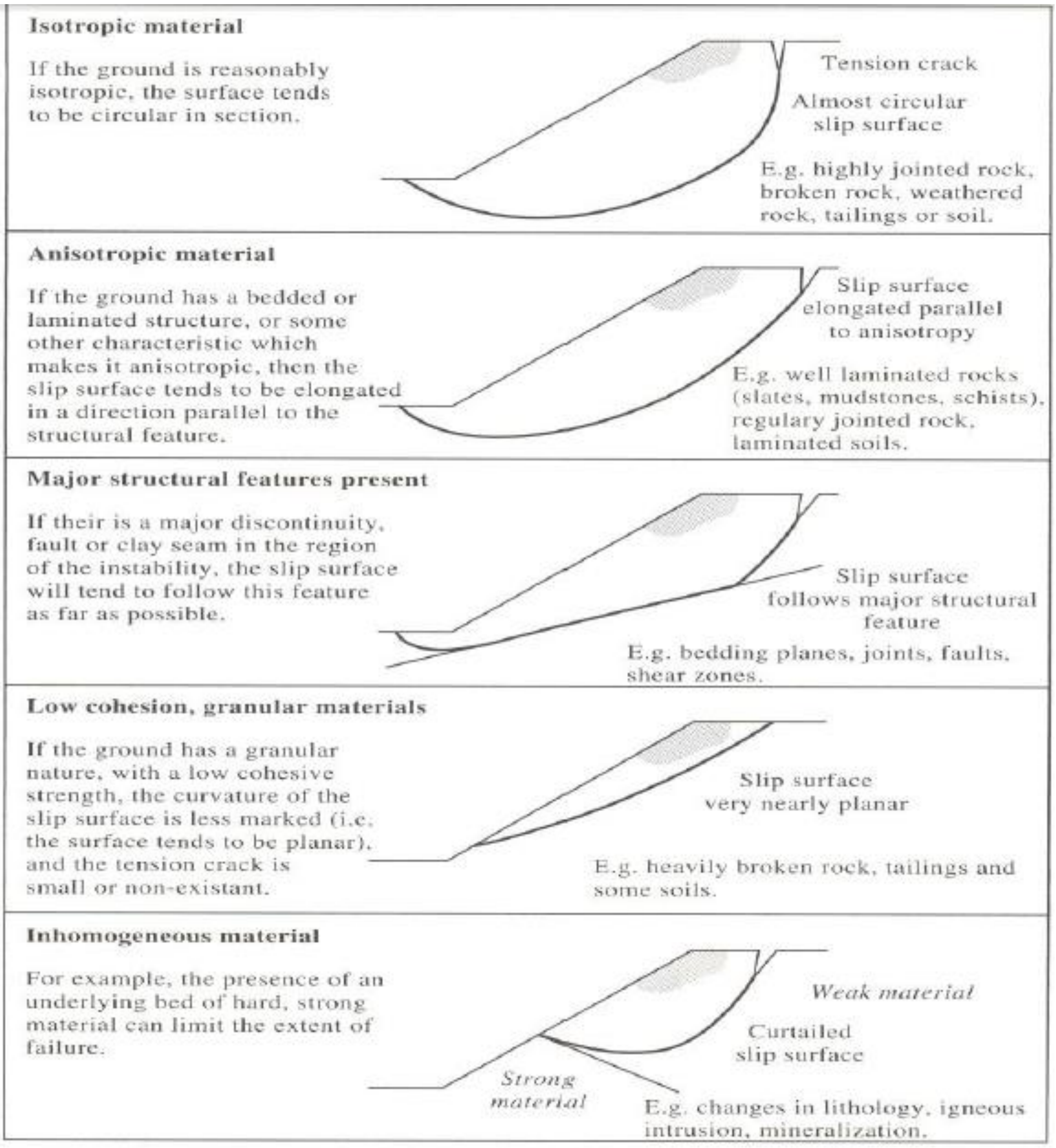

Figure 10: Development of curvelinear slips (Hudson and Harrison, 1997)

The failure surface is curved and usually terminates at a tension crack at the upper ground surface. The strength characteristic of the material, which is dependent on the rock mass structure, defines the shape and location of the slip surface. Sjoberg (1999) commented that numerical simulation particularly in large scale rock slopes might be difficult, however, Sjoberg (2000) managed to conduct a model study of circular failure which showed that failure occurs in stages. Figure 11 below illustrates how failure initiates and progresses in six stages. The failure stages are explained below:

i. This involves elastic displacement caused by removal of rock material by mining.
ii. Yielding which commences at the toe and spreads upwards as more material is removed or as a result of mining to a new and critical slope height.
iii. Shear strain accumulation at the toe of the slope which progresses upwards.

iv. Failure surface fully developed and slope will start showing some displacements, which can be tracked if a good slope monitoring system is in place.
v. The slope fails with time with larger displacements starting from the toe
vi. Failure has occurred, the failing mass can slide away from the slope.

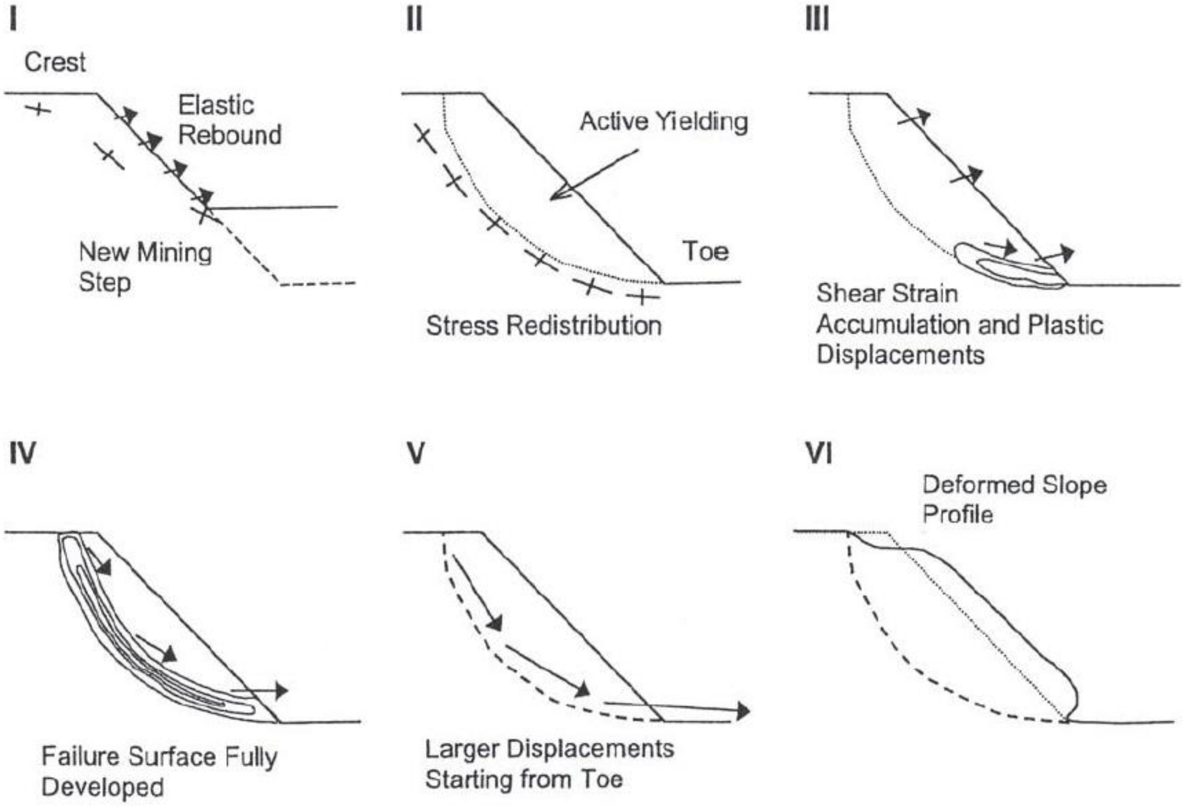

Figure 11: Failure stages for circular shear failure in a slope (Sjoberg, 2000)

2.3.4 Toppling failure

Kliche (1999) describes this type of failure as a mass movement process where the weight vector of a block resting on an inclined plane falls outside the base of the block as shown in Figure 12a. When the vertical weight component, W, is outside the pivot point, potential for toppling increases as can be seen in Figure 12b. Pritchard and Savingy (1990) further added that this movement process is characterized by the down-slope overturning, through rotation and flexure of blocks with steep discontinuities. Slopes whose foliation dips steeply into the slope trending parallel or sub-parallel to the slope crest are generally considered prone to toppling failure. Toppling occurrences are expected at all scales as well as all rock types (de Frietas and Watters, 1973). Sjoberg (2000) said that the following conditions have to be satisfied in order for toppling to occur:

i. The joints must dip relatively steeply into the slope and they must be able to slip relative to each other;
ii. The rock mass must be able to deform substantially for toppling to have room to develop; and
iii. The rock mass tensile strength must be low to allow tensile bending failure at the base of toppling columns.

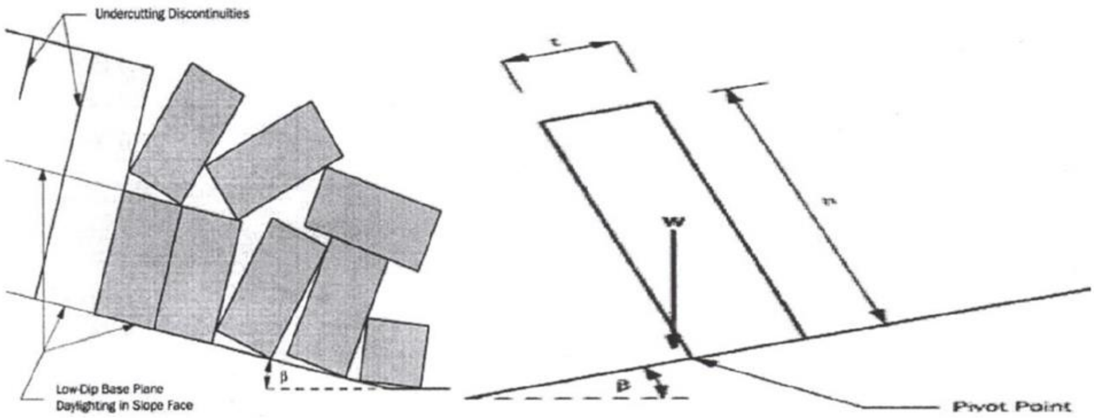

Figure 12: (a) Toppling failure mode. (b) Potential toppling failure when the vertical weight component, W, is outside the pivot point (Kliche, 1999).

Sjoberg (2000) claimed that, like circular failure, toppling failure develops in various stages as well. The failure stages of toppling failure are summarized in Figure 13. A further description of these stages is as below:

i. Elastic rebound on a newly formed bench with joints steeply dipping into the slope.
ii. As a result of stress distribution, failure commences in the form of slip along the steeply dipping joints. Joint slip starts at the toe and progresses toward the crest, with accompanying stress redistribution around this region.
iii. Exaggerated displacements caused by fully developed joint slip whose depth is influenced by slope angle, the friction angle of joints, and the stress state.
iv. Rock columns are compressed, which creates the necessary space for a slight rotation of the columns, starting at the toe. For a high slope, even the elastic deformation of the rock mass can be enough to allow a small rotation. This results in the compression of rock columns, which creates the space for a slight rotation of the columns starting at the toe.
v. This is followed by tensile bending failure at the base of the rotating column, which subsequently progress toward the crest. In a high slope, the elastic deformations of the rock mass can cause a small rotation.
vi. Finally, a base failure surface has developed along which the failed material can slide.

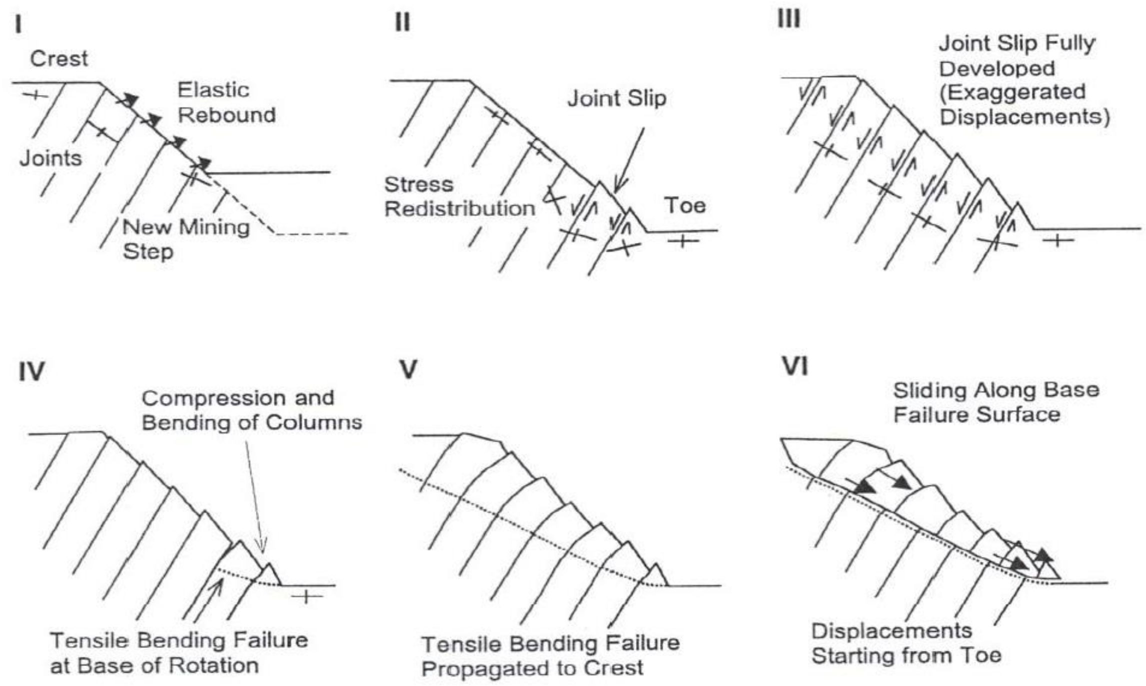

Figure 13: Failure stages for large-scale toppling failure in a slope (Sjoberg, 2000)

de Frietas and Watters (1973) wrote one of the first papers detailing field examples of toppling failure. This paper was key to the acceptance of toppling failure as a distinctive mass-movement and mode of failure. Goodman and Bray (1976) discuss the two distinct methods of stability analysis for toppling failure, as shown in Figure 14, as block toppling and flexural toppling and described the limit equilibrium method for analyzing toppling failure.

According to Wyllie and Mah (2004), block toppling occurs in strong rock containing both a set of discontinuities dipping steeply into the face, and well-developed pre-existing cross joints. It is somewhat a brittle process, leading potentially to large, extremely rapid slope failures.

Flexural toppling on the other hand occurs on a bench scale, since it requires continuous pre-existing discontinuities. Flexural toppling is a ductile, self-stabilizing process which occurs in weak rock masses dominated by a single closely spaced discontinuity set. It is relatively free of cross joints (Nichol et al., 2002). Adhikary and Dyskin (2007) stated that during flexural toppling, the tilting of rock layers into the excavation induces tensile stresses. The stresses induced may initiate tensile structures in rock layers situated in portions of maximum bending moments. The moment at which the tensile (bending) stress in the toe of a column exceeds the tensile strength, failure is initiated (Adhikary et al., 1997).

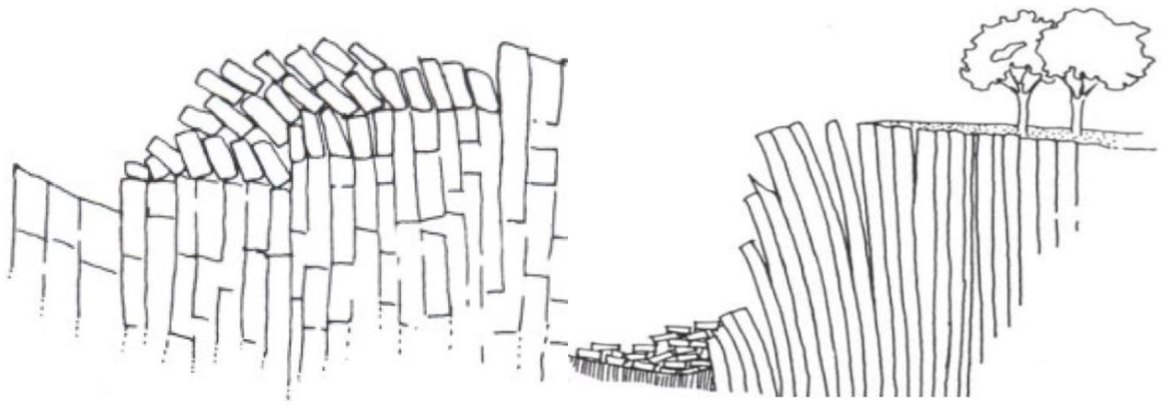

Figure 14: (a) Block toppling example (b) Flexural toppling example (After Goodman and Bray, 1976)

Hoek and Bray (1981) and Glawe (1991) describe secondary toppling as crushing of the slope toe. Secondary toppling failure mechanisms, as classified by Goodman and Bray (1976) are divided into five categories:

i. Slide head toppling;
ii. Slide base toppling or toppling at the toes with shear movement of upper slope;
iii. Tension crack toppling and Toppling and slumping.
iv. Toppling of columns in strong upper material due to weathering of underlying weak material; and
v. Toppling at pit crest resulting in circular failure of upper slope;

These instability phenomena are induced by a toe weakening caused by natural events, such as erosion or human activity such as mining or civil excavation works.

2.4 Rock Mass Classification

Rock mass classification is often used in the primary stage of a project when limited detailed information is available, as a preliminary approach to assess the engineering behavior of rock masses (Hoek, 2007). Rock mass classification methods were introduced about 40 years ago to predict the rock mass quality and excavation support design. The obtained results are an estimate of the stability quantified in subjective terms. Read and Stacey (2009) stated that there are many different classification schemes, however, the ones being mostly utilized in today's open pit slope engineering are:

i. Bieniawski's Rock Mass Rating (RMR) scheme (Bieniawski 1973, 1976, 1979, 1989), originally introduced for tunneling and civil engineering applications;

ii. Laubscher's Rock Mass Rating (IRMR and MRMR) schemes (Laubscher 1977, 1990; Jakubec and Laubscher, 2000; Laubscher and Jakubec, 2001); and
iii. Hoek and Brown's Geological Strength Index (GSI) (Hoek et al., 1995, 2002).

2.4.1 Rock Mass Rating (RMR)

Bieniawski in 1973 developed the Rock Mass Rating or Geomechanics classification system. Significant changes were made to the ratings assigned to different parameters as research continued (Bieniawski, 1989). The value of RMR governs the geotechnical quality of the rock mass (Read and Stacey, 2009). The five parameters below are used to classify rock mass using RMR.

i. Rock Quality Designation (RQD) - Rock Quality Designation (RQD) is an index of the quality of a rock core taken from a borehole. Deere et al. (1967) defined RQD as the percentage of the sum of core lengths greater than 100mm to the total sum of the core run. RQD measures the total length of solid or unbroken pieces of fresh or weathered core longer than 100 mm against the total length of the indicated core run, expressed as a percentage. Deere and Deere (1988) stated that RQD measures the percentage of "good" rock within a borehole.
ii. Rock material strength (UCS) - The rock material strength is the uniaxial compressive strength of intact rock which is the maximum axial compressive stress that a cylindrical rock sample can withstand before failing usually obtained from laboratory testing.
iii. Spacing of discontinuities – also known as joint spacing, it describes the frequency of jointing.
iv. Condition of discontinuities – also known as joint condition, it describes the surface conditions and infilling of the joints or discontinuities.
v. Groundwater condition - gives an estimate of the groundwater conditions that are likely to be encountered during the mining/excavation phase.

RQD, UCS, spacing and condition of discontinuities are either obtained from core logging or surface mapping of structures. A sixth parameter, joint orientation, in relation to the direction of the excavation is applied as shown in Table 1. The table after Read and Stacey (2009) reflects changes to the RMR ratings made by Bieniawski between 1976 and 1979.

Table 1: Bieniawski RMR parameter ratings, 1976 and 1979 (Read and Stacey, 2009).

Parameter	**Rating (1976)**	**Rating (1979)**
UCS	0 – 15	0 – 15
RQD (drill core)	3 – 20	0 – 20
Joint spacing	5 – 30	5 – 20
Joint condition	0 – 25	0 – 30
Groundwater	0 – 10	0 – 15
Basic RMR	**8 – 100**	**8 – 100**
Joint orientation adjustment	0 – -60	0 – -60

The ratings of the five parameters when summed up as well as the sixth adjustment parameter, joint orientation, gives the rock mass rating value.

Rock mass rating values range from 0 to 100 for poor quality rock and good quality rock respectively. The adjustment considers the different joint orientations and applies to that joint set that is more significant than the rest. In instances where no one joint set has particular significance over the rest, the RMR value takes into account the average of the rating values for each set (Read and Stacey, 2009).

Table 2: RMR calibrated against rock mass quality (Read and Stacey, 2009)

RMR rating	**Description**
81 – 100	Very good rock
61 – 80	Good rock
41 – 60	Fair rock
40 – 21	Poor rock
<21	Very poor rock

Read and Stacey (2009) highlight the limitations of using the Bieniawski system in open pit slope design as below:

i. Groundwater parameter: the rock mass should be assumed to be completely dry and the groundwater rating set to 10 (1976) or 15 (1979) according to Table 1 above. Any pore pressures in the rock mass should be accounted for in the stability analysis.

ii. Joint orientation adjustment: joint orientations should be assumed to be very favorable and the adjustment factor set to zero. The effect of joints and other structural defects should be accounted for in the assessment of the rock mass strength (e.g. if using the Hoek-Brown strength criterion) and/or the stability analysis.

iii. RQD parameter: Deere et al. (1967) and Deere and Deere (1988) suggest that the use of RQD as a parameter in Bieniawski's RMR system poses a problem as it is highly subjective (different operators frequently report different values for the same interval of core) and inconsistent, often providing inaccurate and misleading results.

Ultimately, its use should always be coupled with good engineering judgment that takes proper account of the geological characteristics of the rock mass being classified.

2.4.2 Laubscher's IRMR and MRMR

Laubscher's In-situ Rock Mass Rating system (IRMR) and Mining Rock Mass Rating system (MRMR) came about after several modifications of Bieniawski's RMR system for mining applications. The RMR was originally based on civil engineering case histories. Laubscher made several modifications over the years (Laubscher, 1977, 1984; Laubscher and Taylor, 1976; and Laubscher and Page, 1990) in order to make the classification more relevant to mining applications until an independent rock mass classification system, the Mining Rock Mass Rating (MRMR) system was developed. Like Bieniawski's RMR, the MRMR takes into account the same parameters and adjustments as applied to the RMR value.

According to Read and Stacey (2009), the IRMR considers four basic parameters:

i. the intact rock strength (IRS), defined as the unconfined compressive strength (UCS) of the rock sample that can be directly tested;
ii. the rock strength (RBS), defined as the strength of the rock blocks contained within the rock mass;
iii. the blockiness of the rock mass, which is controlled by the number of joints sets and their spacings (JS); and
iv. the joint condition, defined in terms of a geotechnical description of the joints contained within the rock mass (JC).

Figure 15 illustrates the steps to determine IRMR and MRMR. The IRMR value is calculated by adding the Joint Spacing and Joint Condition values to the Rock strength (RBS) value. To calculate MRMR, the IRMR value is adjusted to consider weathering of the rock mass, joint orientation relative to excavation, stress effects, effects of blasting and water (Read and Stacey, 2009).

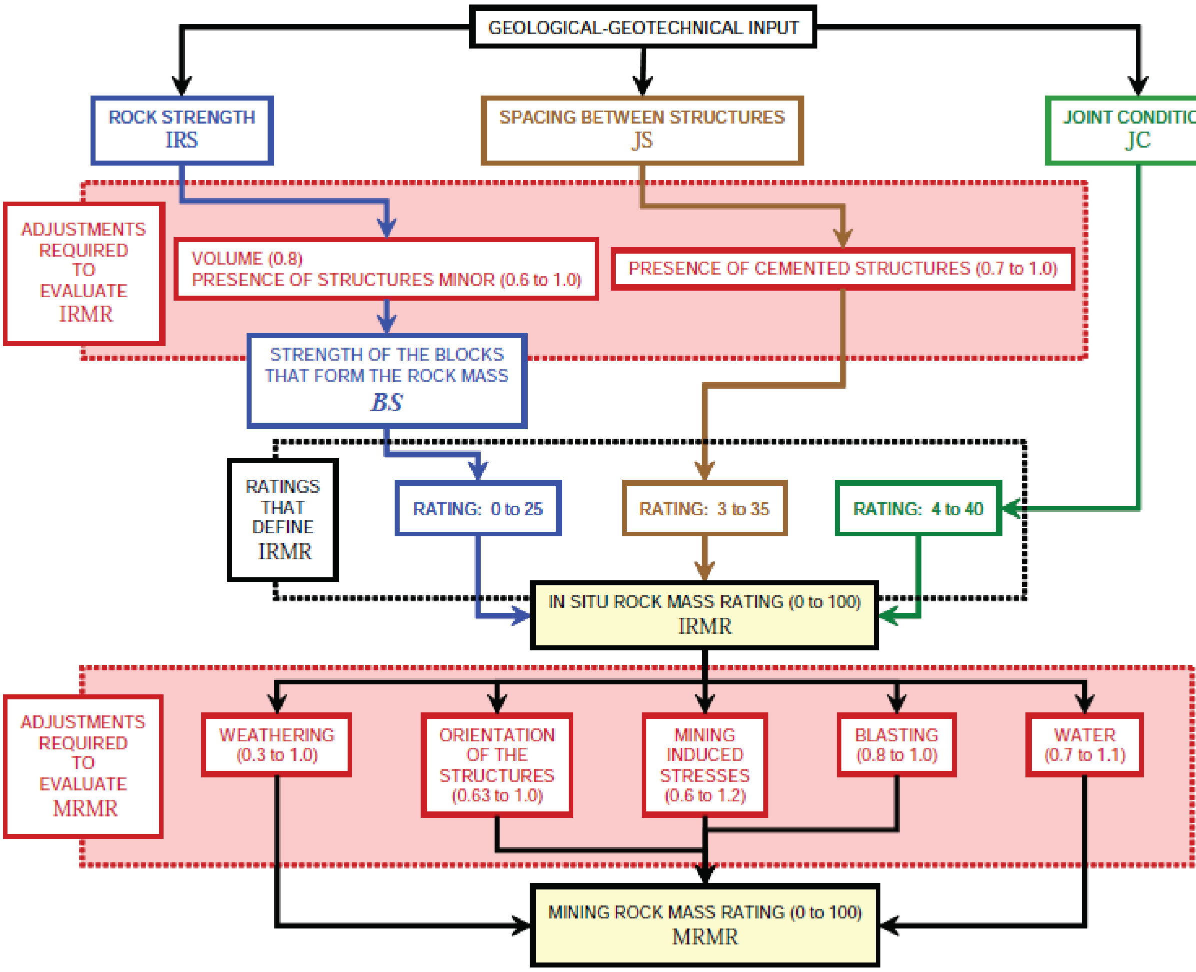

Figure 15: Procedures involved in evaluating IRMR and MRMR (Read and Stacey, 2009)

The adjustment factors once determined can by multiplied with the IRMR value to calculate the MRMR value. Overall, the objective is for the engineering geologist, rock mechanics engineer and planning engineer to adjust the IRMR. It is worth noting that the IRMR procedures and MRMR adjustments described above are the most recently published (Laubscher and Jakubec 2001) of all the adjustment versions. If an earlier version of the procedure is being used, it is important to state the date of the version. Stacey (2007) showed the relationships between RMR and MRMR. The MRMR value is calculated as about 5 points less than the RMR value. The MRMR classification system is better suited to real stability assessment since it is also concerned with cavability.

2.4.3 Hoek-Brown Geological Strength Index (GSI)

The Hoek-Brown Geological Strength Index was after the Hoek-Brown failure criterion which was first presented by Hoek and Brown (1980). The Hoek-Brown Geological Strength Index (GSI) original criterion was developed by Hoek (1983) and Hoek and Brown (1988), to provide a visual method of quantifying rock mass strength for different geological conditions.

Read and Stacey (2009) said that the name GSI officially emerged in 1995 after undergoing numerous changes as a substitution to Bieniawski's RMR in the generalized Hoek-Brown criterion. Values obtained from GSI are related to both the degree of fracturing and the fracture surfaces condition.

Table 3 shows the generalized Hoek and Brown criterion which is a system based more heavily on fundamental geological observations which include values for Young's modulus (*E*) and Poisson's ratio and less on the numbers provided by the RMR system. Further research dealt with the limitations of the system in Table 3 which had expunged the numerical accounting of RMR from the rock mass classification process. This led to the reintroduction of the Geological Strength Index (GSI) in 2000 by Marinos and Hoek as shown in Table 4. The major changes between Table 3 and Table 4 are the display of only the GSI values across each box in the table and the pioneering of the laminated/sheared rock mass structural classification. Read and Stacey (2009) highlight that the most used GSI chart is Table 4 which has been extended to accommodate some of the most variable rock masses and to project information gained from surface outcrops to depth (Hoek et al., 1998; Marinos and Hoek, 2001; Marinos et al., 2005; Hoek et al., 2005).

The principal benefit for replacing the RMR with the GSI concept was that the GSI was deemed a more appropriate means for relating the Hoek-Brown failure criterion to geological observations in the field (Hoek et al., 2002) as it was characterized by the block shapes and the degree of interlock as well as the surface condition of the intersecting defects. Furthermore, the GSI concept recognized the difficulties experienced by the Hoek-Brown criterion when the value of RMR was less than 25 (Hoek et al., 1995). The replacement of RMR put an end to the double counting of joint spacing which is featured in both the RQD and RMR expressions, and repeated consideration of UCS, which is incorporated within RQD and the generalized Hoek-Brown criterion expressions.

Fundamental geological observation is prominent, however, the charted GSI values (Hoek et al., 1998) are still those of Bieniawski RMR (1976) which have been improved slightly. The joint spacing remains double counted, UCS remains double counted and uncertainties of RQD as a parameter for determining rock mass strength (Read, 2007) have not been avoided.

Table 3: Hoek-Brown rock mass classification system (Hoek et al, 1995)

GENERALIZED HOEK-BROWN CRITERION

$$\sigma_1' = \sigma_3' + \sigma_c \left(m_b \frac{\sigma_3'}{\sigma_c} + s \right)^a$$

σ_1' = major principal effective stress at failure

σ_3' = minor principal effective stress at failure

σ_c = uniaxial compressive strength of *intact* pieces of rock

m_b, s and a are constants which depend on the composition, structure and surface conditions of the rock mass

STRUCTURE	SURFACE CONDITION	VERY GOOD Very rough, unweathered surfaces	GOOD Rough, slightly weathered, iron stained surfaces	FAIR Smooth, moderately weathered or altered surfaces	POOR Slickensided, highly weathered surfaces with compact coatings or fillings containing angular rock fragments	VERY POOR Slickensided, highly weathered surfaces with soft clay coatings or fillings
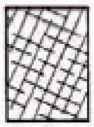 BLOCKY - very well interlocked undisturbed rock mass consisting of cubical blocks formed by three orthogonal discontinuity sets	m_b / m_i	0.60	0.40	0.26	0.16	0.08
	s	0.190	0.062	0.015	0.003	0.0004
	a	0.5	0.5	0.5	0.5	0.5
	E_m	75,000	40,000	20,000	9,000	3,000
	ν	0.2	0.2	0.25	0.25	0.25
	GSI	85	75	62	48	34
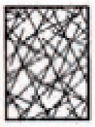 VERY BLOCKY - interlocked, partially disturbed rock mass with angular blocks formed by four or more discontinuity sets	m_b / m_i	0.40	0.29	0.16	0.11	0.07
	s	0.062	0.021	0.003	0.001	0
	a	0.5	0.5	0.5	0.5	0.53
	E_m	40,000	24,000	9,000	5,000	2,500
	ν	0.2	0.25	0.25	0.25	0.3
	GSI	75	65	48	38	25
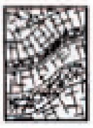 BLOCKY/SEAMY - folded and faulted with many intersecting discontinuities forming angular blocks	m_b / m_i	0.24	0.17	0.12	0.08	0.06
	s	0.012	0.004	0.001	0	0
	a	0.5	0.5	0.5	0.5	0.55
	E_m	18,000	10,000	6,000	3,000	2,000
	ν	0.25	0.25	0.25	0.3	0.3
	GSI	60	50	40	30	20
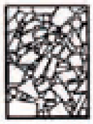 CRUSHED - poorly interlocked, heavily broken rock mass with a mixture of angular and rounded blocks	m_b / m_i	0.17	0.12	0.08	0.06	0.04
	s	0.004	0.001	0	0	0
	a	0.5	0.5	0.5	0.55	0.6
	E_m	10,000	6,000	3,000	2,000	1,000
	ν	0.25	0.25	0.3	0.3	0.3
	GSI	50	40	30	20	10

Read and Stacey (2009) emphasize against the use of the GSI system when a clearly defined, dominant structural system is evident in the rock mass as shown in Table 4. Highly likely, this might be the case for several rock types nominated in some proposed extensions of the system, including bedded or fissile siltstone, mudstone, shale, flysch, schist and gneiss, unless rock types have been tectonically damaged, and their structural preferences lost.

Engineering judgement after assessment of design and failure mechanism is vital regardless of the rock mass classification system used. This is because prediction of failure zone geometries cannot be done accurately and cannot consider the correct mechanism of failure. The prediction however determines the potential volume of failure.

Table 4: Hoek-Brown rock mass classification system (Marinos and Hoek 2000)

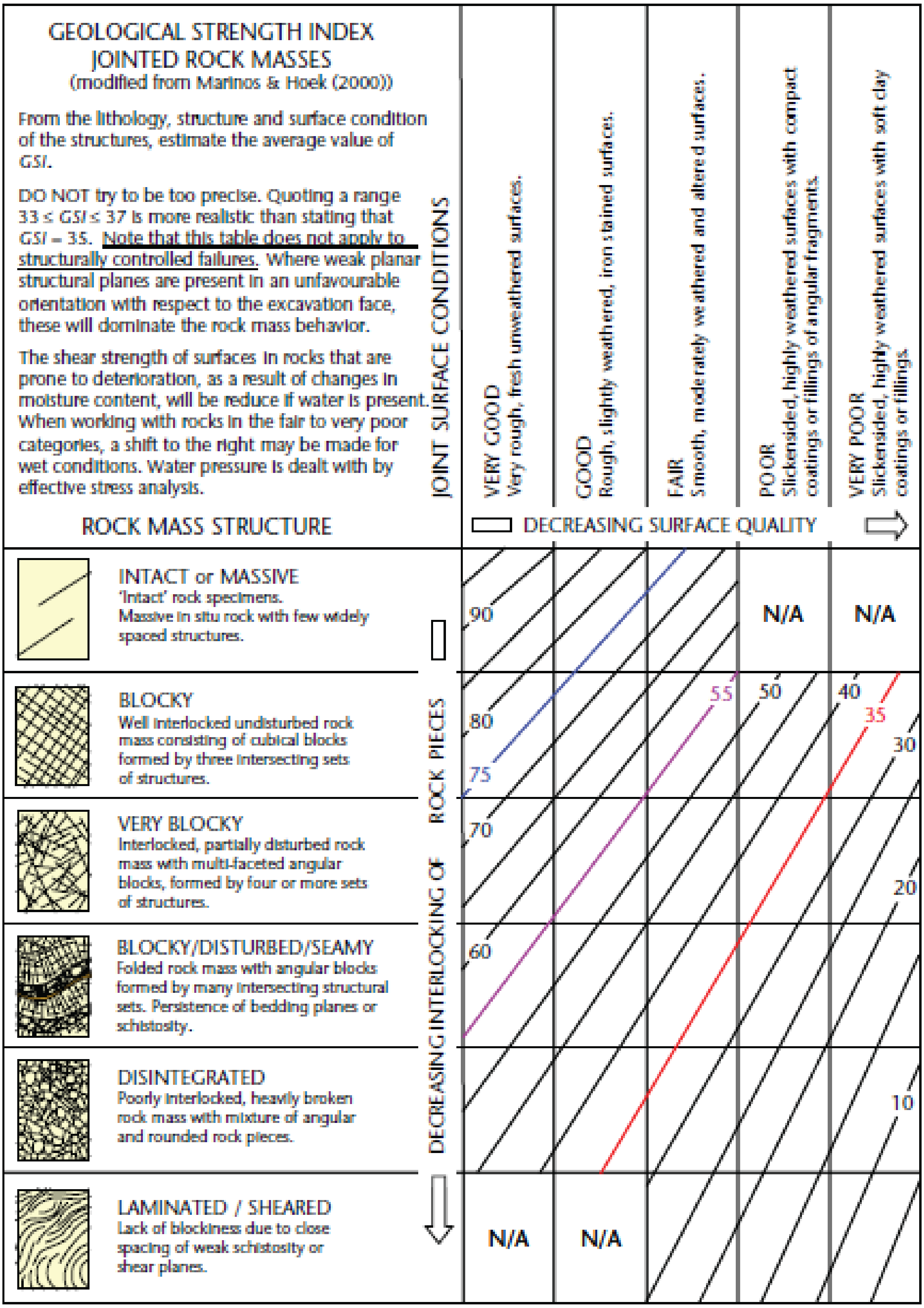

In civil engineering, there is conservatism and usually a large factor of safety is used. This masks any shortcomings in the use of rock mass classification approaches. In mining, however, a lesser margin of error exists and prediction is usually required. Stacey (2007) discussed a few points to consider when using rock mass classification methods:

i. The feel of the rock mass, understanding and interpretation of the rock mass quality number may be lost by the experienced user;
ii. The expectation by many rock engineers for the rock mass to behave according to a rock mass quality number instead of the real in situ rock mass characteristics;
iii. There is a correlation between rock mass quality number, rock mass deformation and strength parameters and this has facilitated sophisticated non-linear numerical stress analysis for design of support. Due to the availability of these correlations, most analysis are often carried out without any necessary understanding of the mechanisms of failure. This can consequently result in incorrect assessment of stability.
iv. The risk involved in variability of input parameters for rock mass classification will not be considered with the use of a single number for the rock mass quality.

2.5 Groundwater conditions

Water can be a nuisance to the mining industry since it causes erosion and accumulation of mud at the bottom of the pit. Apart from being a nuisance, water within the rock or soil considerably decreases stability (Stacey and Swart 2001). The effects of water on a slope occur in two ways: surface water and groundwater. Surface water is detrimental causing erosion channels along relict structures particularly in the saprolite slopes. In instances where the benches are too high or walls are too steep, the ponded water facilitates the saturation of the saprolite material which may cause sloughing.

Groundwater in the rock mass surrounding an open pit excavation can have a detrimental effect on slope stability (Hoek and Bray, 1981). It is therefore expedient to have information on water pressures for designing and maintaining safe slopes (Girard et al., 1998). According to Read and Stacey (2009), fluid pressure acting within discontinuities and pore spaces in the rock mass reduces the effective stress with a consequent reduction in shear strength. However, Mohammed (1997) highlights the fact that there is no doubt that the factor of safety of any given slope can be significantly improved if the water table within it can be lowered. Nevertheless, Stacey and Swart (2001) note that if instability develops in a slope, one of the first measures that should be considered for stabilization is drainage. Azrag et al. (1998) also add that slope instability due to groundwater can be aggravated by the presence of critical features such as foliation, bedding, or a dipping wedge structure in a highwall. The ideal remedy may be the flattening of a wet slope, however, the practical alternative is dewatering of slopes which is more economical and desirable.

Figure 16 presents a flow net which is simply a graphical representation of ground water flow in a rock or soil mass. Flow nets can be used to understand how geology and drainage systems affect possible ground water conditions within a slope. Flow nets consist of two sets of decussating lines as follows (Wyllie and Mah, 2004):

- *Flow lines* are paths followed by the water in flowing through the saturated rock or soil.
- *Equipotential lines* are lines joining points at which the total head *h* is the same.

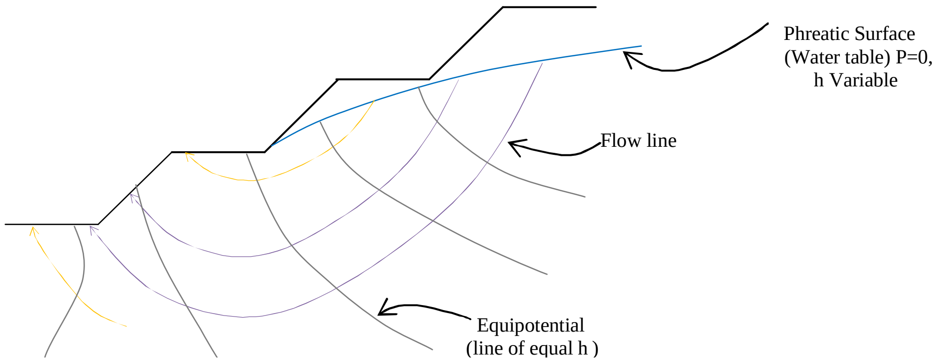

Figure 16: Groundwater Flow Anatomy System in Pit Slope (Hustrulid et al., 2000)

A few authors (Wyllie and Mah, 2004; Read and Stacey, 2009; and Mohammed, 1997) have agreed on the negative effects of groundwater on the stability of a slope as below:

i. Water pressure in a slope minimizes the stability of the slope by decreasing the shear strength of potential failure surfaces, increasing the likelihood of slope failures.
ii. Water pressure in tension cracks or similar near vertical fissures, reduces stability by increasing the forces that tend to induce sliding. The factor of safety is reduced to below unit.
iii. In fissures filled with water due to temperature dependent volume changes, freezing of ground water is likely to cause wedging. On the other hand, freezing of the surface water on slopes can result in a build-up of water pressure in the slope, which may block drainage paths and consequently decrease the stability of the slope.

Read and Stacey (2009) define total normal stress (σ_n) as the pressure acting on the potential failure surface, which is as a result of the lithostatic and hydrostatic loads. This total normal stress is partially opposed by the granular or block components of the formation as well as the fluid pressure within the pores (pore pressure). The pore pressure has a high likelihood to reduce the rock strength by altering the chemical or physical inherent properties of the rock.

This can cause accelerated weathering which decreases shear strength especially in low strength rocks. Moisture has the same effect on the rock strength. Mohammed (1997) further added that more rock strength reduction is expected if the moisture is under pressure. Water pressure U reduces the normal stress σ to an effective stress (σ - U). Wyllie and Mah (2004) define effective normal stress as the distinction between the stress due to the weight of the rock lying above the sliding plane and the uplift pressure which is a resultant of the water pressure.

The water pressure effect, *u* on the shear strength can be expressed in the shear strength equation as follows:

$\tau = C + \sigma_n \tan \phi$ *Equation 1*

which then becomes

$\tau = C + (\sigma_n - u) \tan \phi$ *Equation 2*

where:

- τ = shear strength on a potential failure surface
- u = fluid pressure (or pore pressure)
- σ_n = total normal stress acting perpendicular to the potential failure surface
- ϕ = angle of internal friction
- c = cohesion available along the potential failure surface.

The influence of water pressure acting on the surfaces of a shear specimen is illustrated in Figure 17.

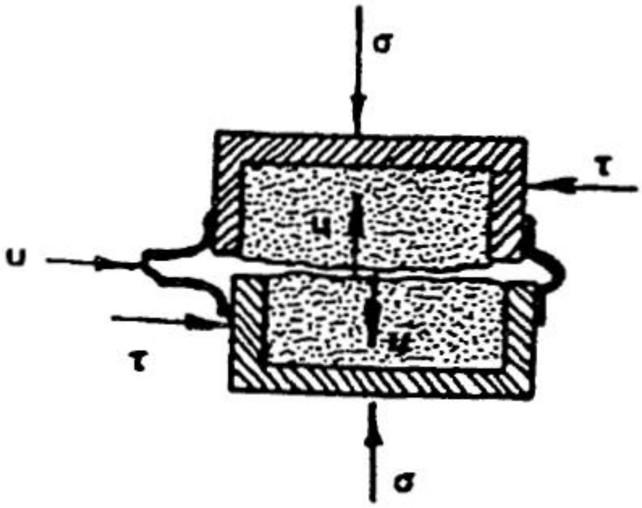

Figure 17: Influence of water pressure on a shear specimen (Mohammed, 1997)

Mohammed (1997) argued that in most hard rocks and in many sandy soils and gravels, the cohesive and frictional properties (c and ϕ) of the materials are not significantly altered by the presence of water and hence reduction in shear strength of these materials is due, almost entirely to the reduction of normal stress across failure surfaces**.** Therefore, it is the water pressure as opposed to the moisture content which is critical in dictating the strength characteristics of the hard rocks. The presence of small volumes of water trapped in the rock mass at high pressure has more detrimental effects than a large volume of water discharging from a free draining aquifer (Mohammed 1997).

2.5.1 The effect of water pressure in a tension crack

Mohammed (1997) considers the case of a block resting on the inclined plane and uses this to discuss the effect of water pressure in a tension crack (figure 18). The block is split by a tension crack which is filled with water whose pressure increases linearly with depth and a total force V. An assumption is made that there is water pressure transmission between the tension crack and the base of the block which causes distribution along the base of the block. This water pressure distribution becomes an uplift force U which lessens the normal force acting across the surface.

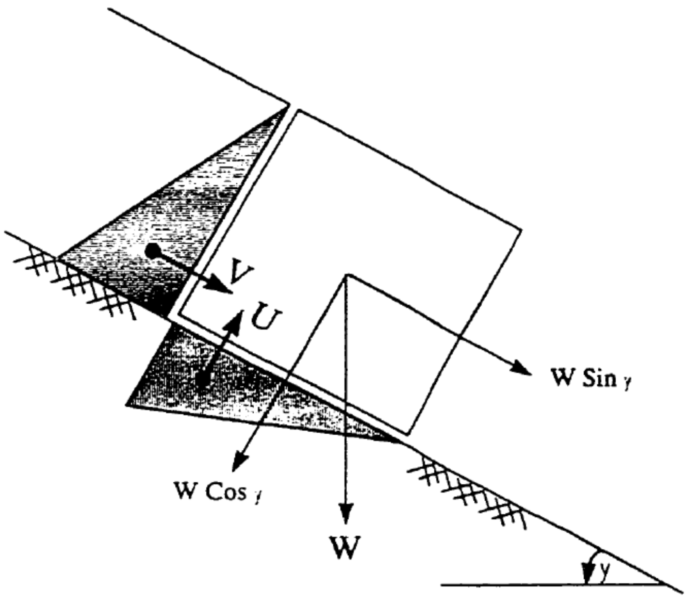

Figure 18: Effect of water pressure in a tension crack (Mohammed, 1997)

The condition illustrated in Figure 18, of a block with its own weight W, acted upon by water forces V and U is defined by:

$W\sin\gamma + V = cA + (W\cos\gamma - U)\tan\gamma$ *Equation 3* where,

C = cohesion along the failure plane

γ = angle of internal friction for the failure plane

A = area of the base of the plane

W = weight of the failure mass

β = dip angle of the failure plane

U = uplift water force

V = Water pressure in a tension crack

Equating driving and resisting forces, the equation for factor of safety (FOS) can be obtained

FOS. = Resisting Forces/Driving Forces *Equation 4*

From this equation it will be seen that the driving force tending to induce sliding down the plane is increased and the frictional force resisting sliding is decreased. Therefore, both V and U result in decrease in stability. The presence of water gives rise to uplift forces but it is the water forces in the tension cracks which critically control the stability of the slopes.

2.6 Effects of Blasting

Blast induced vibrations cause some stress on the slopes, but more importantly, the rock behind the slope face can become fragmented and loosen as a result. Sanchidrian et al. (2007) quantified the energy components in real blasting trials and concluded that only about 7 to 27% of the total explosives energy is used to break the rock, the rest being wasted energy including vibrations into the highwall. Calnan (2015) also agrees that ground vibrations are a resultant of the wasted energy affecting the highwall. Stachura and Cumerlato (1995) highlighted that rock falls from a slope face in a surface mine are largely influenced by poor or improper blasting practices. Wyllie and Mah (2004) further added that not only is the slope face disturbed by blasting, but it also undergoes stress relief, consequently having a higher hydraulic conductivity than the undisturbed rock. Stacey and Swart (2001) estimated that the stable slope angle for a good quality rock mass could, in some cases, be reduced by about 15% due to poor blasting. Stachura and Cumerlato (1995) suggest that presplitting, being one of the most frequently used wall control techniques, can produce a uniform highwall that improves the efficiency in blast operations. Read and Stacey (2009) further discussed several wall control blasting techniques used to reduce blast-induced slope damage which include:

- Pre- or mid-split blasting

- Trim blasting
- Buffer blasting; and
- Line blasting

Konya (2015) said that the choice of the controlled blasting technique depends largely on the slope design and characteristics of the rock mass as each technique has its associated advantages and disadvantages. Read and Stacey (2009) added that all techniques benefit from good horizontal relief away from the slope and therefore consider relief of critical consideration in the design process. Wall control blasting is very critical for the preservation of the final wall quality as slope failure is not only costly but life-threatening. Cebrian et al. (2018) said the objective of an effective wall control blasting technique is to produce on-design and undamaged slopes as well as well-fragmented and loose muck piles.

2.6.1 Presplitting

Sharma (2017) describes a pre-split as a row of small diameter blast holes with decoupled charges, which are usually blasted simultaneously before drilling of production holes to create a fracture plane. According to Read and Stacey (2009), these holes need to be closely spaced in a row and along the designed dig limit. The creation of this fracture plane before the production blast reduces the amount of tensile stresses damaging the highwall by a huge margin. Konya (2015) noted that presplitting is an old technique which is highly recognized for creation of radial cracks. The fissured planes created by presplit blasting restrict back-break and control vibrations from production blasts.

As with other controlled blasting techniques, the presplit performance is dependent on the geology of the rock mass. Read and Stacey (2009) listed the favourable presplit conditions as: massive rock, tight joints, dominant joint orientation more than 30° off strike of the designed face and absence of weak structures that form wedges or daylight on the batter face and catch berm.

According to Konya (2015), presplitting is the most expensive controlled blasting technique, and so its performance must be constantly monitored to achieve its worth. Presplit holes are loaded with decoupled charges, preferably cartridge explosives, to split the gap between holes in tension without causing compressional damage to the slope (Cebrian et al., 2018). Table 5 gives a guide on presplit design parameters and gives a recommendation of assorted charge, spacing and decoupled explosive diameter for a given blast hole diameter.

Table 5: Initial pre-split guidelines (Read and Stacey, 2009)

Blast hole diameter (mm)	Charge (kg/m)	Spacing (m)	Minimum decoupled charge diameter (mm)	Maximum decoupled charge diameter (mm)
76	0.5	1.1	22	25
89	0.6	1.2	22	29
102	0.7	1.4	25	32
114	0.8	1.6	32	38
127	0.9	1.8	32	44
153	1.1	2.1	38	51
165	1.2	2.3	44	51
200	1.4	2.8	51	64
229	1.6	3.2	64	76
270	1.9	3.8	68	89
311	2.2	4.4	78	103

The presplit spacing is approximately 14 hole diameters apart (Read and Stacey, 2009). According to Dyno Nobel (2010), the presplit spacing is supposed to be 12 hole diameters. Rorke and Simataa (2018) however argued that a good presplit design should allow for a range of 10 to 15 hole diameters. According to Read and Stacey (2009) the total charge (kg) in the blast hole must be approximately half the surface area between blast holes (bench height × spacing/2). The uncharged length at the crest of the hole is 10 to 15 times the hole diameters. Typical presplit powder factors are shown in Table 6 (Dyno Nobel, 2010).

Table 6: Typical presplit powder factors (Dyno Nobel, 2010)

Rock type	**Presplit blast Powder factor Kg/m²**
Hard	0.6-0.9
Medium	0.4-0.5
Soft	0.2-0.3

According to Read and Stacey (2009), these guidelines are only rules of thumb for initial design development which will require fine-tuning based on site geological conditions and resultant highwalls. Highly jointed rock requires tighter spacing while massive structures allow the spacing to be increased.

Bulk charges are typically ten times cheaper than continuous cartridge explosives and work well in weak slightly jointed rock mass. Adverse geological conditions however require continuous decoupled charges which provide excellent energy distribution. This relationship on choice of explosive product is shown in Figure 19.

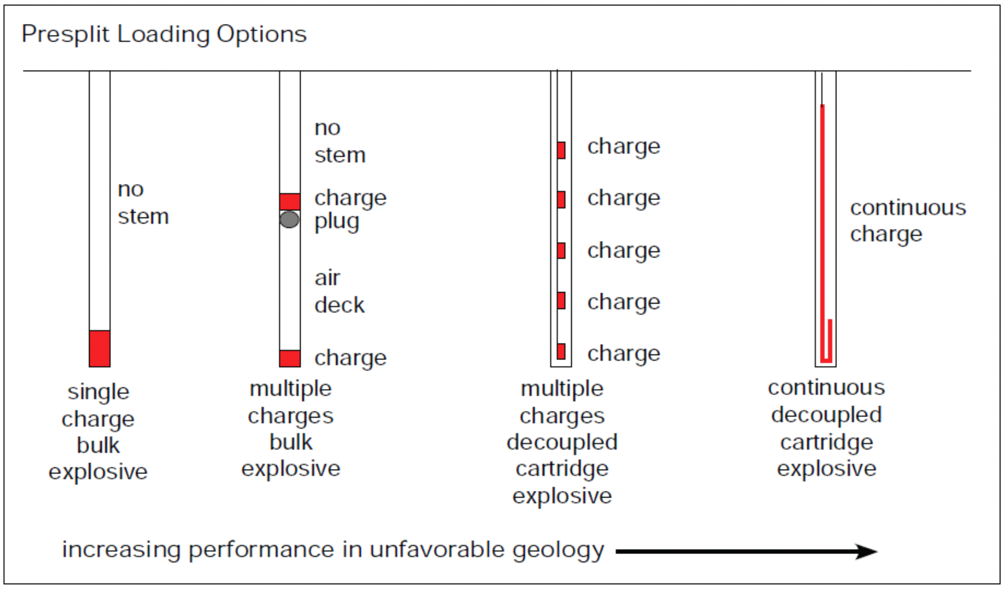

Figure 19: Presplit loading options (Read and Stacey, 2009)

Konya (2015) encourages stemming of presplits whereas most authors including Read and Stacey (2009) say presplit holes must be left unstemmed unless air overpressure needs to be controlled. Stemming of a pre-split hole has likelihood of causing cratering of the top of the bench as illustrated in Figure 20. It is recommended that the pre-split row be drilled 10–20° from the vertical for most geological structures. This positions the crest further away from the adjacent buffer row, which helps to reduce damage. The key factor in controlling overbreak is the standoff of the toe row from the pre-split. In some cases, the use of pre-splitting is not recommended due to narrow bench widths or highly fractured rock and next to loaded holes, the detonation of the pre-split can cause column shift.

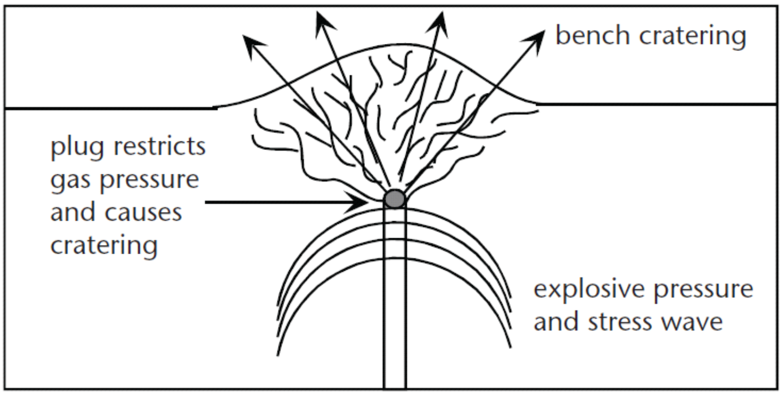

Figure 20: Crest damage caused by stemming pre-split holes (Read and Stacey, 2009)

According to Sharma (2017), pre-split charges are fired simultaneously by using detonating cord, electronic detonators or instantaneous electric detonators. However, whenever noise is a problem, a small pyrotechnic delay detonator is used to reduce the maximum charge mass per delay. Cracking occurs under the influence of blast induced stresses as shown in Figure 21. Rorke and Botes (2000) said that the generated borehole pressure must exceed the tensile strength of the rock, but must not exceed the compressive strength of the rock in order to achieve cracking and not crushing. Further reduction of noise levels can be achieved by burying surface lines of detonating cord with sand or drill chippings.

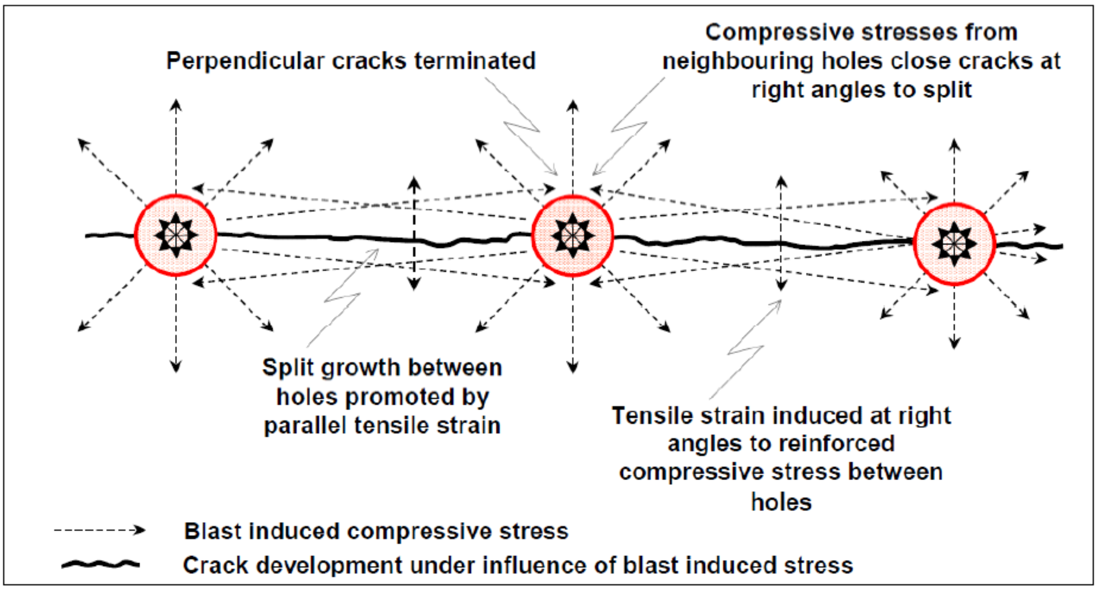

Figure 21: Pre-split formation through instantaneous initiation of closely spaced holes (Dunn and Cocker, 1995)

2.6.2 Trim Blasts

Trim blasts are the most commonly used controlled blasting technique specially designed to protect the highwall from blast induced damage (Sharma, 2017). Rorke and Simataa (2018) and Read and Stacey (2009) have made recommendations for trim blast designs to assist in preserving highwall integrity in highly jointed rock mass. The principles of trim blast designs are listed and explained below.

i. Trim width should be kept narrow to limit the accumulated amount of energy generated by the blast propagating into the final walls. Normally a width of about two bench heights or three to six rows provides for limited confinement of the blasted rock. In rock mass with adverse geological conditions, extra rows may be required to protect the slope from damage as a result of the production blast.
ii. Maintain block powder factor: Lowering the powder factor promotes back damage because each hole has to work much harder to break out the burden. Reduce the

charge mass in the back holes, but maintain the block powder factor. This can be achieved by tightening the burdens and spacings.

iii. Reduce spacings and burdens for holes along the final wall. The relationship between burden and spacing becomes inverted where the burden has to be bigger than the spacing, or a ratio of 1:1 is adopted along the final wall to promote breakage between the toe holes. Smaller burdens translate to less back damage. The spacing is initially set at half the normal spacing to make it easier to tie-in.

iv. A staggered pattern should be adopted and blasting should be done into a free face, preferably two free faces.

v. Lower charge mass per hole = less energy = less vibration: Charge mass per hole should be lowered without reducing powder factor. This can be achieved by reducing the diameter for the back holes. A reduced diameter means less linear charge and less charge mass per hole and consequently less charge mass per delay. This produces less energy and consequently less damaging vibration.

vi. No sub-drill for holes above berm width of subsequent bench

vii. A pre-shear row or buffer row is included in the trim blast design where necessary. The inner buffer row is designed to define the crest, therefore, careful determination of its charge and standoff from the batter face is required.

viii. Application of air decks on the holes above the lower level berm or in the toe and inner buffer rows to reduce blast hole pressures and to increase fragmentation in the top portion of the bench. The air deck provides a cushion that significantly diminishes the shock wave that is transmitted to the rock.

ix. Timing is critical. Shots should be timed to achieve single hole firing and a wide breakage angle.

Rorke and Simataa (2018) emphasized that these recommendations should not be applied in isolation because singly, they might make matters worse by increasing confinement. Table 7 presents the initial trim blast design guidelines which show the correlation between blast hole diameter, burden and the back row spacing. Continuous assessment of the resultant highwall will be necessary so that tweaks to the design can be made to achieve optimal results.

Table 7: Initial trim blast guidelines (Read and Stacey, 2009)

Blast hole diameter (mm)	Charge (kg/m)	Burden (m)	Spacing (m)a	Offset from toe (m)
76	0.6	1.7	1.4	0.30
89	0.75	1.9	1.5	0.36
102	0.9	2.0	1.7	0.41
114	1.2	2.4	1.9	0.46
127	1.4	2.6	2.0	0.51
153	2.0	3.1	2.4	0.61
165	2.3	3.3	2.6	0.66
200	3.4	4.1	3.1	0.80
229	4.6	5.0	3.5	0.92
270	6.0	5.5	4.1	1.08
311	7.8	6.1	4.8	1.24

a: Spacing may need to be half the inner buffer row spacing to help pattern tie-in

2.6.3 Buffer Blasting

Buffer (or cushion) blasting is the simplest of the wall control blasting techniques. It is typically used for competent rocks and involves modification of the last row in a production blast to alter the energy and consequently reduce wall damage. The common modifications are reduction of the explosive energy as well as reduction of the burden and spacing. The scaled depth of burial is increased by the reduction in explosive energy. Though buffer blasting is the most economical wall control technique, it is not the most effective of techniques when used in isolation. It is more effective when used in conjunction with other techniques such as trim blasting and presplitting.

2.6.4 Line Drilling

Konya (2015) and Wyllie and Mah (2004) describe line drilling as a wall control technique where blast holes are normally drilled close to one another usually within two to four hole diameters. Read and Stacey (2009) however say that, in weak rock mass, the spacing should be around 12 hole diameters, whereas in hard massive rock, the spacing should be reduced to three to six hole diameters. These holes are unloaded with explosives and normally drilled on the final limit. Sharma (2017) considers this technique as seldom used due to the cost implication of drilling closely spaced holes. Line drilling is used in areas where a presplit or trim blast cannot be done, usually in weak or highly fractured rock mass.

Read and Stacey (2009) and Konya (2015) both agree that a breakage plane occurs when the material between the holes is placed under tension from the adjacent blast and the holes act as stress concentrators, as functions of the rock mass strength and hole spacing. Sharma (2017) says that accurate drilling (hole spacing and angles) determine the success or failure of this technique.

2.6.5 Timing for Limiting Back Damage

According to Read and Stacey (2009), once a controlled blast design involving the techniques discussed above has been developed, the timing configuration needs to allow for relief and promote horizontal displacement away from the highwall. Wyllie and Mah (2004) suggested that damage to the highwall can also be caused by a production blast and so timing of a production blast should equally be looked at. Correct timing designs when applied with the trim blast principles such as implementation of staggered pattern and shooting to two free faces, can make a good blast design perform better (Read and Stacey, 2009). Emphasis on the free faces was also made by Wyllie and Mah (2004) when they discouraged against choke blasting into excessive burden or broken muck piles. Excessive front row blast hole burdens restrain horizontal movement of material during blasting (Rorke and Simataa, 2018). The point of initiation should be at a point of maximum relief which in this case is the corner as shown by Read and Stacey (2009) in Figure 22.

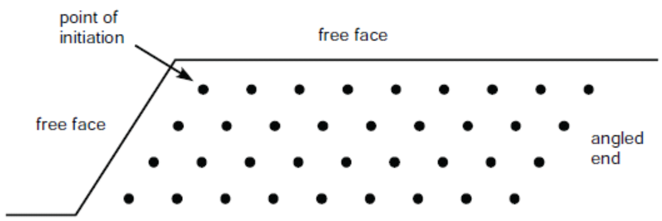

Figure 22: Point of initiation and double free faced trim (Read and Stacey, 2009)

Different authors have proposed (Rossmanith, 2003 and Chiappetta, 2007) that short delays are the way to go for blasting while others have opposed this (Bergmann et al., 1974 and Katsabanis et al., 2006). The application of more or longer delays within a blast promotes highwall stability. Wyllie and Mah (2004) and Rorke (2007) agree that adequate delays and timing intervals ought to be used for good movement towards free faces and the creation of new free faces for following rows as the blast progresses. Rorke and Simataa (2018) further added that highwall stability is promoted by ensuring obtuse (wide) breakage angles or acute (low) angles of displacement for the holes along the blast perimeter as shown in Figure 23.

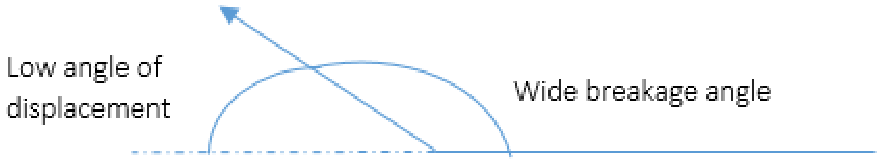

Figure 23: Back row breakage angles (Rorke and Simataa, 2018)

This method of timing (slowing down to achieve large breakage angles) always succeeds in trim blasts. However, slowing down of timing should not be applied in isolation. The charge distribution in the back of a blast is equally critical. Read and Stacey (2009) agree that reduction of overbreak is achieved by attaining low angles of direction of displacement to the desired crest (Figure 24) and not perpendicular to the wall (Figure 25). Wyllie and Mah (2004) further added that delays should be used to control the maximum instantaneous charge. Furthermore, satisfactory results are obtained by detonating each hole along the final line on separate delays, and it is not necessary to use a single delay for the full length of the final wall blast.

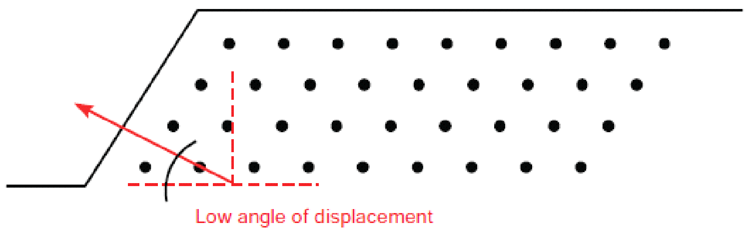

Figure 24: Preferred angle of displacement (Read and Stacey, 2009)

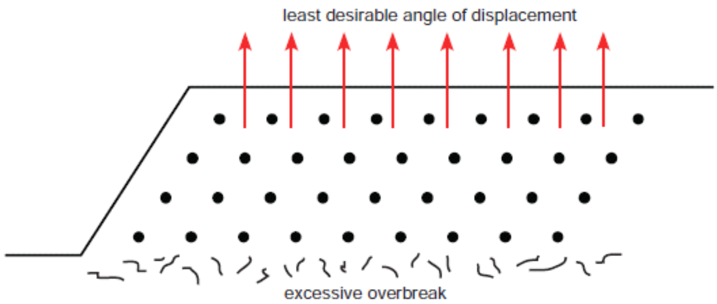

Figure 25: Adverse angle of displacement (Read and Stacey, 2009)

Wyllie and Mah (2004) say that trim blasts should be shot to two free faces to ensure maximum relief, however, instances occur when only one free face is available. In such instances, blasting a flat chevron or V configuration should be used to minimize back break as shown in Figure 26 (Read and Stacey, 2009). Deep V patterns however generate excessive back break, usually at the point of the V (Figure 27).

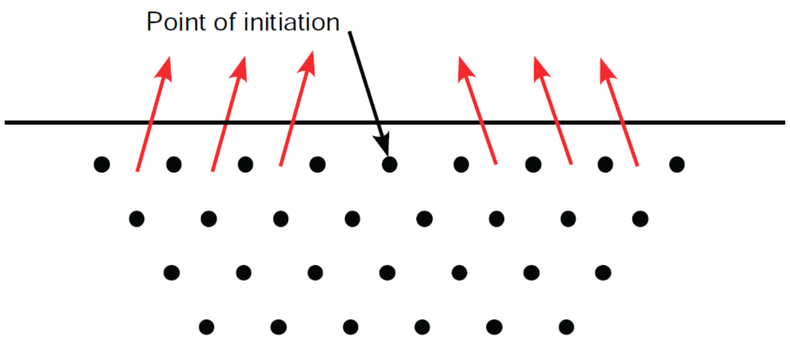

Figure 26: Flat V displacement (Read and Stacey, 2009)

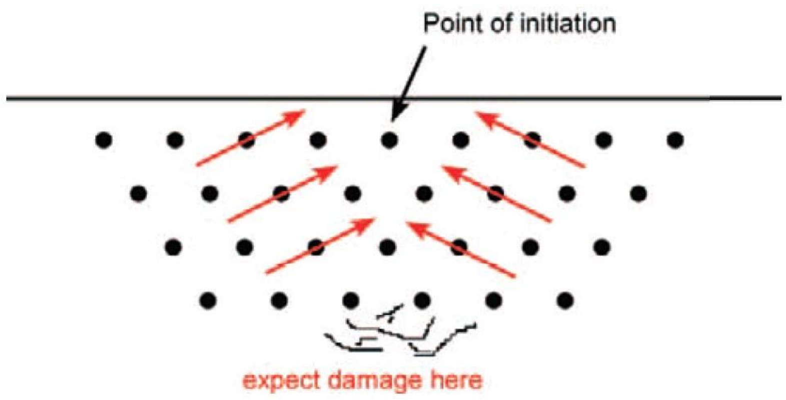

Figure 27: Deep V damage (Read and Stacey, 2009)

To reduce confinement along the highwall, the beginning and end of the blast should be angled (Read and Stacey, 2009). The joint orientation of the dominant structure to the azimuth of the crest will determine the initiation direction as it influences the amount of overbreak produced. Blasting against the direction of the dominant joints presses the joints together and limits back damage whereas blasting in the same direction as the dominant jointing rips the joints apart as shown in Figures 28 and 29.

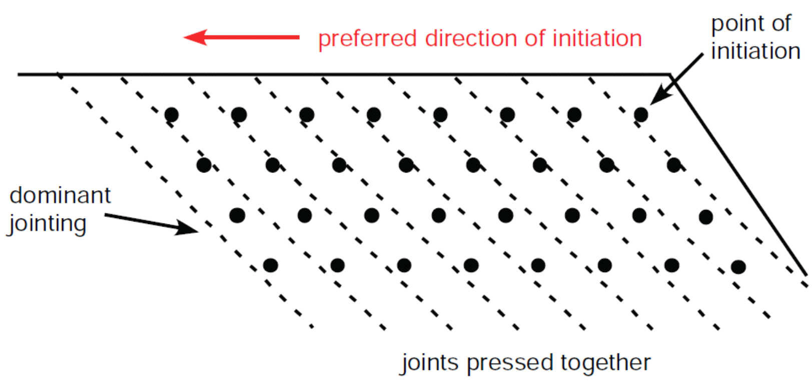

Figure 28: Direction of initiation that limits wall damage (Read and Stacey, 2009)

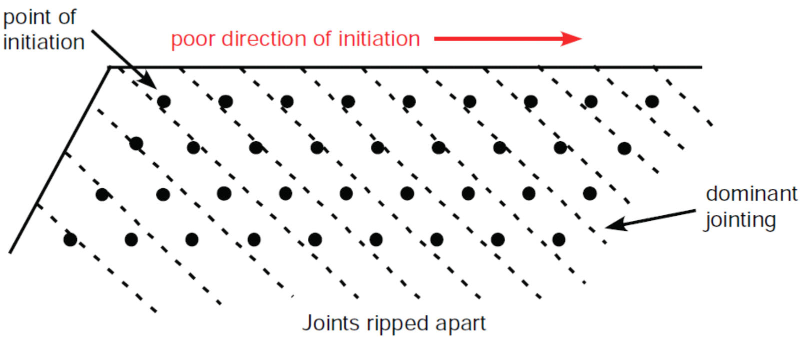

Figure 29: Direction of initiation that increases wall damage (Read and Stacey, 2009)

2.6.6 Blastability Index (BI)

Xiao et al. (2015) define rock mass blastability as a measure of the resistance of a rock mass to blasting and crushing. Blasting is affected by the synchronization, to various extents, of physical and mechanical properties, as well as structural characteristics of rocks. Founded by Lilly (1986), the Blastability Index has four main parameters that contribute significantly to blasting performance. These parameters and their influence are summarized below:

i. **Structural Nature (RMD):** If a rock mass has a blocky composition, that characteristic is likely to supersede the effect of explosive energy and the associated rock breaking mechanisms in the determination of the size of fragments that result from the blasting process. Conversely, in a massive rock mass, the formation of fragments is primarily brought about by the interaction of the explosive energy with the rock.

ii. **Joint Plane Spacing (JPS):** In the context of Lilly's (1986) work, joint planes refer to all planes of weakness observed in a rock mass: bedding planes, planes of foliation or schistocity, fault planes, and geological and mining-induced joints. This parameter has bearing on the size and shape of the fragments achievable. Rocks with closely spaced joints require relatively low levels of explosive energy to achieve the desired blasting outcome. The joint plane spacing plays a primary role in the effectiveness of wall control blasting.

iii. **Joint Plane Orientation (JPO):** The dip and dip direction can be used to assess the ease with which rock responds to blasting. The orientations of planes of weakness also affect the profile of the rock that remains on the periphery of the block that was blasted; that is, the highwalls and floor.

iv. **Specific Gravity (SGI) and Hardness (H):** In general, harder, heavier rock requires more explosive energy to break and move than lighter rock. Such rock also tends to behave in a brittle fashion in response to stress.

Chatziangelou and Christaras (2015) support the determination of BI before blasting in order to aid with the blast design process. The differentiation in BI values obtained has an immediate effect on excavation cost which always depends on factors like explosion, vibration, disintegration, powder creation. The BI is calculated by the following formula proposed by Lilly (1986), based on rock mass description, joint spacing and orientation, specific gravity and hardness:

BI = 0.5 x (RMD+JPS+JPO+SGI+H (Lilly, 1986) *Equation 5*

Where, BI = Blastability Index

RMD (Rock mass Description) = 10 (for Powdery/Friable rock mass), 20 (for Blocky rock mass), 50 (for Totally Massive rock mass)

JPS (Joint Plan Spacing) =10 (for closely spaced discontinuities), 20 (for intermediate spaced discontinuities), 50 (for widely spaced discontinuities)

JPO (Joint Plane Orientation) = 10 (for Horizontal), 20 (for Dip out of the Face), 30 (for Strike Normal to Face), 40 (for Dip into Face)

SGI (Specific Gravity Influence) = 25 x Specific Gravity of rock (t/m^3) – 50

H = Hardness in Mho Scale (1-10)

The rock hardness factor (H) ratings were calculated using the following empirical equation after the work of Lilly by Rorke (2003):

$$H = \frac{UCS+23.7}{47.6}$$ *Equation 6*

The outcome of the BI value computed is such that a low BI represents difficult blasting rock conditions and a high BI representing easy to blast rock conditions (Lilly, 1986). Christaras and Chatziangelou (2014) came up with a rock mass blastability classification standards after Lilly's work as included in Appendix G.

Lilly (1986) emphasized that the index is heavily biased towards the nature and orientation of weakness planes in the rock mass and is largely dependent on the four main parameters that contribute significantly to blasting performance.

2.7 Effects of mining (Excavation and scaling)

The effects of excavation and scaling on pit wall stability can be reviewed in tandem with mining compliance to designed bench geometry. In open pit mining operations, excavators are used to scale bench faces in order to achieve designed bench face angles. The key is:

- Selection of the right excavator sizes or "kits" which determine safe bench face scaling for the operator and the ripability of the soil or rock mass to be mined/scaled;
- Use of skilled operators for scaling operations; and
- Use of surveyed markers/guide pegs to ensure bench geometry is consistent, more especially in more weathered soil or rock formations.

The focus on the above factors is in line with the final bench face geometry to ensure a straight face is excavated rather than a concave or convex shaped bench face. According to Read and Stacey (2009), the final and crucial stages in achieving a safe and optimum slope in an open pit are excavation and scaling of the bench faces. Wyllie and Mah (2004) mention that these stages are usually carried out by excavating equipment such as rope shovels, excavators and bulldozers. Unlike in production loading where an operator's performance is judged in terms of productivity, in final wall excavation, primary performance criteria involve achieving the design batter face angle, bench width and minimizing rock fall hazards along the bench faces (Read and Stacey, 2009). Large loading equipment is more efficient for excavation in large open pits, however, it is not suited for scaling bench faces nor is it cost effective in that role. It is more appropriate to have specific teams with separate equipment for phase and ultimate slope excavation, cleanup and scaling.

Primary excavation in large open pit mines is done by rope shovels and hydraulic excavators while excavators operating in either a front shovel or backhoe configuration or wheeled front-end loaders may be used in small open pits. L'Amante and Flora (2012) and Read and Stacey (2009) both agree that large shovels excavate to a maximum of 15 - 16m whereas smaller equipment excavates to 10 - 12m. The operating bench height is generally regulated to a maximum of 1.5m above the excavating equipment reach. Overburden and weathered or weaker rocks can often be free-dug with large equipment, or alternatively, ripped and dozed, whereas strong rock requires blasting and excavating by primary loading equipment.

Read and Stacey (2009) further explain how powerful large items of equipment are and how they are not appropriate for highwall excavation because of the high potential of over digging benches, especially where there is blast damage. Over digging on the bench face by large equipment can be avoided by cutting a trench face with a smaller excavator. This consequently clarifies the dig line or excavation limit to which the operator should mine, thus reducing the tendency to create overhang at the crest of the bench. It is difficult for large equipment such as rope shovels to efficiently mine along the crest of benches without significant over spill. High production rates in large open pits normally contribute to the creation of overhang that will need to be attended later.

Wyllie and Mah (2004) describe scaling as cleaning of highwalls or the removal of loose rock, soil and vegetation on the face of a slope which is an important part of the excavation cycle. The cleaning of highwalls is normally conducted by a hydraulic excavator (backhoe or face shovel). L'Amante and Flora (2012) highlighted that the correct selection and implementation of wall control blasting strategies minimizes scaling activities. For this reason, highwall cleaning is considered as a reactive strategy. Read and Stacey (2009) consider scaling to be very significant especially in double-benched configurations as it minimises the accumulation of debris on the bench following excavation, consequently preserving valuable catchment volume. It is affected by the nature of the rock mass, the effective bench height, the size of the equipment used, operator experience and design catchment berm width. Scaling can be done from the bench above by dragging a chain across the face with a dozer or backhoe; and from the bench below by an excavator configured as a backhoe. At no point shall the face be scaled from the bench above using a backhoe as the balance of the machine may be disturbed by large rocks (Read and Stacey, 2009).

2.8 Empirical Slope Stability Assessments

2.8.1 Saprolite and Saprock Slopes

Hoek and Bray (1981) produced a set of charts corresponding with five different groundwater conditions. Only three of these have been included for this evaluation purpose:

i. Dry conditions: the presence of a pit or quarry will result in groundwater drawdown conditions, with the consequence that the soil adjacent to the excavation is likely to be in a dry or only partially saturated condition. It is to be borne in mind that South Africa is a semi-arid country;
ii. Saturated conditions: this condition is included to take account of a worst-case situation which could occur after sustained rainfall; and
iii. A partially saturated condition intermediate between the dry and saturated conditions.

Stacey and Swart (2001) highlight the above conditions on the slope stability chart in Figure 30. The input data necessary to decipher the chart are itemized below:

- C cohesion of the soil mass (kPa)
- γ density of the soil mass (kg/m^3)
- ϕ angle of internal friction of the soil mass (˚)
- H height of the slope (m)

The parameters for the soil mass (cohesion, angle of friction and density) should be determined by means of laboratory and field testing. It must be ensured that these values are relevant to, and representative of, the condition of the slope. As a guide, however, Table 8 gives consistency of soil descriptions and corresponding typical values for the parameters. These values do not consider any soil structure that may be present in the soil mass.

Table 8: Typical values of soil parameters (Stacey and Swart, 2001)

Soil description	**Density (kN/m^3)**	**Cohesion (kPa)**	**Friction angle (°)**
Loose sand/gravel	16	Zero	35
Medium dense sand/gravel	18	Zero	37
Dense sand/gravel	20	Zero	40
Loose silt	16	2	29
Medium dense silt	17	5	30
Dense silt	18	10	31
Soft clay	16	5	23
Moderately stiff clay	17	10	24
Stiff clay	18	25	25

The method of determination of factor of safety of a slope using charts according to Stacey and Swart (2001) is as follows:

i. Calculate the value of $C/(\gamma H.tan\ \phi)$ and find the corresponding point on the circumference of the chart.

ii. Translate radially inwards on the chart from this point to meet the required slope angle isoline.

iii. For this intersection point, read off the corresponding ordinate value $Tan\ \phi\ /F$ (or the abscissa value) and hence calculate the value of the factor of safety *F*.

The chart is a means of determining factors of safety of slopes very rapidly. It can also be used for back analysis of slopes, as well as to determine, for example, the value of cohesion necessary for stability. It can also be used to investigate the effect of variability in soil properties on the stability (Wyllie and Mah, 2004).

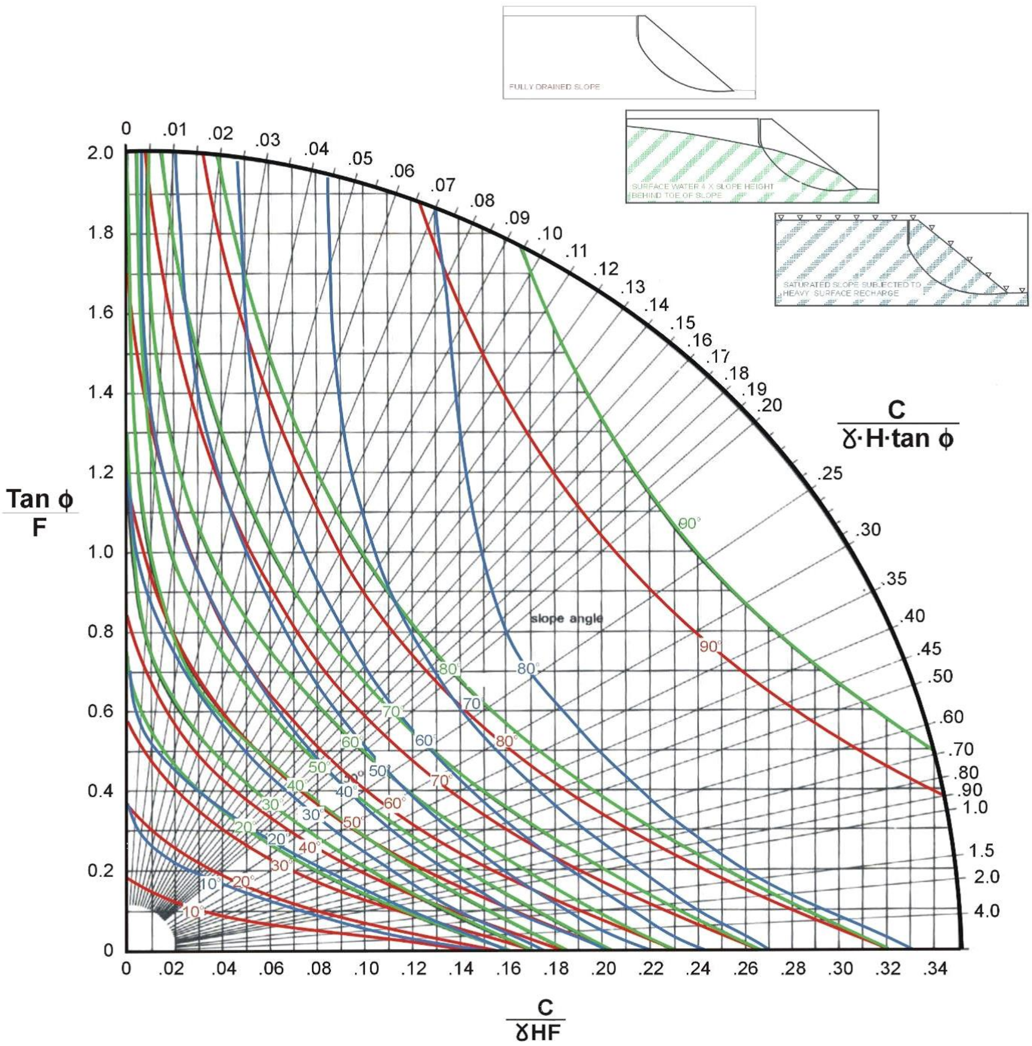

Figure 30: Slope stability chart for soil and weathered rock slopes (Stacey and Swart, 2001)

2.8.2 Hard/Fresh Rock Slopes

Kinematic analysis

The results of scanline and window mapping are input into a graphical and statistical analysis computer programme (Rocsience's DIPS, for instance), to analyze and visualize structural data, following the same technique used in stereonets. Assumptions for the internal angle of friction are made in the absence of results from a lab-based material (mechanical) property programme.

A sensitivity analysis is conducted on the slope angle and the probabilities of the various modes of failure against slope face angles, are recorded and tabulated in Chapter 3.

Empirical stability analysis

The Mining Rock MMass Rating (MRMR) classification is better suited to real stability assessment since it is also concerned with cavability. The RMR is multiplied by an adjustment percentage to give the MRMR. The adjustment percentages are empirical, having been based on numerous observations in the field. The adjustment procedure requires that the engineer assess the proposed mining activity in terms of its effect on the rock mass. Application of the MRMR system involves assigning in-situ ratings to a rock mass based on measurable geological parameters (Laubscher, 1990). The geological parameters are weighed according to their relative importance, with a maximum possible total rating of 100. Rating values between 0 and 100 cover five rock mass classes comprising ratings of 20 per class, ranging from very poor to very good, which reflect the relative strengths of the rock masses (Laubscher, 1990). Each rock mass class is further sub-divided into a division A and B.

Table 9 shows the adjustments for joint condition from a dry condition to a fully saturated joint with severe groundwater pressure. Adjustments are applied to the MRMR value to take account of weathering of the rock mass, joint orientation relative to the excavation, mining-induced stresses and blasting effects. The magnitudes of these adjustments are described in Tables 10 to 12.

- Weathering

Certain types of rock weather readily, and this must be taken into consideration in decisions on the size of the excavation. Weathering is time-dependent and influences the timing of support installation and the rate of mining. The three parameters that are affected by weathering are the Intact Rock Strength (IRS), Rock Quality Designation (RQD) or fracture frequency per metre (FF/m), and joint condition (Laubscher, 1990). The RQD percentage can be decreased by an increase in fractures. The IRS refers to the Uniaxial Compressive Strength (UCS) of intact rock between discontinuities and can decrease significantly as chemical changes take place. Alteration of the host rock and gouge material affects the joint condition.

A weathering adjustment is relevant when rock types occur which are susceptible to deterioration over time. The adjustment percentages are given in Table 10.

Table 9: Adjustments for Joint Condition and Groundwater (Laubscher, 1993)

Parameter	Description		Dry Condition	Wet Conditions: Moist	Wet Conditions: Moderate pressure 25-125 1/mm	Wet Conditions: Severe Pressure >125 1/min
A Joint Expression (large scale irregularities)	Wavy	Multi-Directional	100	100	100	95
	Wavy	Uni-Directional	95 90	95 90	90 85	80 75
	Curved		89 80	85 75	80 70	70 60
	Straight		79 70	74 65	60	40
B Joint Expression (small scale irregularities or roughness	Very rough		100	100	95	90
	Striated or rough		99 85	99 85	80	70
	Smooth		84 60	80 55	60	50
	Polished		59 50	50 40	30	20
C Joint Wall Alteration Zone	Stronger than wall rock		100	100	100	100
	No alteration		100	100	100	100
	Weaker than wall rock		75	70	65	60
D Joint Filling	No fill surface staining only		100	100	100	100
	Non softening and sheared material (clay or talc free	Coarse Sheared	95	90	70	50
		Medium Sheared	90	85	65	45
		Fine Sheared	85	80	60	40
	Soft sheared material (eg talc)	Coarse Sheared	70	65	40	20
		Medium Sheared	65	60	35	15
		Fine Sheared	60	55	30	10
	Gouge thickness <amplitude of irregularity		40	30	10	
	Gouge thickness <amplitude of irregularity		20	10	Flowing material 5	

Table 10: Weathering Adjustment (Laubscher, 1993)

Rate of weathering and adjustments (%)					
Description of weathering extent	**6 months**	**1 year**	**2 years**	**3 years**	**4 + years**
Fresh	100	100	100	100	100
Slightly	88	90	92	94	96
Moderately	82	84	86	88	90
Highly	70	72	74	76	78
Completely	54	56	58	60	62
Residual soil	30	32	34	36	38

In explanation of the adjustments given in table 10, if the rock will weather to a residual soil in 6 months, the adjustment is 30%; if it will be only slightly weathered after 3 years, the adjustment is 94%.

- Joint Orientation

According to Laubscher (1990), rock mass behaviour is a function of the size, shape and orientation of an excavation. The stability of an excavation is significantly affected by the attitude of the discontinuities, and whether or not the bases of the blocks formed by the discontinuities are exposed. The joint orientation adjustment depends on the orientations of the joints with respect to the vertical axis of the block. The adjustment percentages are given in Table 11 (Laubscher, 1993).

Table 11: Adjustments for MRMR due to joint orientation (Laubscher, 1993)

Number of joints defining the block	**Adjustment (%) Number of faces inclined away from the vertical**				
	70	75	80	85	90
3	3	-	2	-	-
4	4	3	-	2	-
5	5	4	3	2	1
6	6	5	4	3	2 or 1

A shear zone or a fault can have a significant influence on stability. Adjustments applicable, with respect to the dip of the feature relative to the development, are 0° to 15° – 76%; 15° to 45° – 84%; 45°to 75° – 92%.

- Mining-induced stresses

The re-distribution of regional stress fields, due to mining activities, results in mining-induced stresses. Stress adjustments cater for the magnitude and orientation of the principal stress. Spalling, crushing of pillars and the plastic flow of soft zones can all be caused by the maximum principal stress (Jakubec and Laubscher, 2000). The stresses acting around the mining excavations influence the stability of those excavations. The adjustments for mining induced stresses are essentially based on judgement. Good confinement enhances stability and the maximum positive adjustment is 120%. Poor confinement, associated with numerous, closely spaced joint sets, does not promote stability, and the maximum negative adjustment is 60%.

- Effect of Blasting

Blasting creates new fractures, loosens the rock mass and causes movement along existing joints (Laubscher, 1990). The quality of blasting has an influence on the fracturing and loosening of the rock mass. Four excavation techniques are considered in applying adjustments to blasting: Boring, Smooth wall blasting, Good conventional blasting and Poor blasting.

Adjustments for blasting effects are given in Table 12 (Laubscher, 1993).

Table 12: Adjustments for Blasting Effects (Laubscher, 1993)

Excavation Technique	**Adjustment (%)**
Boring	100
Smooth wall blasting	97
Good conventional blasting	94
Poor blasting	80

The above adjustments are cumulative, being applied as multipliers to the MRMR. The MRMR result is used on the Haines-Terbrugge empirical design chart (Figure 31) to determine:

- The bench/wall height; and
- The Factor of Safety (FOS) of the wall being assessed

Acceptable design Factors of Safety are:

- Temporary wall (i.e. a wall that will remain static for a period not exceeding 1 year) = 1.2
- Permanent/Final wall = 1.5

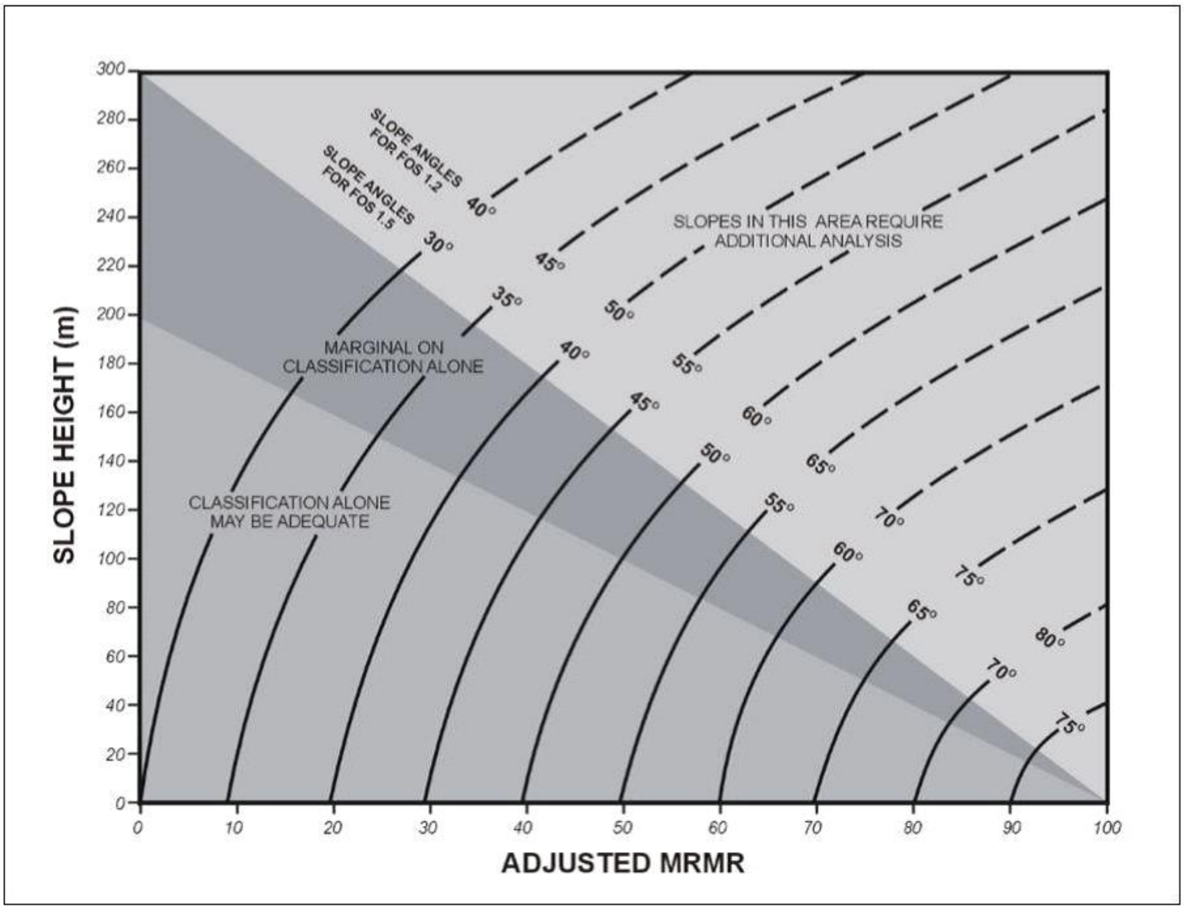

Figure 31: Empirical slope design chart (Haines and Terbrugge, 1991)

2.8.3 Numerical Modelling

All the geological, hydrogeological and mechanical data collected for the study allow the building of a geomechanical model of the rock mass, which will be used for numerical modelling using computational tools tailored to the mechanisms of deformation and failure identified above.

However, the contexts of modelling that first require clarity are particularly:

i. the geometric scales of the problem - stability of a single bench, a set of three, four, five benches, or the entire pit side, 100 m, 300 m, 600 m or more in height;

ii. the type of mechanical loading - short and medium term stability of slope during the mining operations phase, long-term stability of final pit slopes at the end of the mining operation and after rehabilitation processes, stability in extreme conditions (e.g. hazard studies) corresponding to specific hydraulic loading or specific dynamic loadings (earthquake);

iii. the accuracy of the geological, hydrogeological and geotechnical data collected for the study, which will always give partial knowledge of the real natural environment. In order to overcome the problem of accuracy in some datasets, it is necessary to perform a parametric analysis considering a realistic variation range for the poorly known parameters, and by comparing responses from the expected deformation and failure in the soil or rock masses.

After the definition of the problem, calculation of deformation and stability parameters can be undertaken. Factor of Safety calculations are based on the theory of limit equilibrium. The mechanical problem is simplified and the stability of the slope is defined using the concept of Factor of Safety (FOS) which is defined by the ratio between the maximum resisting forces or moments and the acting forces of moments along a potential failure surface. More O'Ferrall (2018) explained that, from a theoretical point of view, the slope is stable if the FOS is greater than one; but in practice, the theoretical level of safety must be adapted to the accuracy of the input data. For short-term stability analyses, safety factors of 1.2 to 1.3 would be acceptable, while for long-term stability, factors of safety usually range between 1.4 and 1.5. It is wise to perform these calculations using both average values of mechanical parameters and also lower realistic values. These latter values are always the basis of the design process.

2.8.3.1 Finite Element Analysis Method

In the finite element method, the so-called shear strength reduction (SSR) technique (Dawson et al., 1999) can be applied. The angle of dilatancy, soil modulus or the solution domain size are not critical parameters in the SSR technique (Ling and Cheng, 1997). The safety factor can be obtained, assuming a Mohr-Coulomb failure criterion, by reducing the strength parameters incrementally, starting from unfactored values $\phi_{available}$ and $c_{available}$, until no equilibrium can be found in the calculations. The corresponding strength parameters can be denoted as $\phi_{failure}$ and $c_{failure}$ and the safety factor η_{fe} is defined as:

$$\eta_{fe} = \frac{\tan \varphi_{available}}{\tan \varphi_{failure}} = \frac{c_{available}}{c_{failure}}$$

Equation 7

Duncan's (1969) review of the finite element (FE) analysis of slopes concentrates mainly on deformation rather than stability analysis of slopes; however, attention is drawn to some important early papers in which elasto-plastic soil models are used to assess stability. Taylor's (1937) charts presented results of $\phi_u = 0$ slopes. Zienkiewicz et al. (1975) consider a c', ϕ' slope and obtain good agreement with slip circle solutions. Griffiths and Lane (1999) extend this work to show reliable slope stability results over a wide range of soil properties and geometries as compared with charts of Bishop and Morgenstern (1960). Subsequent use of the FE method in slope stability analysis has added further confidence in the method (Griffiths and Lane, 1999). Duncan (1969) mentions the potential for improved graphical results and reporting utilizing FE, but cautions against artificial accuracy being assumed when the input parameters themselves are so variable. Zienkiewicz et al. (1975) give a useful summary of potential sources of error in the FE modelling of slope stability.

Advantages of the finite element method

The advantages of a FE approach to slope stability analysis over traditional limit equilibrium methods can be summarized as follows:

i. No assumption needs to be made in advance about the shape or location of the failure surface. Failure occurs 'naturally' through the zones within the soil mass in which the soil shear strength is unable to sustain the applied shear stresses.

ii. Since there is no concept of slices in the FE approach, there is no need for assumptions about slice side forces. The FE method preserves global equilibrium until 'failure' is reached.

iii. If realistic soil compressibility data are available, the FE solutions will give information about deformations at working stress levels.

iv. The FE method is able to monitor progressive failure up to and including overall shear failure.

2.8.3.2 Limit Equilibrium Method

Limit equilibrium methods are the most commonly used approaches in slope stability analysis. The fundamental assumption in these methods is that failure occurs through sliding of a mass along a slip surface. The reputation of the limit equilibrium methods is principally due to their relative simplicity, the ability to evaluate the sensitivity of stability to various input parameters, and the experience geotechnical engineers have acquired over the years in calculating the factor of safety. The assumptions in the limit equilibrium methods are that the failing soil mass can be divided into slices and that forces act between the slices, whereas different assumptions are made with respect to these forces in different methods. Some common features and limitations for equilibrium methods in slope stability analysis are summarized in Table 13. All methods use the same definition of the factor of safety:

$$FOS = \frac{Shear\ strength\ of\ soil}{Shear\ stress\ required\ for\ equilibrium} \qquad \text{Equation 8}$$

The factor of safety is the factor by which the shear strength of the soil would have to be divided to carry the slope into a state of barely stable equilibrium. The features and limitations of traditional equilibrium methods in slope stability analysis are in Table 13.

Table 13: Features and Limitation for Traditional Equilibrium Methods in Slope Stability Analysis (Duncan and Wright, 1980)

Method	Features and Limitation
Slope Stability Charts (Janbu, 1968)	• Accurate enough for many purposes. • Faster than detailed computer analysis.
Ordinary Method of Slices (Fellenius, 1927)	• Only for circular slip surfaces. • Satisfies moment equilibrium. • Does not satisfy horizontal or vertical force equilibrium.
Bishop's Modified Method (Bishop, 1955)	• Only for circular slip surfaces. • Satisfies moment equilibrium. • Satisfies vertical force equilibrium. • Does not satisfy horizontal force equilibrium.
Force Equilibrium Methods (e.g. Lowe and Karafiath, 1960, Army Corps of Engineers, 1970)	• Any shape of slip surfaces. • Does not satisfy moment equilibrium. • Satisfies both vertical and horizontal force equilibrium.
Janbu's Generalized Procedure of Slices (Janbu, 1968)	• Any shape of slip surfaces. • Satisfies all conditions of equilibrium. • Permit side force locations to be varied. • More frequent numerical problems than some other methods.
Morgenstern and Price's Method (Morgenstern and Price, 1965)	• Any shape of slip surfaces. • Satisfies all conditions of equilibrium. • Permit side force orientations to be varied.
Spencer's Method (Spencer, 1967)	• Any shape of slip surfaces. • Satisfies all conditions of equilibrium. • Side forces are assumed to be parallel.

2.9 Summary

Previous research that has been conducted concerning slope stability and the parameters that can influence it have been reviewed in this Chapter. Different authors have had different opinions over the years as research was carried out. The literature discussed was compared against the data collected.

The approach to rock slope analysis requires to be continuously updated as different failure criteria are discovered. It is possible for rock mass to display complex or hybrid failure modes and mechanisms. Authors such as Sjoberg (2000) express the possibility of the existence of unknown or poorly investigated mechanisms for higher and steeper slopes than those presently existing. Stacey (2007) further quoted several unexpected slope failures from several publications. It is therefore conclusive that the four common slope failure modes that have been used for many years as the basis of stability analysis and slope design are not sufficient to explain some of the failure mechanisms which have been recently encountered in different parts of the world.

From the literature collected, it is evident that rock mass properties play an important role in blast performance (fragmentation). The same rock mass properties play a pivotal role in the control of blast damage, particularly when it comes to perimeter walls. Lilly’s (1986) blastability index is equally affected by the same rock mass properties.

Read and Stacey (2009) contributed significantly to the research surrounding wall control blasting techniques. Their contribution has undeniably assisted many rock engineers to understand the correlation between rock type and expected blasting effects.

CHAPTER THREE

3.0 DATA COLLECTION

In order to reach the objectives stated in Chapter 1, information had to be collected and consolidated, tests had to be conducted on samples collected and validation of the samples and data collected had to be undertaken. The validation is intended to adopt model parameters that are not biased or tendentious, but instead should generate the most representative results of the data at hand.

The data acquired will be used in the kinematic stability assessment of the slope as well as improvement of the blast design.

3.1 Hydrogeology

Hydrogeological testing of boreholes at Sentinel Copper Mine was conducted by SRK Consulting Ltd. The hydrological testing in the phyllite units mainly included packer testing. Airlift pumping and recovery testing was done on other boreholes in the other rock types but not in the phyllites. The cores at which hydrogeological testing was conducted were drilled for geotechnical purposes and not drilled to specifically target any features associated with the occurrence of groundwater.

The objective of the hydrogeological testing was to estimate the hydraulic conductivity of various intervals intersected at different boreholes. This information would later be used by the mine for updating the site groundwater numerical model. A similar exercise was conducted in 2013 and the results of the current hydraulic conductivity were compared to those from 2013 as can be seen in Table 14.

Table 14: Comparison of hydraulic conductivity results - 2013 vs 2017

Hydrostratigraphic unit	**Hydraulic conductivity range (m/d)**		**Average hydraulic conductivity (m/d)**	
	2013 study	**2017 study**	**2013 study**	**2017 study**
Saprolite	5.0×10^{-2} to 5.0×10^{0}	7.7×10^{3} to 9.4×10^{-2}	N/A	4.1×10^{-2}
Sentinel phyllite	1.0×10^{-3} to 5.0×10^{-1}	1.6×10^{-3} to 3.4×10^{-1}	3.0×10^{-2}	5.2×10^{-2}
Northern schist	1.0×10^{-4} to 4.0×10^{-3}	Not tested	2.0×10^{-3}	Not tested
Southern schist	3.0×10^{-1} to 5.0×10^{0}	Not tested	2.5×10^{0}	Not tested
Meta-carbonate	4.5×10^{-3} to 2.0×10^{-2}	Not tested	8.2×10^{-3}	Not tested

Derived hydraulic conductivity values in the phyllite range from 1.6 x 10^{-3} m/d at borehole number KALGT0027 in the central area of the pit to 3.4 x 10^{-1} m/d at borehole number KALGT0024 at the southeast of the pit (Figure 35). The obtained upper limit K value in the phyllites is slightly on the higher side. Comments on the hydraulic conductivity values being low, medium or high are relative and adopted from Itasca Denver (2012). The universal values are based on Freeze and Cherry (1779). Values of K less than about 1x 10^{-3}m/d are generally not measurable or quantifiable in the field using standard testing equipment. K value decreases with depth. SRK summarized the hydrogeology of the Sentinel Pit area described by Schlumberger Water Services (2013) as follows:

- The pre-mining ground water elevations in the pit area ranged from 1185 to 1225 m above mining sea level (mamsl), with the groundwater levels ranging between 2.3 and 12.5 m below ground level (mbgl). In general, groundwater flows from the NE towards the SW across the sentinel deposit and reflects the fall of the ground surface towards the Musangezhi River. The average hydraulic gradient of the ground water system in the area of the deposit is 0.3 to 0.5%.

- Artesian conditions were noted between February and August indicating discharge conditions during this period, and there seemed to be a local effect associated with the low permeability characteristics of the wetlands and the intersection of the groundwater table with topography.

- The recharge rate of the groundwater system is still undetermined. However, the recharge rate assumes a range of between 5% and 30% of the annual average rainfall. For the catchment area upstream of the deposit (258 km^2), recharge would be on the order of 0.5m^3/s to 3.3m^3/s. For the catchment area downstream of the Musangezhi dam and on the western edge of the Sentinel deposit, groundwater recharge would be in the order of 0.13m^3/s to 0.78m^3/s.

3.1.1 Packer testing

The conventional double packer assembly with a fixed 1 m test interval was used to test the boreholes listed in Table 15. The test intervals selected were all inferred fractured zones identified from the core. When the test sections were determined and the packers set in place, water was injected under predetermined pressures into the rock formation. The pressures and water flow into the rock formation were recorded at predetermined time intervals. Pressure and flow rates were used to calculate the hydraulic conductivity, K using the Thiem equation given by the formula:

$$K = \left(\frac{Ln\left(\frac{R}{r}\right)}{2\pi L}\right)\frac{\Delta Q}{\Delta P}$$

Equation 9

Where:

R = radius of influence (m)

r = radius of the borehole (m)

L = Length of the test section (m)

Q = Injection rate (m^3/d)

P = net injection pressure (m H_2O)

Table 15: Packer testing borehole (SRK Consulting, 2018)

Hole ID	X-Coordinate (m)	Y-Coordinate (m)	Elevation (mamsl)	Orientation (˚)	Depth (mdh)
KALGT0024	317385.3	8643898.5	1222.0	-90	120
KALGT0025	316220.8	8644104.5	1172.7	-90	120
KALGT0026	316799.3	8643758.8	1223.8	-90	120
KALGT0027	312330.0	8644471.0	1110.6	-65	80
KALGT0028	315404.9	8644207.9	1112.3	-60	80
KALGT0029	317284.4	8644267.8	1221.6	-70	83
KALGT0030	317309.6	8644265.5	1221.7	-70	70

Figure 32 shows the positions of the drilled boreholes, including the ones in Table 15, in the Sentinel pit (SRK Consulting, 2018)

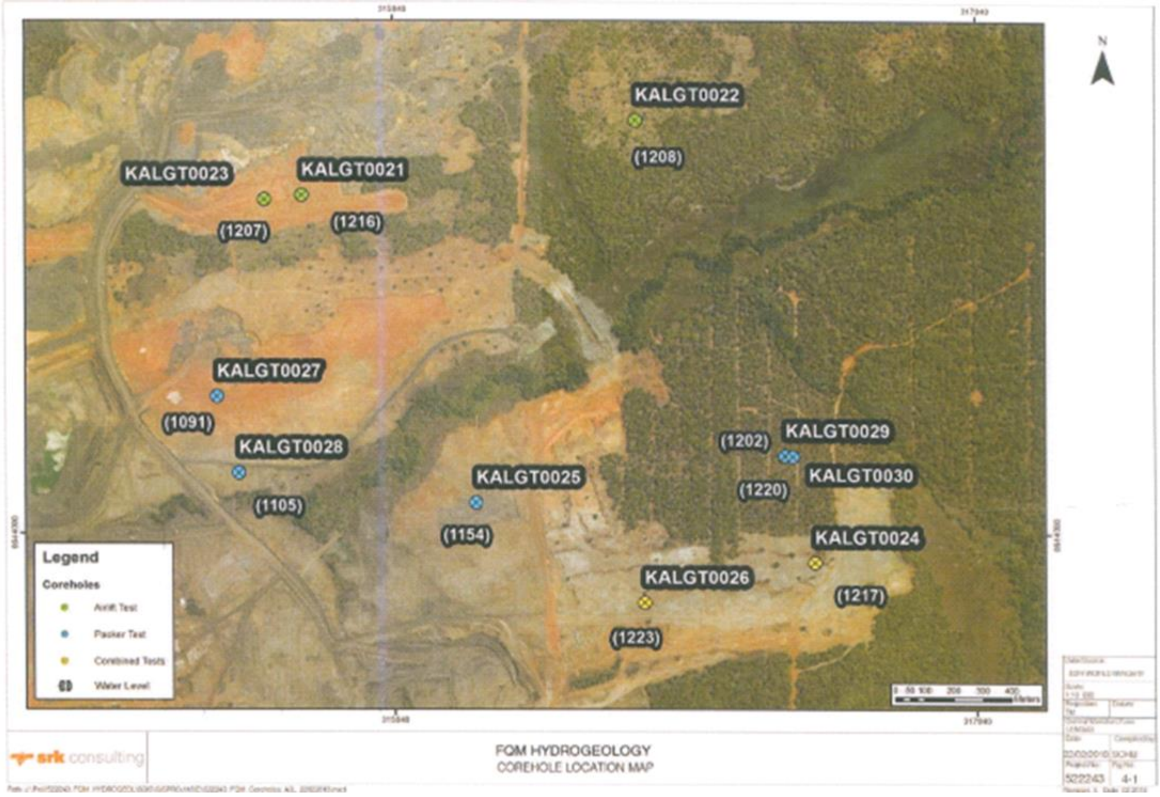

Figure 32: Position of the drilled boreholes in the Sentinel pit

3.2 Geotechnical core logging

Two boreholes were drilled in the phyllites close to the western wall for UCS computation. Six specimens were picked from each of the boreholes and used in the evaluation of deformation properties of the rock. The rock sample was loaded at 1KN/s until failure. The average dimensions of the samples KALGT27 and KALGT28 are tabulated below. The height to diameter ratio of specimens was between 2.5 - 3 as recommended by the ISRM Committee (1979).

The closest of the boreholes to the western wall being KALGT0027 yielded an average UCS value of 120 MPa and a Poisson's ratio of 0.24 GPa at failure. The rest of the individual sample information is included in Appendix C.

Table 16: Results of uniaxial compression tests with elastic modulus and Poisson ratio

Sample ID	Diameter mm	Height mm	Ratio of Height to Diameter	Mass g	Density g/cm³	Failure Load kN	Strength (UCS) Mpa	Tangent Elastic Modulus @50% UCS Gpa	Secant Elastic Modulus @50% UCS Gpa	Poisson's Ratio Tangent @50% UCS	Poisson's Ratio Secant @50% UCS	Linear Axial Strain at Failure mm/mm	Failure Mode
KALGT27	60.77	161.10	2.70	1319.00	2.82	350.00	120.87	56.30	57.40	0.24	0.20	0.002390	Shear
KALGT28	60.77	160.90	2.60	1287.00	2.76	249.70	86.10	44.60	40.90	0.22	0.16	0.002210	

3.3 Rock Mass Classification

Geotechnical data on the West Wall of the Sentinel pit was collected by conducting geotechnical wall mapping in order to provide geological structure data for input into the Rock Mass Classification systems.

All Rock Mass Classification systems consider a few of the key rock mass parameters and assign numerical values to the classes within which these parameters lie for a given rock type. These systems provide guidance for engineering design and also provide a simple way of describing the rock mass properties that are difficult to assess e.g. the prediction of rock mass strength and deformability. Three Rock Mass Classification systems discussed earlier in Chapter 2 were deemed to be adequate for the study i.e. Bieniawski's Rock Mass Rating (Bieniawski, 1989), Laubscher's Mining Rock Mass Rating (Laubscher and Jakubec, 2001) and Barton's Q-system (Barton, 1993).

The wall was divided into three different windows and mapping was done according to the three windows. These window mapping sheets as well as images are included in Appendix D.

Calculation of RMR for window 1

RMR = Rock strength + spacing rating + RQD + Joint condition rating + Joint water + orientation adjustment *Equation 10*

RMR = 7 + 15 + 8 + 25 + 7 + (-5) = 57

The average RMR according to Bieniawski is 57.

The adjusted MRMR according to Laubscher is 35. Computation of the MRMR is shown in Equation 11. From the adjustment tables, adjustments of weathering was taken as 82%, 85% for joint orientation, 110% for mining induced stresses, and 80% for blasting effects.

Adjusted MRMR = RMR_{89} x Adjustments (weathering, Orientation, Stress and blasting effects) *Equation 11*

Adjusted *MRMR* = 57 x 0.82 x 0.85 x 1.1 x 0.8 = 35

Results of scanline and window mapping of the walls as well as geotechnical core logging are used to determine the MRMR.

Barton's Q system

$Q = RQD/J_n \times J_r/J_a \times J_w/SRF$ *Equation 12*

Q = 10.617

GSI = 55 - 60

All the classification system's ratings are showing that this is fair to good rock (refer to Tables A-1 to A-3 in Appendix A).

Rock Mass Characterization of the western final wall was conducted using the Geological Strength Index which utilizes average values of rock mass strength for jointed rocks which are estimated from visual assessment. The visual assessment considers the lithology, structure and surface conditions of the discontinuities.

3.4 Geologic Structural Mapping

Geologic structural data was collected using a Gekom Pro-stratum compass, which measures the orientation (dip and dip direction) of a geological structure. Field strength estimates, making use of a geological hammer, were conducted to determine the strength of the rock comprised on the west wall (based on the number of blows from a geologic hammer a rock can sustain before failure).

3.4.1 Geotechnical Data Analysis - Scanline Survey

According to the scanline mapping conducted on the Sentinel Mine West wall, the outcrop phyllite can be described as very hard to extremely hard rock varying between R4 to R5 i.e. a uniaxial compressive strength (UCS) ranging between 50MPa – 250MPa (i.e. requiring multiple blows with a geologic hammer to fracture) as indicated by the blue box in Figure 33.

Grade	*Description*	*Field identification*	*Approx. range of uniaxial compressive strength (MPa)*
R6	Extremely strong rock	Specimen can only be chipped with geological hammer.	>250
R5	Very strong rock	Specimen requires many blows of geological hammer to fracture it.	100–250
R4	Strong rock	Specimen requires more than one blow of geological hammer to fracture it.	50–100
R3	Medium strong rock	Cannot be scraped or peeled with a pocket knife, specimen can be fractured with single firm blow of geological hammer.	25–50
R2	Weak rock	Can be peeled by a pocket knife with difficulty, shallow indentations made by firm blow with point of geological hammer.	5.0–25
R1	Very weak rock	Crumbles under firm blows with point of geological hammer and can be peeled by a pocket knife.	1.0–5.0
R0	Extremely weak rock	Indented by thumbnail.	0.25–1.0
S6	Hard clay	Indented with difficulty by thumbnail.	>0.5
S5	Very stiff clay	Readily indented by thumbnail.	0.25–0.5
S4	Stiff clay	Readily indented by thumb but penetrated only with great difficulty.	0.1–0.25
S3	Firm clay	Can be penetrated several inches by thumb with moderate effort.	0.05–0.1
S2	Soft clay	Easily penetrated several inches by thumb.	0.025–0.05
S1	Very soft clay	Easily penetrated several inches by fist.	<0.025

Figure 33: Field estimates of uniaxial compressive strength of intact rock

Following the scanline survey, the highwall can be described as slightly weathered to unweathered (fresh) with linear macro joints consisting of sporadic iron staining surfaces. Furthermore, micro joints slightly undulate with soft infill material and rough or irregular joint surface conditions. This maybe a result of the water flowing along the joint planes on the south end of the wall (Figure 35).

Gray et al (2015) in the Trident project brief (NI-43101) described the geometry of the host phyllite as recumbent, typically asymmetric, folds and several detachments that truncate the lower limbs of these folds. The phyllite is terminated to the northeast by the northwest-southeast trending Kalumbila Fault and to the south by a sub east-west cross-cutting structure, thought to be a detachment surface. The S-shape surface expression of the phyllite is indicative of non-cylindrical folding, likely resulting from differences in speeds of transport along the fold axis during progressive deformation within the shear environment.

Figures 34 and 35 are photographs of some portions of the mapped wall on the 1112 reduced level (RL).

The foliation on the northern side of the western wall and southern side differ slightly due to the undulation of the foliation as is evident from the scanline survey conducted.

Figure 34 indicates a small portion of the mapped area on the West wall (north), whose foliation dips at 42° and dip direction being 346°. The face angle at the point indicated is 76°.

Figure 34: Main face orientation on the northern side: Strike = 297° and Dip = 76° East

Generally, the predominant geological structure on the south side of the West wall (Figure 35) indicates foliation dipping 30° towards north with the dip direction being 348°.

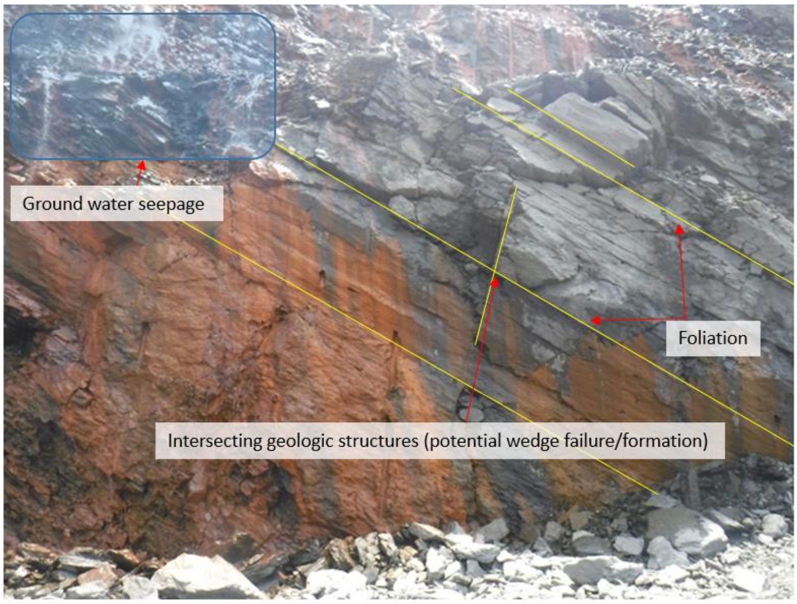

Figure 35: Photograph taken from the southern side of the western wall showing Strata (foliation) dipping 30° towards the north

For the wall to yield favourable results after pre-splitting, the joints must intersect the face at greater than 30°. Anything less will cause fractures to intersect the jointing planes having large pieces of material fallout from the face during scaling of the wall. Figure 36 is a typical example of material falling out from the face during scaling of the wall. This is slightly in agreement with what Gray et al. (2015) discussed in the Trident project brief (NI-43101). The project brief mentioned that the dominant foliation dips towards north-northwest, at an average of 20-30°, typically parallel to the fold axial plane of the pervasive drag folds. These low foliation angles are more evident on the southern side of the western wall and the southern wall itself. The recumbent folding, detachments, and dominant foliation are likely expressions of top-north directed shearing. Both low-angle thrusting along detachment horizons and shear-related folding are evident in the phyllite stratigraphy at Sentinel.

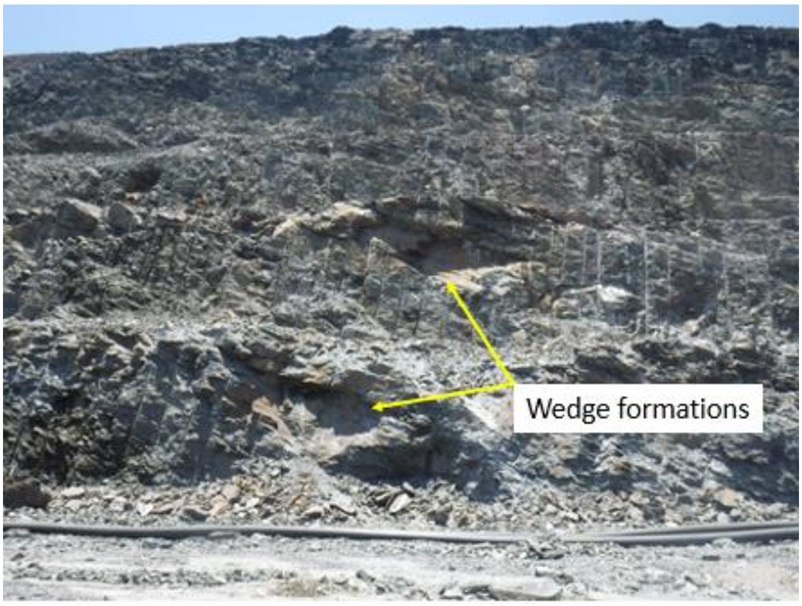

Figure 36: Dislodged blocks of rock during scaling of the bench faces

The foliation of the wall and random joints intersecting tend to result in wedge formations or wedge failures after satisfaction of the conditions of wedge failure formation as discussed in Chapter 2. The weakness planes forming wedges are easily dislodged during scaling of the highwall.

3.5 Kinematic stability analysis

Instabilities of benches are generally associated with geological structure, including relict structures i.e. in the saprolite and laterite benches. These instabilities take the form of circular, planar, wedge, flexural and direct toppling, multi-causal and rotational failure; all associated with geological structure.

The kinematic stability analysis conducted on the West wall indicates a low potential for instability. Table 17 shows the kinematic property assumptions used for the analysis:

Table 17: Kinematic stability analysis properties

Kinematic Properties	**Unit (Degrees)**
Friction Angle	30
Lateral limits	20
Sets from cluster analysis (cone radius)	30

Table 18 shows the results of the kinematic stability analysis conducted on the wall with the probability of failure expressed as a percentage. The dip and dip directions obtained from the scanline survey comprised the input parameters of the kinematic stability analysis. Dips v7.0 was the software that was used for the analysis.

Table 18: Probability of failure expressed as a percentage

Failure mode	Probability of Failure
Planar sliding	0.00%
Wedge sliding	6.31%
Direct toppling	15.44%
Flexural toppling	4.69%

According to the kinematic stability analysis conducted on the wall, the most probable mode of failure is by direct toppling. The least probable mode of failure is through planar sliding, which is evident through visual assessment (visual assessment suggest having no visible planes daylighting on the slope face to result in any possible planar failures).

Refer to Appendix B for the contour plots of the kinematic stability analysis. The input parameters for kinematic stability analysis, specifically the slope dip of 49 degrees was attained using Surpac software, by way of measuring the inter-ramp angle of the as-built geometry, from the top most bench on the west wall (1191 RL crest) to the elevation where the scan line mapping was conducted (1112m RL). The phyllite host rock which constituted the mapping area was observed to have two prominent joint sets: foliation (shallow dipping foliation towards the north i.e. dips between 20 degrees - 40 degrees) and the other dipping at 88 degrees 359 dip direction as well as random joints. Joint spacing/defect spacing for the predominant foliation ranges between 0.3m to 1m with the second joint set defect varying between 1m to 3m. Assumption of the kinematic properties are due to a lack of information.

The kinematics has shown slight back break due to the foliation coupled with poor drilling/blasting practices and potentially development of wedge instabilities which results in loss of the berm width. Based on the wedge analysis, the as-built inter-ramp slope of 49 degrees poses a 6.31% probability of failure. With good controlled blasting practices, the inter-ramp angle wedge formation and dislodging risk may potentially be reduced.

3.6 Blasting

The geology of the final West Wall (foliation dipping 30° towards north), when damaged by blasting, result in rock slippage along the planes and crest failures on each bench. This consequently results in reduced or missing catchment berms, which increases the risk of major wall failure.

Although the rock seems bedded, the bedding planes are bonded. There is however a need to prevent failures of the bonding between the bedding planes, caused by blast induced shock waves and high-pressure gas penetration. If the integrity of the bedding planes can be maintained, the risk of failure along the final wall will be significantly reduced.

Wall control blasting techniques currently employed on the western wall include presplitting and trim blasting. A few blast audits were conducted on the trims and presplits on the western wall. Table 19 shows a summary of the audited parameters. 32mm diameter cartridges (splitex) continuously coupled onto a detonating code are used in 140mm diameter presplit holes. These are tied to a 5 grams detonating code on surface for initiation purpose. Extracts from the presplit audits conducted are included in Appendix H showing deviation per hole audited.

Table 19: Presplit audited parameters

	Number of hole Depths measured	Number of holes deviated	Deviation %	Number of hole spacings measured	Number of holes deviated	Deviation %
Audit 1	102	32	31	101	30	30
Audit 2	92	14	15	90	31	35
Audit 3	125	91	73	98	32	33
Audit 4	142	38	27	141	40	29
Average % Deviation			**36**			**31**

The pre and post blast photographs of the presplits are shown in Figures 37 to 40 with more photographs included in Appendix H. The results of some of the splits was crushing at the collar of the holes, overbreak and toes on the catchment berm. Generally, the west wall has suffered significant back break on the 1112 RL compromising the arresting capacity of the berm. The sentinel phyllite unit exhibits a moderate to high permeability on the south west corner of the pit. The observed aquifer is identified from the visible iron staining, slightly visible water seepage and water percolation on figure 37. For wedge instabilities to be kinematically possible, one of the three criterions discussed in Chapter 2.3.2 must be met. The water seepage on the wall assists in inducing release of the wedge.

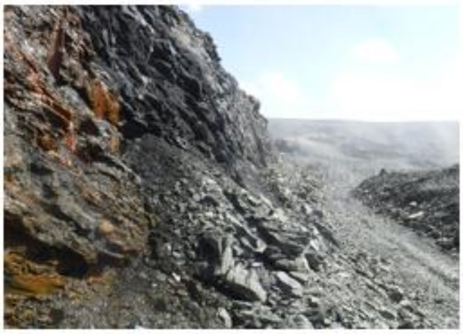

Over break of the wall during excavation

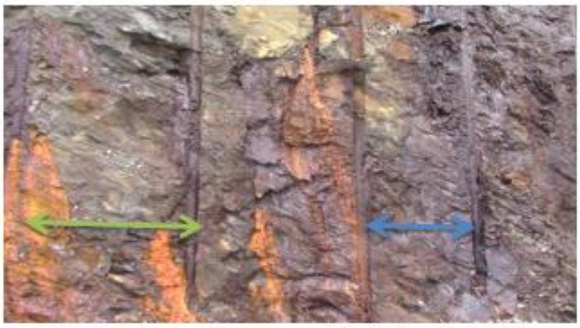

Spacing inconsistency and deviation in drilling

Wedge failure- Effect on geological discontinuity

Toe burden not blasted caused by poor charging or poor drilling

Figure 37: A few examples of poor presplit results on the western wall

Figure 38: photographs of the western wall from the northern perspective

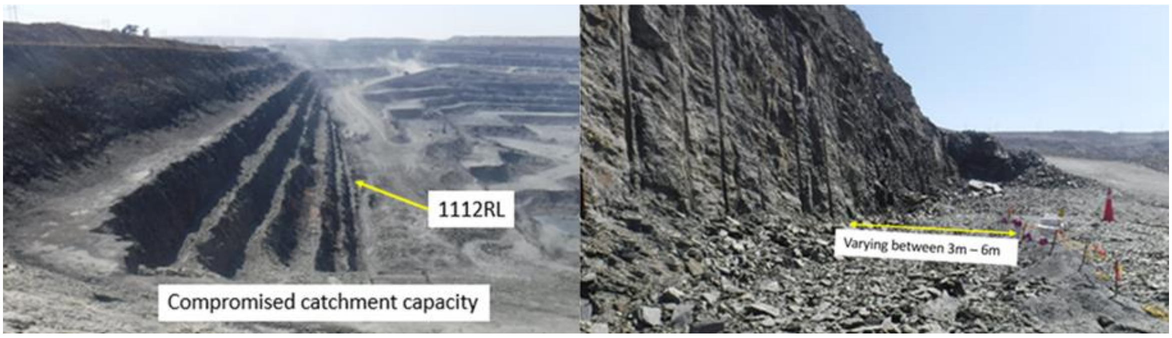

Figure 39: Photographs of the western wall from the southern perspective

Figure 40: Poor pre-split blast on the 1112 RL

Below were the findings of the audits (possible causes) on the contributing factors to the poor quality presplits

- Standoff of trim blast back line from presplit holes
- Initiating presplit together with trim blast (post splitting)
- Drilling deviation visible on some portions of the wall
- Some holes were lost and some were recorded as short holes after measurement (Most holes in water logged areas were collapsing)
- Decoupling ratio of the explosives in the presplit holes

3.6.1 Blast induced ground vibrations

Ground vibrations and air over pressure levels were measured for a few blasts on the 1112 level which comprised the trim and presplit. A seismograph was instrumented for a few blasts (within a 50m radius from the splits and 36m above blast elevation near the power substation – see Appendix F) for near field measurement of blast induced ground vibrations. The maximum peak particle velocity recorded from the measured blasts was 48.26mm/s at 17.6Hz and a maximum air over pressure of 148dB at 34.1Hz was measured. The rest of the results are presented in Table 20.

Table 20: Near field blast induced ground vibration measurements

Block ID	Radial		Vertical		Transverse		Acoustic	
	PPV (mm/s)	Freq (Hz)	PPV (mm/s)	Freq (Hz)	PPV (mm/s)	Freq (Hz)	PPV (dB)	Freq (Hz)
000_013	16.256	42.6	13.589	30.1	15.748	18.2	140	23.2
000_003	22.182	30.5	16.261	21.2	19.621	17.8	142	28.3
000_011	42.672	16.0	43.688	34.1	48.26	17.6	148	34.1

3.6.2 Blastability Index

A blastabilty index of the rock mass was calculated using average values as collected through the mapping exercises conducted along the wall.

BI = 0.5 x (RMD+JPS+JPO+SGI+H) (Lilly, 1986) *Equation 13*

BI= 0.5 x (20+30+30+10+3)

BI = 46.5

A BI value of 46.5 according to Christaras and Chatziangelou (2014) is indicative of the rock being very easy to blast.

3.7 Summary

The data collected from the field which is useful in the kinematic stability analysis as well as overall slope stability analysis was presented in Chapter 3. Standard industry practices were used for the data collection. Even though standard industry practices were used, most of the assessments are dependent on the expertise of the Engineer and are a conversion from a qualitative description to a quantitative one. It is critical for the Engineer conducting the data collection exercise to be knowledgeable on the subject matter.

Hydrogeological data, geotechnical data and blasting data were collected from the field. Even though there is water seeping through the wall, the geotechnical core logging conducted as well as rock mass classification are indicating that the wall is fairly competent. However, it is when blasting is introduced that the cementing between the discontinuities is weakened. The blasting audits conducted on the presplits further indicate that apart from the analysis of the drill and blast design, the execution of the design in the field is not in agreement with the design itself.

The biggest issue when it comes to the execution of the drill and blast design is the presence of the water which causes collapsing of some holes as soon as the drill retracts the drill rod from the hole. The audits conducted at the mine brought several operational inconsistencies to the fore that were suspected to contribute to the problem experienced by the mine. Operational discipline in the execution of drilling and blasting plans is important, but it is preceded by understanding and application of the rock mass fundamental inputs at the design stage.

A combination of the foliation as well as the presence of water and an additional influence of poor blasting practices is the source of the failure. If these had to occur in isolation, the wall would not have been that unstable. Drill and blast designs should therefore be adjusted to account for the source of the failure until a stable wall with a clean cut presplit is attained. It was concluded that data that is collected periodically at the mine can be used to establish meaningful relationships between rock mass characteristics and effects of designs using rock mass classification as a medium.

CHAPTER 4

4.0 PROPOSED BLAST DESIGN

The only controllable variable amongst the parameters affecting slope stability discussed in the earlier Chapters is blasting. The mining rock mass rating (MRMR) assumes a degree of blast induced damage. It has been observed that the rock mass on the western wall is stable and cemented before the introduction of blasting. A design which takes into cognizance the blasting techniques, discussed in sections 2.6.1, 2.6.2 and 2.6.5, could assist in preserving highwall stability. It is important not to overlook the existence of prominent geological structures which tend to terminate the developing split and spoil the end effect.

Following the findings of the blast audits in Chapter 3, the implication might be that the presplit design and blasts are working, evident in portions where the presplit audited parameters scored very high ratings. However, the damage to the layers in the footwall rock is being caused by the trim blasts.

4.1 Presplit design

Drilling

It is recommended to maintain the current presplit design parameters as listed in Table 21. An emphasis should be placed on the quality control and ensure improvement of the parameters that directly affect the results of the split. The hole diameter was pre-determined as 140mm, as this is the smallest blasthole drill at the mine. A presplit powder factor for hard rock, of not less than 0.6kg/m^2 was used as a guide for calculating the spacing. The spacing was calculated at 11 times hole diameter. Furthermore, if the presplit is to be blasted together with the trim blast pattern, it is recommended to introduce a buffer row before the presplit with a smaller burden.

Charging

The conclusion is that the currently applied 32mm x 600mm splitex cartridges have increased the decoupling ratio. Consideration should be given to trial 50mm x 580mm cartridges coupled on 10g detonating code due to the calculated borehole pressure for this cartridge size.

Table 21: presplit parameters

	Planned
Spacing (m)	1.6
Hole Depth (m)	13.2
Hole Orientation (°)	80
Charge Mass per hole (kg)	14.18
Hole Diameter (mm)	140
Borehole pressure (MPa)	110
Split factor (kg/m^2)	0.68

The decoupled borehole pressure referred to in table 21 can be estimated using the following equation:

$$Pb = 1.255\ \rho V^2 \left(\sqrt{c}\frac{De}{Dh}\right)^{2.4}$$ *Equation 14*

Where Pb is the decoupled borehole pressure in MPa, ρ is the explosive density in g/cm³, V is the velocity of detonation (VOD) of the explosive in m/s, *c* is the percent explosive in a hole as a fraction = (Length of explosive)/(Length of hole), *De* is the diameter of explosive in mm and *Dh* is the diameter of hole in mm.

With 50mm x 580mm cartridges, the calculated borehole pressure is 105 MPa which is greater than the tensile strength but less than the UCS of the rock. The UCS of the rock is 120 MPa and the tensile strength is calculated as 12 MPa. This then satisfies the condition $T<Pb\leq UCS$. Energy that exceeds the compressive strength of the rock will cause counter-productive crushing damage to the wall; particularly at the hole collar where confinement is reduced.

Parallel geological structures (joints) act as points of least resistance, to which the excavation tends to break regardless of the pre-split. Further adjustments to the split design should be considered in cases where geology has a large effect.

4.2 Trim blast designs according to rules of thumb

Trim blasting should be a norm or standard whenever blasting close to the western wall. Rules of thumb were used to come up with the trim blast parameters listed in Table 22. These parameters can then be adjusted until favourable results are achieved. The width of the trim blast should be restricted to 2.5 times the bench height. A recommendation of trim blast parameters per row is shown in Table 22.

Table 22: Trim blast parameters for the different rows

Trim Blast Design									
	Row 1	Row 2	Row 3	Row 4	Row 5	Row 6	Row 7	Row 8	Row 9
Bench Height (m)	12	12	12	12	12	12	12	12	12
Batter Angle (Deg)	80	80	80	80	80	80	80	80	80
Hole Diameter (mm)	140	140	140	140	140	140	140	140	140
Hole Depth (m)	12	12	12	12	14	14	14	14	14
Sub-drill (m)	0	0	0	0	2	2	2	2	2
Offset from top of batter (m)	2.5	2.6	2.6	3.5	3.5	3.5	3.5	3.5	3.5
Burden (m)	2.6	2.6	3.5	3.5	3.5	3.5	3.5	3.5	3.5
Spacing (m)	3	3	4	4	4	4	4	4	4
Charge Length (m)	7	7	7	7	10	10	10	10	10
Charge Diameter (mm)	140	140	140	140	140	140	140	140	140
Air Deck Length (m)	1	1	1	1	0	0	0	0	0
Stemming Length (m)	4	4	4	4	4	4	4	4	4
Powder Factor (kg/m3)	1.29	1.29	0.88	0.88	1.1	1.1	1.1	1.1	1.1

BME’s wallpro software was used for the analysis of blast impacts. The software works on the Holmberg–Persson approach in the attenuation of blast waves in the rock mass, consequently giving an insight into what the rock mass may be experiencing during the blasting process. Holmberg and Persson (1980) models blast wave attenuation by defining two site specific constants (K and α). The approach further requires the measurement of peak particle velocity at several locations resulting from a known explosive source.

The wallpro software works under the following assumptions:

- A radiating blast wave obeys charge weight scaling laws.
- The peak particle velocity due to each small element of charge within the blast hole is numerically additive.
- For practical purposes, the velocity of detonation (VOD) of the explosive charge is neglected.
- the effect of free face boundaries is also neglected.
- For damage assessment purposes, it assumes that PPV is proportional to the dynamic strain experienced by the rock mass.

When the parameters in Table 22 are input into BME’s wallpro software, it generates a visual output with contour levels in mm/s (Figure 41). The main aim of this revised design will be to prevent opening of the bedding planes through high vibration amplitudes and high pressure gases entering the bedding planes as well as minimising footwall and back damage based on a damaging vibration limit of 1500mm/s. This is achievable by adjusting the trim drilling design as well as its timing. A collar standoff of 2.5m from the presplit is required. The first four rows of holes from the highwall have an air deck at the toe of the hole.

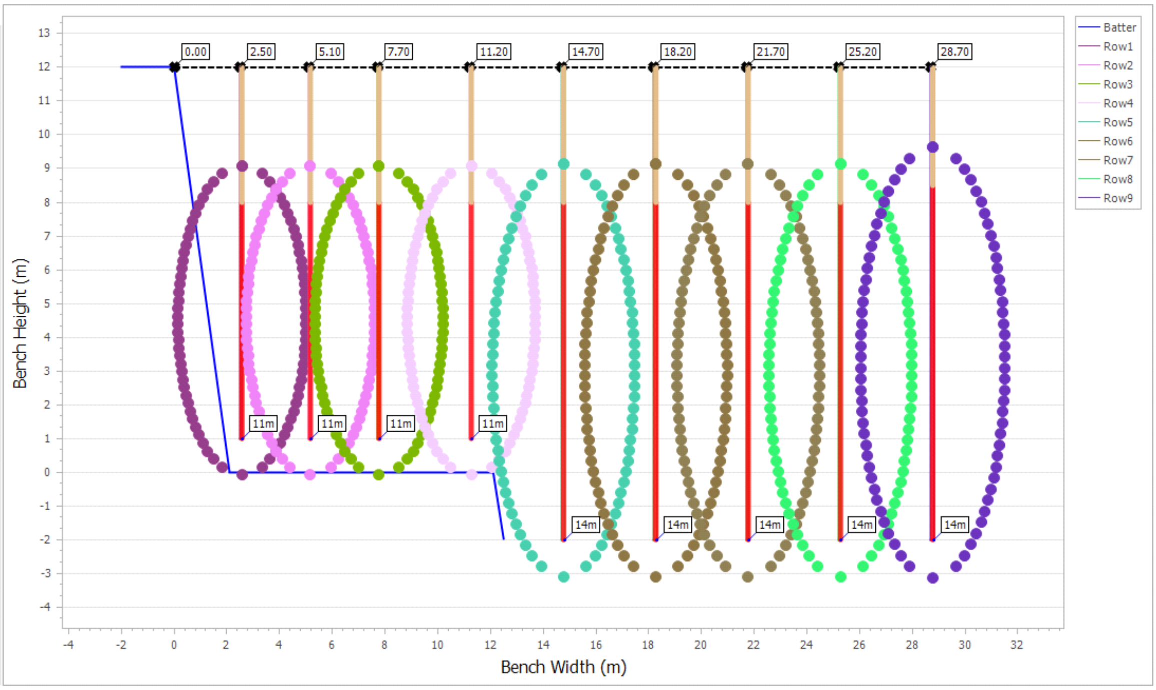

Figure 41: Trim blast design simulation from BME's Wallpro software

The vibration contours for the design are presented in different colours for each line of holes (Figure 41). The cross-section shows 1500mm/s contour curves for each line of holes. The contours are based on the Holmberg and Persson (1980) near field vibration estimates and on charge mass, charge location and hole length. The wallpro software model is unable to simulate bottom air decks in its calculations, so the scenario has been estimated by modelling the first four rows as shorter holes. On the portion above the berm of the subsequent bench, the solid rock replaces air in the hole bottoms thus transferring shock more efficiently. This will then result in less hole bottom damage. If an option of dewatering the holes exists, water should be removed in any of the holes in the back four rows of the trim blast before charging commences. Water will negate the effect of the bottom air decks as it will transfer shock energy efficiently.

A proposal of a timing design is given in Figure 42, yielding wide breakage angles for highwall control as can be seen in Figure 43. The timing design assumes an ideal case of two free faces. The material will be cast in a direction orthogonal to the contours generated by the timing design. The timing configuration needs to allow for relief and promote horizontal displacement away from the highwall. Obtuse (wide) breakage angles or acute (low) angles of displacement for the holes along the blast perimeter are essential for wall control.

The application of longer delays within a blast promotes progressive formation of new free faces for the following rows as the blast progresses and consequently promotes highwall stability. This creation of new free faces is termed as burden relief, which can also be defined as the creation of sufficient void volume into which the burden can move and expand. Prout (2015) states that typical intra row timing delay should lie in the range of 3ms/m to 6ms/m of burden for hard and soft rocks respectively, while inter row delay values should range between 10ms/m and 30ms/m of burden for hard and soft rocks respectively. The empirical figures suggested by Prout serve as a means of estimation in the absence of rock response data. Ideally, the minimum rock response time (Tmin) for that particular rock mass would have to be determined in order to establish the most suitable timing. The rock mass is relatively hard rock, however, for highwall control, engineering judgement is necessary. Therefore, delays of 5ms/m of burden and 11ms/m of burden will be used for intra row and inter row timing respectively. This translates into intra row delay of 20ms and inter row delay of 44ms with an incremental inter row delay towards the highwall as applied in figure 42. This recommendation of longer inter row timing will be easy to implement as the mine uses electronic delay detonators which are fully programmable, flexible and precise, suited for any timing complexity.

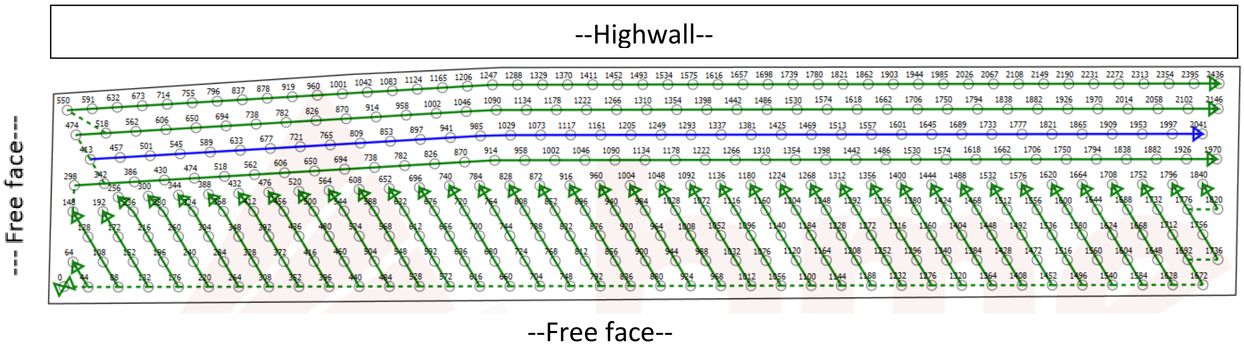

Figure 42: Proposed timing design simulated using BME's Blastmap software

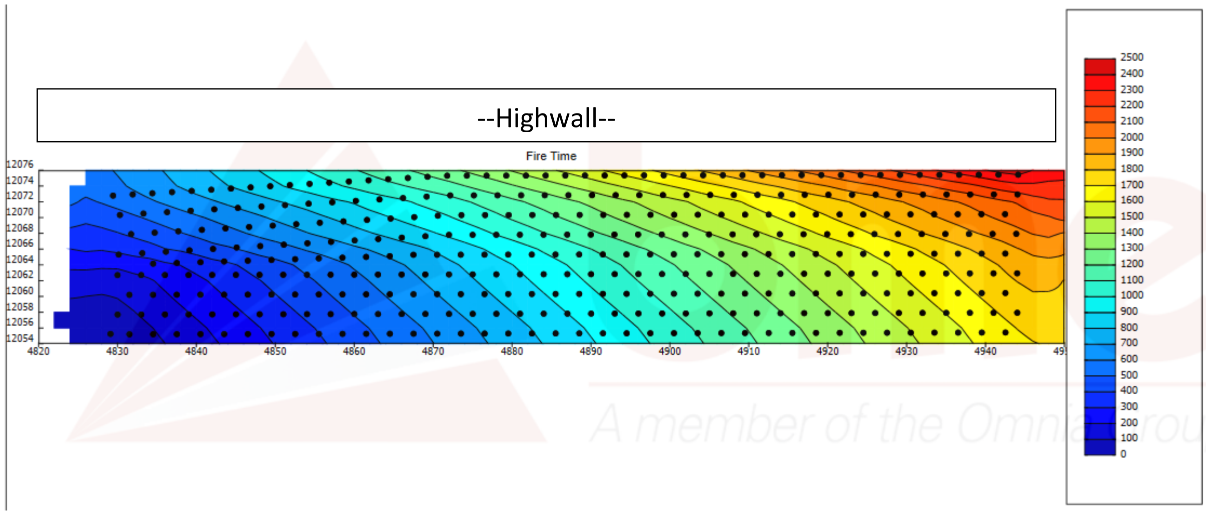

Figure 43: Contours indicating direction of throw of the material

The beginning and ends of the blast should be angled to reduce confinement along the highwall. Blasting direction is very critical. The joint orientation of the dominant structure influences the amount of overbreak produced. Blasting against the direction of the dominant joints presses the joints together and limits back damage whereas blasting in the same direction as the dominant jointing rips the joints apart. The initiation point of a pattern should be on the end where the dip direction is oriented towards. The direction of fire should be in the opposite direction to the dip direction.

4.3 Summary

The design proposals made in Chapter 4 are conservative and more adjustments are required as more rock mass information comes available.

Ultimately, drilling smaller diameter holes on trim blasts improves the energy distribution within the trim block while reducing the energy directed towards the highwall per delay (charge mass per delay).

The author believes that problems that face blasting engineers in many instances are the lack of rock mass information to aid in analyses and the tendency of having generic blast designs across varying rock strata. The proposed drill and blast designs should be seen as guidance without ignoring the engineering judgement following careful field observations, and alterations following results obtained.

CHAPTER 5

5.0 CONCLUSIONS AND RECOMMENDATIONS

5.1 Conclusions

The evaluation of slope stability in heavily jointed rock mass is always very challenging especially if other factors such as geological structures, presence of groundwater and blasting are in play. These factors have a significant influence on the stability of a slope.

Hydrogeological testing (Packer and airlift tests) was conducted by SRK Consulting to estimate the hydraulic conductivity of various intervals intersected at different boreholes. Recharge to the groundwater system is still undetermined, however, the average hydraulic conductivity of 5.2 x 10^{-2} m/d measured is on the higher side.

A Uniaxial Compressive Strength value of 120 MPa and a Poisson's ratio of 0.24 were recorded from the core samples collected. The significance is that rock mass with low Poisson's ratios react favourably to wall control blasting techniques such as pre-splitting (Williams et al, 2009). Different rock mass classification techniques were employed. Bieniawski's Rock Mass Rating (RMR_{89}), Laubscher's Mining Rock Mass Rating (MRMR) and Barton's Q-system gave rating values of 57, 35 and 10.617 respectively. The Geological Strength Index value was calculated as 55-60. These values imply that the rock is fair to good rock (Bieniawski, 1989).

A kinematic stability analysis was conducted which indicated a low potential for instability. The analysis of the scanline mapping suggests that the most probable mode of failure is by direct toppling.

The quality of the final result of a highwall is directly proportional to the amount of time and effort invested into the blasting techniques employed. A combination of wall control blasting techniques, that is, trim blasting, buffer blasting and presplitting should always be applied as a standard whenever blasting close to the western wall. Parallel geological structures (joints) act as points of least resistance, to which the excavation tends to break regardless of the pre-split. Adjustments to the split design should be considered in cases where geology has a large effect. The joint orientation of the dominant structure influences the amount of overbreak produced. Blasting against the direction of the dominant joints presses the joints together and limits back damage whereas blasting in the same direction as the dominant jointing rips the joints apart.

Effects of mining including size of loading equipment and operator experience have a very small effect as localized failures will be driven by the predominant factors (geology and blasting). Scaling of the highwall still remains an important phase of the mining process.

5.2 Recommendations

Adequate attention has to be paid to the orientation and alignment of blast patterns relative to the structural orientation of the rock mass.

More geotechnical mapping needs to be conducted in order to make informed decisions during the slope design process. In areas with extreme geological structures, the slope angles need to be redesigned or occasionally larger catchment berms designed in order to avoid toppling.

Further research is necessary to quantify the amount of energy released into the final wall due to blasting. Modelling near field peak particle velocity (PPV) attenuation due to blasting by use of the Holmberg and Persson site specific constants (K and a) can assist in the attenuation of blast waves released in the rock mass. An Alternative approach to determine the Holmberg–Persson Constants for modelling near field Peak Particle Velocity attenuation discussed by Onederra and Esen (2004) should be considered.

More geotechnical information is required to build a robust database of slope failures on this mine and other mines in the region. The aim of this database will be to ease prediction of failures especially in greenfield projects. Validation of the slope failure prediction model should be carried out in order to attach a confidence level to the results obtained.

The scientific basis of the standards used for blastability classification of rock masses is not confirmed as it is purely based on literature. For this research, a small sample area was used for the determination of the blastability index. Sufficient rock mass sample data (collection of rock mass data on different elevations from the south end to the north end) needs to be collected for more accurate calculation and analysis of the blastability index.

More detailed investigations demanding time and resources need to be conducted on the effects of the dimensions of face machinery on the benches. This will assist in drawing quantitative conclusions on the effects of loading machinery on slope stability.

REFERENCES

Abramson, L.W., 2002, Slope stability and stabilization methods. *Wiley, New York*.

Adhikary, D. P., Dyskin, A. V., Jewell, R. J., and Stewart, D. P., 1997, A study of the mechanism of flexural toppling failure of rock slopes, *Rock Mech. Rock Engineering*, Vol. 30, pp 75 – 93.

Adhikary, D. P., and Dyskin, A. V., 2007, Modelling of progressive and instantaneous failures of foliated rock slopes, *Rock Mech. Rock Engineering*, Vol. 40, pp 349 – 362.

Army US Corps of Engineers, 1970, Stability of Earth and Rockfill Dams, *Engineering Manual EM 1110-2-1902, US Government Printing Office, Washington, DC*, pp 75 – 93.

Azrag, E.A., Ugorets, V.I., and Atkinson, L.C., 1998, Use of a finite element code to model complex mine water problems. Presented at the Proc. Symposium on mine water and environmental impacts, *International Mine Water Association, Johannesburg, South Africa*, pp 31– 41.

Barton, N., 1993, Application of Q-system and index tests to estimate shear strength and deformability of rock masses, *Workshop on Norwegian Method of Tunnelling, New Delhi, India*, pp 66–84.

Bergmann, O.R., Wu F.C., and Edl J.W., 1974, Model Rock Blasting Measures Effect of Delays and Hole Patterns on Rock Fragmentation, *McGraw-Hill Inc., 1221 Avenue of the Americas, New York.*

Bieniawski, Z. T., 1973, Engineering Classification of Jointed Rock Masses, *Transactions of the South African Institution of Civil Engineers*, Vol. 15, pp 335 - 344.

Bieniawski, Z. T., 1976, Rock mass classification in rock engineering, *Exploration for Rock Engineering, Proc, Symp.* Vol. 1, Cape Town, Balkema, pp 97 – 106.

Bieniawski, Z. T., 1979, The geomechanics classification in rock engineering applications, *Proceedings of 4th Congress of International Society of Rock Mechanics*, Montreux, vol. 2, Balkema, Rotterdam, pp 41– 48.

Bieniawski, Z. T., 1989, Engineering rock mass classifications, *New York, Wiley*.

Bishop, A. W., 1955, The use of the slip circle in the stability analysis of slopes, *Geotechnique*, Vol. 5, pp 7 - 17.

Bishop, A. W., and Morgenstern, N., 1960, Stability coefficients for earth slopes, *Geotechnique*, Vol. 10, pp 129 –150.

Call, R. D., 1982, Monitoring of Pit Slope Behaviour, in Stability in Surface Mining, *Society of Mining Engineers, Denver, Co.* Vol. 3, Chap. 9.

Calnan, J., 2015, Determination of explosive energy partition values in rock blasting through small-scale testing, *PhD thesis, University of Kentucky.*

Cebrian, B., Rocha, M., Morales, B., Castanon, L.J. and Floyd, J., 2018, Full wall control blasting optimization, *The Journal of Explosives Engineering, July/August 2018,* pp 6 - 14.

Chatziangelou, M. and Christaras, B., 2015, A Geological Classification of Rock mass Quality for Intermediate Spaced Formations, *International Journal of Engineering and Innovative Technology,* vol. 4, no.9, March, pp 52 – 61.

Chiappetta F., 2007, Using Electronic Detonators, Air Decks, Stem Charges and Very short Hole Delays, *BME Drilling and Blasting Conference, November 2007,* Pretoria, South Africa.

Christaras B. and Chatziangelou M., 2014, Blastability Quality System (BQS) for using it, in bedrock excavation, Structural Engineering and Mechanics, Techno-Press Ltd., vol. 51, no.5, pp 823 – 845.

Coates, D. F., 1977, Pit slope manual – Design, *CANMET (Canada Centre for Mineral and Energy Technology),* pp 126.

Coates, D. F., 1981, Rock Mechanics Principles, *Canadian Centre for Mineral and Energy Technology (CANMET),* Ottawa, Canada, 410pp.

Dahner-Lindqvist, C., 1992, Liggvagga Stabiliteten I Kiirunavaara, *Proceedings Bergmekanikdagen*, Papers presented at Rock Mechanics meeting, Stockholm, Sweeden, pp 37 – 52.

Dawson, E. M., Roth, W. H. and Drescher, A., 1999, Slope stability analysis by strength reduction, *Géotechnique,* Vol. 49, pp 835–840.

de Frietas, M. H. and Watters, R. J., 1973, Some field examples of toppling failure. *Geotechnique*, Vol, 23, pp 495 – 514.

Deere, D. U., Hendron, A. J., Patton F. and Cording E. J., 1967, Design of surface and near surface excavations in rock, *Proceedings of 8th US Symposium on Rock Mechanics: Failure and Breakage of Rock*, pp 237– 302. AIME, New York.

Deere, D. U. and Deere, D. W., 1988, The rock quality designation (*RQD*) index in practice. In *Rock Classification Systems for Engineering Purposes*, pp 91–101. ASTM STP 984, American Society for Testing and Materials, Ann Arbor, Michigan.

Duncan N., 1969, Engineering Geology and Rock Mechanics, *Leonard Hill, London*, vol. 1.

Duncan, J. M. and Wright, S. G., 1980, The accuracy of equilibrium methods of slope stability analysis, *Engineering Geology*, Vol. 16, pp 5–17.

Dunn, P. and Cocker, A., 1995, Pre-Splitting-Wall Control for Surface Coal Mines, *Proceedings Explo Conference, pp* 299-305.

Dyno Nobel, 2010, Blasting and Explosives Quick Reference Guide, *Dyno Nobel Asia Pacific Pty Limited*, pp 1-10.

Eberhardt, E., 2003, Rock slope stability analysis—utilization of advanced numerical techniques, *Earth Ocean Sci. UBC Vanc.* Canada.

Eberhardt, E., Stead, D. and Coggan, J. S., 2004, Numerical Analysis of Initiation and Progressive Failure in Natural Rock Slopes – the 1991 Randa Rockslide, *International Journal of Rock Mechanics & Mining Sciences,* Vol. 41, pp 69-87.

Fellenius, W., 1927, Erdstatische Berechnungen mit Reibung und Kohäsion (adhäsion) und unter Annahme kreiszylindrischer Gleitflächen, *Verlag Ernst and Sohn, Berlin*.

Freeze, A. R. and Cherry, J. A., 1979, Groundwater, *Prentice Hall, New York*.

Girard, J. M., Mayerle R. T. and McHugh, E. L., 1998, Advances in Remote Sensing Techniques for Monitoring Rock Falls and Slope Failures, *Proceedings of the 17th International Conference on Ground Control in Mining, NIOSHTIC-2,* No 20000186, pp 326-331.

Glawe, U., 1991, Analysis of Failure Mechanisms for a Large Scale Slope Movement, *Master of Science Thesis, Royal School of Mines, Imperial College of Science and Technology*, London, pp 71.

Goodman, R. E., and Bray, J. W., 1976, Toppling of rock slopes, *Proceedings of ASCE Speciality conference, Rock Engineering for Foundation and Slopes*, Boulder, CO, 2, pp 201 – 234

Goodman, R. E., 1989, Introduction to rock mechanics (2nd Edition), *John Wiley & Sons.*

Goodman, R. E. and Kieffer, D. S., 2000, Behaviour of rock in slopes, *J. Geotech. Geoenviron. Engng*. ASCE, Vol. 126, pp 675 – 684.

Gray, D., Michael, L. and Briggs, A., 2015, *NI 434-101 Technical report*, Perth, Australia.

Griffiths, D. V. and Lane, P. A., 1999, Slope stability by finite elements, *Colorado School of Mines, Golden, USA, Geotechnique 39, no. 3,* pp 387 – 403.

Haines, A. and Terbrugge, P. J., 1991, Preliminary estimate of rock slope stability using rock mass classification, *7th Cong. Int. Soc. of Rock Mech., Aachen, Germany,* pp 887–892.

Hoek, E., 1983, Strength of jointed rock masses, 23rd Rankine Lecture. Géotechnique 33(3), pp 187- 223.

Hoek, E. and Bray, J. W., 1981, Rock Slope Engineering, *Institution of Mining and Metallurgy, London.*

Hoek, E. and Brown, E. T., 1980, Emprical strength criterion for rock masses. *J. Geotech. Engng Div*., ASCE 106 (GT9), pp 1013 – 1035.

Hoek, E. and Brown, E.T., 1988, The Hoek-Brown failure criterion – a 1988 update. In Rock Engineering for Undergraound excavations, Proc. 15th Canadian Rock Mech. Symp. (edited by Curran J.C.), *Toronto, Dept. Civil Engineering, University of Toronto,* pp 31-38.

Hoek, E., Kaiser, P. K. and Bawden, W. F., 1995, Support of Underground Excavations in Hard Rock, *Balkema, Rotterdam*.

Hoek, E., Marinos, P. and Benissi, M., 1998, Applicability of the Geological Strength Index (GSI) classification for very weak and sheared rock masses, *The case of the Athens Schist Formation, Bull. Engng. Geol. Env.,* Vol. 57(2), pp 151 – 160.

Hoek, E., Read, J., Karzulovic, A. and Chen, Z. Y., 2000, Rock slopes in civil and mining engineering, *An International Conference on Geotechnical & Geological Engineering*, Vol. 1, pp 643 – 658, Melbourne, Australia.

Hoek, E., Carranza-Torres, C. and Corkum, B., 2002, Hoek-Brown failure criterion, *Proc. NARMS-TAC Conference, Toronto,* Vol. 1, pp 267 – 273.

Hoek, E., Marinos, P. and Marinos, V. P., 2005, Characterization and engineering properties of tectonically undisturbed but lithologically varied sedimentary rocks, *International Journal of Rock Mechanics and Mining Science,* Vol. 42, pp 277–285.

Holmberg, R. and Persson, P.A., 1980, Design of Tunnel Perimeter Blast Hole Patterns to Prevent Rock Damage, *Trans. Inst. Mining Metal,* Vol. 89, pp A37–A40.

Hudson, J. A. and Harrison, J. P., 1997, Engineering rock mechanics, *Elsevier, Oxford, UK*, pp 444.

Hustrulid, W. A., McCarter, M. K. and Van Zyl, D. J. A., 2000, Slope stability in surface mining*, Society for Mining, Metallurgy, and Exploration, Littleton, Colorado*, pp 81-88.

ISRM Committee, 1979, Suggested Methods for Determining the Uniaxial Compressive Strength and Deformability of Rock Materials, *International Journal of Rock Mechanics and Mining Sciences & Geomechanics Abstracts,* Vol. 16 (2), pp 135 – 140.

Itasca Denver, Inc., 2012, Predicted Inflow Rate to Sublevel Retreat Mining at Aurora Mine, Technical Memorandum submitted to SRK Consulting (Canada) Inc., 24 October.

Jakubec, J. and Laubscher, D. H., 2000, The MRMR rock mass rating classification system in mining practice, *Proceedings of MASSMIN 2000,* Brisbane, pp 413–422, AusIMM, Melbourne.

Janbu, N., 1968, Slope stability computations, *In Soil Mech. and Found. Eng. Rep. Technical University of Norway,* Trondheim, Norway.

Katsabanis, P.D., Tawadrous, A., Braun, C. and Kennedy, C., 2006, Timing Effects on Fragmentation of small-scale blocks of granodiorite. Int J Blast Fragm, Vol. 10, pp 83 – 93.

Kliche, C., 1999, Rock Slope Stability*, Society for Mining, Metallurgy and Exploration*, Inc, Colorado, pp 253.

Konya, C., 2015, Rock Blasting and overbreak control, *Fifth edition, National Highway Institute.*

L'Amante, D. and Flora, A., 2012, Effects of the excavation procedure on the stability of diaphragm wall panels, *Taylor & Francis Group, London*.

Laubscher, D. H. and Taylor, H. W., 1976, The importance of geomechanics classification of jointed rock masses in mining operations, *Exploration for Rock Engineering, Proceedings of International Symposium*, Johannesburg, Vol. 1, A.A. Balkema, pp 119-128.

Laubscher, D.H., 1977, Geomechanics classification of jointed rock masses – mining applications, *Trans. Instn. Min. Metal*. Vol. 86, pp 1 – 8.

Laubscher, D. H., 1984, Design aspects and effectiveness of support systems in different mining conditions, *Transactions of Institute of Mining and Metallurgy, Section A: Mining Industry,* pp 70 – 81.

Laubscher, D.H., 1990, A geomechanics classification system for the rating of rock mass in mine design, *J.S Afr. Inst. Min Metall,* vol. 90 (10), pp 257 – 273.

Laubscher, D. M. and Page, C. H., 1990, The design of rock support in high stress or weak rock environments, *Proc. 92nd Can. Inst. Min. Metall*, AGM, Ottawa, pp 91 – 102.

Laubscher, D. H., 1993, Planning mass mining operations, *Comprehensive Rock Engineering: Principles*, Vol 2, Pergamon Press, Oxford, pp 547-583.

Laubscher, D. H. and Jakubec, J., 2001, The MRMR rock mass classification for jointed rock masses, *Underground Mining Methods: Engineering Fundamentals and International Case Studies*, Society of Mining Engineers, AIME, New York, pp 474 – 481.

Lilly, P., 1986, An Empirical Method of Assessing Rock mass blastability, *In Proceedings of AUSIMM–IE Aust. Newman Combined Group, Large Open Pit Mining Conference*, pp 89 – 92.

Ling, H. I. and Cheng, A. H. D., 1997, Rock sliding induced by seismic forces, *Int. J. Rock Mech. Mining Sci.,* Vol. 34(6), pp 200 – 220.

Low, B. K., 1997, Reliability analysis of rock wedges, *J. Geotech. Geoenviron. Engng*. ASCE, Vol. 123, pp 498 – 505.

Lowe, J. and Karafiath, L., 1960, Stability of earth dams upon drawdown, Proceedings of the 1st Pan-Am. Conf. on Soil Mech. And Found. Eng., Mexico, pp 537-552.

Marinos, P. and Hoek, E., 2001, Estimating the geotechnical properties of heterogeneous rock masses such as Flysch, *Bulletin of Engineering Geology Environment,* Vol. 60, pp 85–92.

Marinos, V., Marinos, P. and Hoek, E., 2005, The geological strength index: applications and limitations, *Bulletin of Engineering Geology Environment*, Vol. 64, pp 55–65.

Mohammed, M. M., 1997, Effects of Groundwater on Stability of Rock and Soil Slopes, *Master's thesis, McGill University*.

More O'Ferrall, G. C., 2018, Standard Operating Procedure; Evaluation of Bench Face Angle design, *First Quantum Minerals Operations, Zambia*.

Morgenstern, N. R. and Price, V. E., 1965, The analysis of the stability of general slip surfaces, *Geotechnique*, Vol. 15, pp 79 – 93.

Nathanail, C. P., 1996, Kinematic analysis of active/passive wedge failure using stereographic projection, *Int. J. Rock Mech. Min. Sci. & Geomech. Abstr*. Vol. 33, pp 405 – 407.

Nichol, S. L., Hungr, O. and Evans, S. G., 2002, Large-scale brittle and ductile toppling of rock slopes, *Can. Geotech. J*, Vol. 39, pp 773 – 778.

Nicholas, D. E. and Sims, D. B., 2000, Collecting and using geological structure data for slope design. *Slope Stability in Surface Mining*, Hustrulid, McCarter & Van Zyl (eds), SME, Colorado, pp 11 – 26.

Onederra, I. and Esen, S., 2004, An alternative approach to determine the Holmberg–Persson constants for modelling near field Peak Particle Velocity attenuation, *Taylor & Francis Ltd,* Vol. 8, No. 2, pp 61–84.

Piteau, D. R., and Martin, D. C., 1981, Mechanics of rock slope failure, *3rd International Conference on Stability in Surface Mining,* Edited by C. O. Brawner, pp 133 – 169.

Pritchard, M. A. and Savingy, K. W., 1990, Numerical modelling of toppling, *Can. Geotech. J*, Vol. 27, pp 823 – 834.

Prout, B., 2015, MINN7091: Blasting for Surface Mines, *University of the Witwatersrand. Johannesburg: Department of Mining Engineering*, South Africa, pp 51 – 53.

Read, J. R. L., 2007, Predicting the behaviour and failure of large rock slopes, In *Proceedings of 1st Canada–US Rock Mechanics Symposium* (eds E Eberhardt, D Stead & T Morrison), 27–31 May, Canada, pp 1237–1243. Taylor & Francis, London.

Read, J. and Stacey, P., 2009, Guidelines for Open Pit Slope Design, *CSIRO Publishing*. https://doi.org/9780415874410

Rocscience, 2001, SWEDGE – Probabilistic analysis of the geometry and stability of surface wedges, *Rocscience Ltd., Toronto, Canada*.

Rorke, A. J., 2003, BME Training Module: Pre-Splitting. *Bulk Mining Explosives*, Johannesburg. South Africa.

Rorke, A. J., 2007, An evaluation of precise short delay periods on fragmentation in blasting, *EFEE Conference*, Vienna, Austria.

Rorke, A. J. and Botes, J., 2000, Highwall control measures at Optimum Colliery, *BAI 2000 International High Tech Blasting Seminar*, Orlando, USA.

Rorke, A. J. and Simataa, E., 2018, Drill and blast evaluation – Otjikoto Mine, *B2 Gold, Namibia.*

Rossmanith, H. P., 2003, The Mechanics and Physics of Electronic Blasting. *Proceedings of the 33rd Conference on Explosives and Blasting Technique,* ISEE, Nashville, TN.

Sanchidrian, J. A., Segarra, P. and Lopez, L. M., 2007, Energy Components in Rock Blasting, Rock Mechanics and Rock Engineering, Springer Verlag, Volume 44, pp 130-147.

Schlumberger Water Services Pty Ltd, 2013, Dewatering program Sentinel Copper Project, Zambia, P*hase 1 – Initial field investigation and preliminary Hydrogeological assessment,* Perth.

Sharma, A., 2017, Estimating the effects of blasting vibrations on the high-wall stability, Master's Thesis, *University of Kentucky.*

Sjoberg, J., 1996, Large Scale Stability in Open Pit Mining- A Review, *Technical Report,* Lulea University of Technology, Lulea, Sweden, pp 16-17, 229.

Sjöberg, J., 1999, Analysis of large scale rock slopes, *Doctoral thesis, University of Technology*, Luleå.

Sjöberg, J., 2000, Failure mechanisms for high slopes in hard rock, *Slope Stability in Surface Mining*, Hustrulid, McCarter and Van Zyl (eds), SME, Colorado, pp 71 – 80.

Spencer, E., 1967, A method of analysis of stability of embankments assuming parallel interslice forces, *Geotechnique,* Vol. 13, pp 11-26.

SRK Consulting, 2018, Hydrogeological testing at the Sentinel Copper Mine, *Project number 522243/2, Solwezi.*

Stacey, T. R. and Swart, A. H., 2001, Booklet Practical Rock Engineering Practice for Shallow and Opencast Mines, *Johannesburg: The Safety In Mines Research Advisory Committee (SIMRAC).*

Stacey, T. R., 2007, Slope stability in high stress and hard rock conditions, *International Symposium on rock slope stability in open pit mining and civil engineering,* Perth, Australia, Australian Centre for Geomechanics, pp 187 – 200.

Stachura, V. J. and Cumerlato, C. L., 1995, Highwall damage control using presplitting with low-density explosives, *International Society of Explosives Engineers*, Vol. 2, pp 187-197.

Taylor, D. W., 1937, Stability of Earth Slopes, *J. Boston Soc. Civil Engineers*, Vol. 24, pp 197 – 246.

Watts, C. F. and Associates, 2001, ROCKPACK III For the analysis of rock slope stability, *United States of America*.

Williams, P., Floyd, J., Chitombo, G. and Maton, T., 2009, Design implementation in Guidelines for Open Pit Slope Design, *CSIRO Publishing*, pp 265-326.

Wittke, W. W., 1990, Rock Mechanics, Theory and Applications with Case histories. *Berlin. Springer.*

Wyllie, D. C. and Mah, C. W., 2004, Rock Slope Engineering, *Civil and Mining, 4th Edition*, Spon Press, New York.

Xiao, S., Li, K., Ding X. and Liu, T., 2015, Rock Mass Blastability Classification Using Fuzzy Pattern Recognition and the Combination Weight Method, *China University of Mining and Technology,* Xuzhou, Jiangsu 221116, China.

Zienkiewicz, O. C., Humpheson, C. and Lewis, R. W., 1975, Associated and non-associated visco-plasticity and plasticity in soil mechanics, *Géotechnique,* Vol. 25(4), pp 671–689.

APPENDICES

Appendix A – Guidelines of the different classification systems

Table A-1: Guidelines for classification of discontinuity condition in RMR_{89}

RMR_{89}	**Class**	**Rock mass quality**
100-81	I	Very Good rock
80-61	II	Good rock
60-41	III	Fair rock
40-21	IV	Poor rock
<20	V	Very Poor rock

Table A-2: Q-system classification for rock masses

Q	**Rock mass quality**
400	Exceptionally Good rock
400-100	Extremely Good rock
100-40	Very Good rock
40-10	Good rock
10-4	Fair rock
4-1	Poor rock
1-0.1	Very Poor rock
0.1-0.01	Extremely Poor rock
<0.01	Exceptionally Poor rock

Table A-3: GSI classification for rock masses

GSI	**Rock mass quality**
100-81	Very Good rock
80-61	Good rock
60-41	Fair rock
40-21	Poor rock
<20	Very Poor rock

Appendix B - Contour plots of the kinematic stability analysis

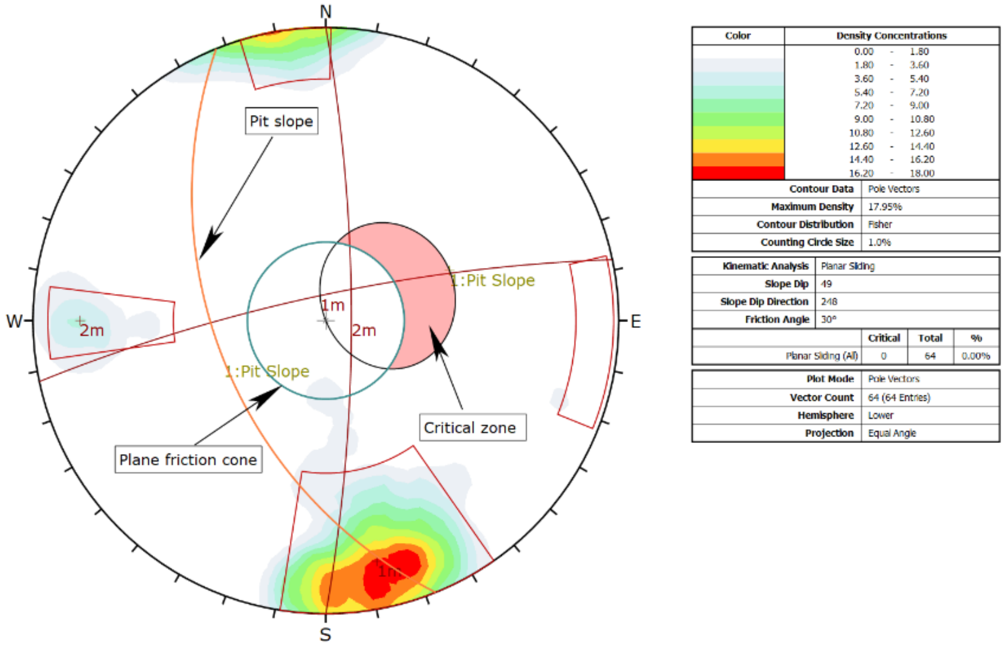

Figure B-1: Planar sliding contour plots

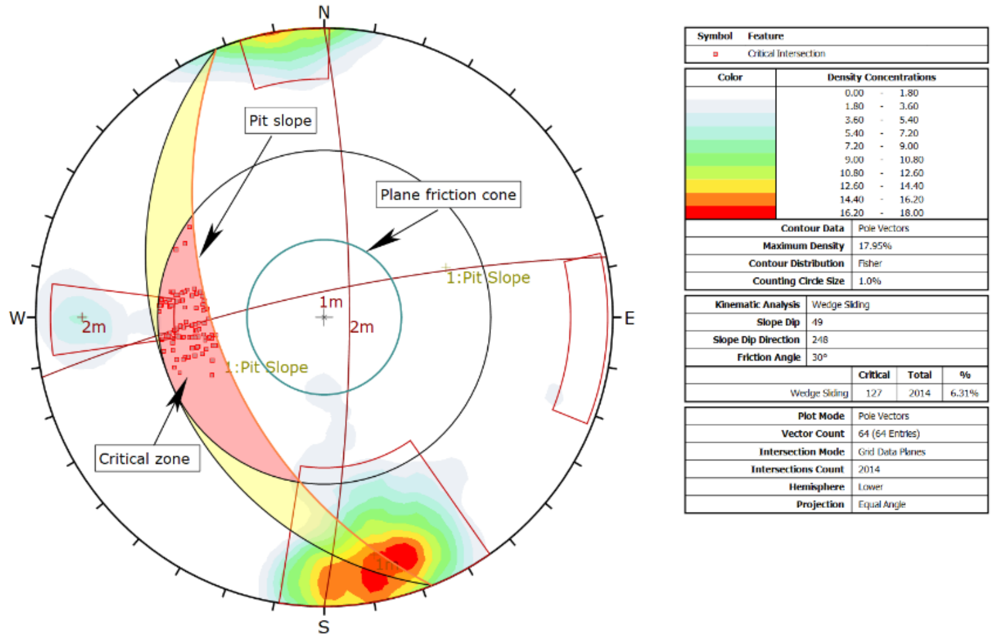

Figure B-2: Wedge sliding contour plots

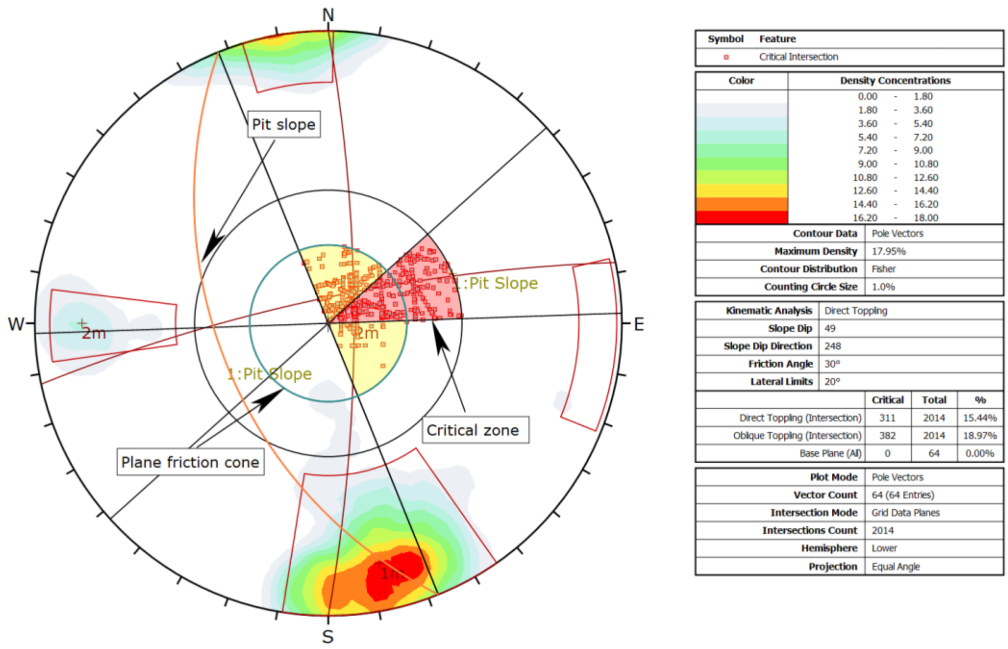

Figure B-3: Direct toppling contour plots

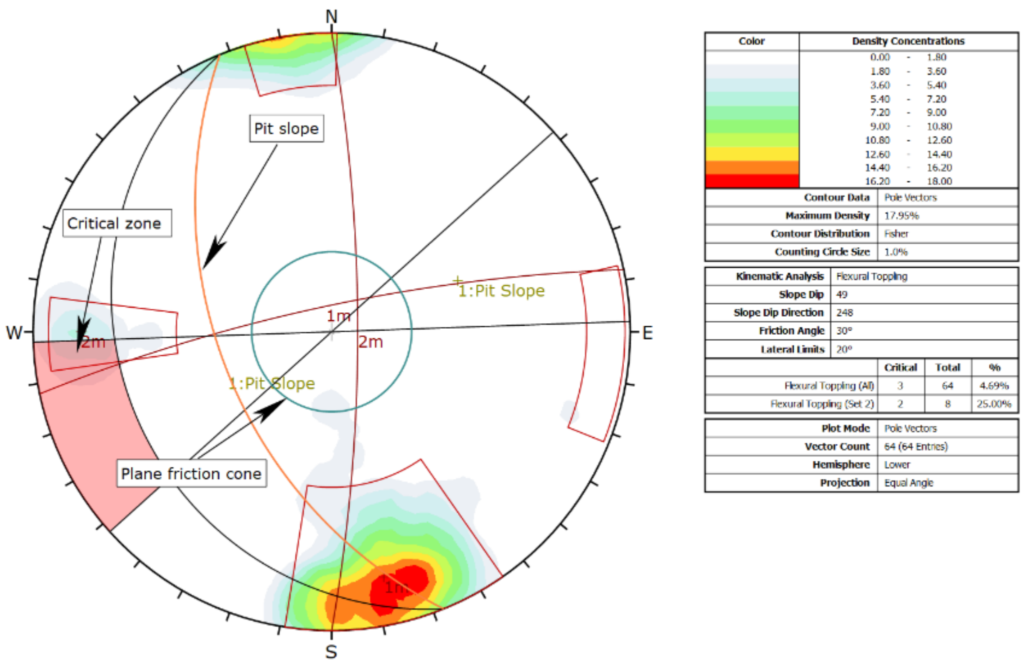

Figure B-4: Flexural toppling contour plots

Appendix C – Geotechnical logging

Table C-1: Scanline survey mapping data for kinematic stability analysis

Date: 13-09-18

Location: Sentinel Pit-West wall

Mine grid Coordinates: X: Y: Z:

Logger: MC

Chainage	Joint Set or Structure	Joint Orientation		Rock Type	Joint Persistence	Joint Aperture	Geotech Interval	From (m)	To (m)	Rock				Joint Condition						Joint Spacing						Water
		Dip	Dip Direction							Rock Code	Rock Type	Hard	Weath	Mic	Mac	Fill	Fill Thickness (mm)	Alt	Joint Condition	J1 (m)	J2 (m)	J3 (m)	J4 (m)	J5 (m)	Joint Spacing (RMR)	
	Joint	80	14	Phyllite	1-3m	1-5mm				MPH		3	1	6	2	9		1	5							2
	Joint	75	268	Phyllite	3-10m	>5mm				MPH		3	1	3	1	7	7	1	2							2
	Joint	84	268	Phyllite	3-10m	1-5mm				MPH		3	1	3	1	7	7	1	2							2
	Joint	65	358	Phyllite	1-3m	1-5mm				MPH		3	1	3	1	9		1	1							2
	Joint	64	6	Phyllite	3-10m	0.1-1.0mm				MPH		3	1	3	2	10		1	1							2
	Joint	83	76	Phyllite	3-10m	1-5mm				MPH		3	1	3	2	9		1	1							2
	Joint	85	34	Phyllite	3-10m	1-5mm				MPH		3	1	3	2	9		1	1							2
	Joint	84	20	Phyllite	3-10m	1-5mm				MPH		3	1	3	1	9		1	1							2
	Joint	85	22	Phyllite	3-10m	>5mm				MPH		3	1	3	1	8		1	1							2
	Joint	81	17	Phyllite	3-10m	>5mm				MPH		3	1	3	1	8		1	1							2
	Joint	85	32	Phyllite	3-10m	1-5mm				MPH		3	1	3	2	9		1	1							2
	Joint	80	178	Phyllite	1-3m	0.1-1.0mm				MPH		3	1	3	1	9		1	2							2
	Joint	85	169	Phyllite	1-3m	1-5mm				MPH		3	1	3	1	9		1	1							2
	Joint	73	93	Phyllite	1-3m	1-5mm				MPH		3	1	3	1	9		1	1							2
	Joint	74	94	Phyllite	1-3m	1-5mm				MPH		3	1	3	1	9		1	1							2
	Joint	89	95	Phyllite	1-3m	1-5mm				MPH		3	1	3	1	9		1	1							2
	Joint	36	334	Phyllite	3-10m	1-5mm				MPH		3	1	3	1	9		1	1							2
	Joint	52	2	Phyllite	1-3m	1-5mm				MPH		3	1	3	1	9		1	1							2
	Joint	82	68	Phyllite	3-10m	1-5mm				MPH		3	1	3	1	9		1	1							2
	Joint	84	72	Phyllite	1-3m	1-5mm				MPH		3	1	3	1	9		1	1							2
	Joint	86	258	Phyllite	3-10m	1-5mm				MPH		3	1	3	1	9		1	1							2
	Joint	90	99	Phyllite	1-3m	1-5mm				MPH		3	1	3	1	9		1	1							2
	Joint	85	22	Phyllite	1-3m	1-5mm				MPH		3	1	3	1	9		1	1							2
	Joint	89	195	Phyllite	1-3m	1-5mm				MPH		3	1	3	1	9		1	1							2

Table C-2: Results of uniaxial compression tests on boreholes with elastic modulus and Poisson's ratio, measurements by means of strain gauges

Client: Kalumbila Minerals, Zambia | Project: | 08-05-2018

SPECIMEN PARTICULARS						SPECIMEN DIMENSIONS					SPECIMEN TEST RESULTS								
Rocklab Specimen No 7473-	Sample ID	Rock Type	Hole ID	From	To	Diameter mm	Height mm	Ratio of Height to diameter	Mass g	Density g/cm³	Failure Load kN	Strength (UCS) MPa	Tangent Elastic Modulus @ 50% UCS GPa	Secant Elastic Modulus @ 50% UCS GPa	Poisson's Ratio Tangent @ 50% UCS	Poisson's Ratio Secant @ 50% UCS	Linear Axial Strain at Failure mm/mm	Failure Code	Note
UCM-01	KALUCS2701	Phyllite	KALGT0027	5.80	6.00	60.83	161.5	2.7	1321.8	2.82	333.0	114.6	51.4	50.9	0.29	0.23	0.002391	6B	
UCM-02	KALUCS2702	Phyllite	KALGT0027	17.80	18.00	60.76	161.4	2.7	1319.2	2.82	382.6	132.0	55.2	52.6	0.29	0.23	0.002609	5B	
UCM-03	KALUCS2703	Phyllite	KALGT0027	28.90	29.10	60.72	161.4	2.7	1330.5	2.85	439.8	151.9	63.4	67.1	0.28	0.21	0.002934	XA	
UCM-04	KALUCS2704	Phyllite	KALGT0027	50.60	50.80	61.01	160.9	2.6	1337.6	2.84	124.5	42.6	56.5	56.5	0.16	0.16	0.000779	5B	
UCM-05	KALUCS2705	Phyllite	KALGT0027	58.30	58.50	60.61	160.7	2.7	1296.7	2.80	428.7	148.6	54.0	56.7	0.25	0.19	0.002976	XA	
UCM-06	KALUCS2706	Phyllite	KALGT0027	70.60	70.80	60.71	160.8	2.6	1307.9	2.81	392.6	135.6	57.2	60.6	0.18	0.16	0.002649	6B	
UCM-07	KALUCS2801	Phyllite	KALGT0028	5.93	6.13	60.80	161.0	2.6	1291.9	2.76	265.3	91.4	55.4	55.9	0.23	0.20	0.001757	5B	
UCM-08	KALUCS2802	Phyllite	KALGT0028	23.10	23.30	60.77	160.7	2.6	1269.8	2.72	226.7	78.2	37.3	30.0	0.20	0.13	0.002439	XA	
UCM-09	KALUCS2803	Phyllite	KALGT0028	33.70	33.90	60.77	160.5	2.6	1277.2	2.74	183.4	63.2	30.7	26.1	0.20	0.14	0.002538	4B	
UCM-10	KALUCS2804	Phyllite	KALGT0028	51.70	51.90	60.71	161.7	2.7	1296.2	2.77	229.4	79.2	41.9	33.4	0.29	0.20	0.002134	5B	
UCM-11	KALUCS2805	Phyllite	KALGT0028	62.70	62.90	60.72	161.0	2.7	1307.2	2.80	308.5	106.5	54.5	54.0	0.19	0.13	0.001998	XA	
UCM-12	KALUCS2806	Phyllite	KALGT0028	72.50	72.70	60.82	160.5	2.6	1285.2	2.76	284.8	98.0	47.7	45.7	0.19	0.15	0.002391	4B	

Appendix D – Window mapping for rock mass classification purposes

Figure D-1: Photograph of window 1 type rock mapped

Table D-1: Window 1 mapping data

Window Mapping Logsheet

Site Location:	Sentinel Mine		Window 1		Date:	12-Dec-18	
(N):		(E):		Z (RL):	1124rl	Mapped By:	
						Dip	Dip Dir
Window Height:	12	Window length:	30	Face Orientation:			

Rock Type

Rock Type	Phyllite			
Weatheing	None	Slight	Moderate	Highly

Rock Strength

>250 MPa	100-250 MPa	50-100 MPa	24-50 MPa	5-25 MPa	1-5 MPa	<1 MPa
15	12	7	4	2	1	0

Joint Number and Spacing

Joint Set Number (Jn)		Spacing		Joint Set	Spacing	1/spacing
Massive, no or few joints	0.5	>2m	20	J1	0.1	10
One joint set	2	0.6-2m	15	J2	2.1	0.476190476
One plus random	3	200-600mm	10	J3		
Two joint sets	4	60-200mm	8	J4		
Two plus random	6	<60mm	5	Jv = sum of the inverse spacings		10.47619048
Three joint sets	9					
Three plus random	12	No of Joint Sets	2			
Four or more	15					

Rock Quality (RQD)

	100-90 %	90-75 %	75-50 %	25-50 %	0-25 %
Bieniawski	20	17	13	8	5
Barton	RQD = 115 – 3.3 Jv		80.4285714		

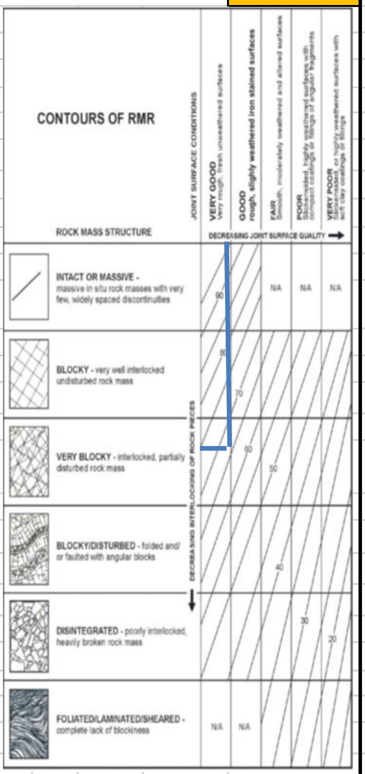

Joint Condition

		Joint Roughness (Jr)	
Very Rough, Not continuous, No seperation, Unweathered walls	30	Discontinuous	4
Slightly rough, Seperation <1mm, Slightly weathered	25	Rough, Irregular, Undulating	3
		Smooth Undulating	2
Slightly rough, Seperation <1mm, Highly weathered	20	Slickensided, Undulating	1.5
		Rough or irregular, planar	1.5
Slickensided or Gouge <5mm thick or Seperation 1-5mm, Continuous	10	Smooth, planar	1
		Slickensided, planar	0.5
Soft gouge >5mm thick or Seperation >5mm, Continuous	0	**Joint Alteration (Ja)**	
		Tightly healed	0.75
		Unaltered, staining only	1
		Slightly altered	2
		Hard infill material	3
		Soft infill material	4

Joint Water

	Compl. Dry	Damp	Wet	Dripping	Flowing
Bieniawski	15	10	7	4	0
Jw	1	0.88	0.66	0.5	0.33

Stress Reduction Factor

Description	UCS /σ_1	σ_t/ σ_1	SRF Value
Low stress, near-surface	>200	>13	2.5
Medium stress	200-10	13-0.66	1.0
High stress, very tight structure (usually favourable to stability, may be unfavourable for wall stability)	10-5	0.66-0.33	0.5-2
Mild rock burst (massive rock)	5-2.5	0.33-0.16	5-10
Heavy rock burst (massive rock)	<2.5	<0.16	10-20

Orientation Adjustment	0
Favourable	-5
Fair	-25
Unfavourable	-50

Q Value	10.617
RMR	57
GSI	60 - 55

Figure D-2: Photograph of window 2 type rock mapped

Table D-2: Window 2 mapping data

Window Mapping Logsheet

Site Location:	Sentinel Mine		Window 1		Date:	12-Dec-18
(N):		(E):		Z (RL): 1124rl	Mapped By:	
					Dip	Dip Dir
Window Height:	12	Window length:	30		Face Orientation:	

Rock Type

Rock Type	Phyllite			
Weatheing	None	Slight	Moderate	Highly

Rock Strength

>250 MPa	100-250 MPa	50-100 MPa	24-50 MPa	5-25 MPa	1-5 MPa	<1 MPa
15	12	7	4	2	1	0

Joint Number and Spacing

Joint Set Number (Jn)		Spacing		Joint Set	Spacing	1/spacing
Massive, no or few joints	0.5	>2m	20	J1	0.4	2.5
One joint set	2	0.6-2m	15	J2	1.5	0.666666667
One plus random	3	200-600mm	10	J3	0.3	3.333333333
Two joint sets	4	60-200mm	8	J4		
Two plus random	6	<60mm	5	Jv = sum of the inverse spacings		6.5
Three joint sets	9					
Three plus random	12	No of Joint Sets		2		
Four or more	15					

Rock Quality (RQD)

	100-90 %	90-75 %	75-50 %	25-50 %	0-25 %
Bieniawski	20	17	13	8	5
Barton	RQD = 115 – 3.3 Jv		93.55		

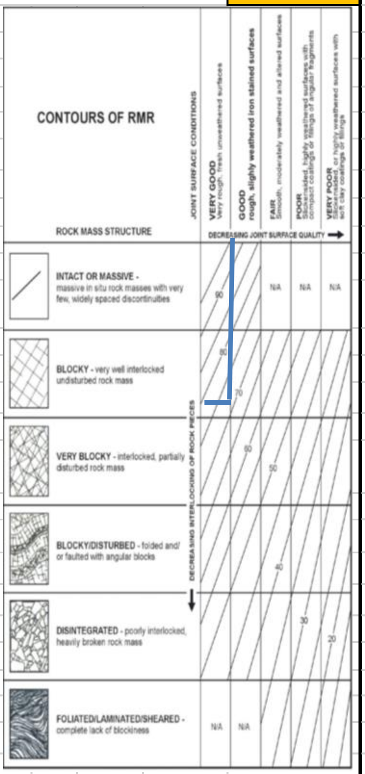

Joint Condition

Very Rough, Not continuous, No seperation, Unweathered walls	30	**Joint Roughness (Jr)**	
		Discontinuous	4
Slightly rough, Seperation <1mm, Slightly weathered	25	Rough, Irregular, Undulating	3
		Smooth Undulating	2
Slightly rough, Seperation <1mm, Highly weathered	20	Slickensided, Undulating	1.5
		Rough or irregular, planar	1.5
Slickensided or Gouge <5mm thick or Seperation 1-5mm, Continuous	10	Smooth, planar	1
		Slickensided, planar	0.5
Soft gouge >5mm thick or Seperation >5mm, Continuous	0	**Joint Alteration (Ja)**	
		Tightly healed	0.75
		Unaltered, staining only	1
		Slightly altered	2
		Hard infill material	3
		Soft infill material	4

Joint Water

	Compl. Dry	Damp	Wet	Dripping	Flowing
Bieniawski	15	10	7	4	0
Jw	1	0.88	0.66	0.5	0.33

Stress Reduction Factor

Description	UCS / σ_1	σ_t / σ_1	SRF Value
Low stress, near-surface	>200	>13	2.5
Medium stress	200-10	13-0.66	1.0
High stress, very tight structure (usually favourable to stability, may be unfavourable for wall stability)	10-5	0.66-0.33	0.5-2
Mild rock burst (massive rock)	5-2.5	0.33-0.16	5-10
Heavy rock burst (massive rock)	<2.5	<0.16	10-20

Orientation Adjustment	0
Favourable	-5
Fair	-25
Unfavourable	-50
Q Value	16.4648
RMR	69
GSI	65 - 70

Figure D-3: Photograph of window 3 type rock mapped

Table D-3: Window 3 mapping data

Window Mapping Logsheet

Site Location:	Sentinel Mine		Window 1		**Date:**	08-Aug-18	
(N):		**(E):**		**Z (RL):**	1112rl	**Mapped By:**	
						Dip	Dip Dir
Window Height:	12	**Window length:**	30	**Face Orientation:**			

Rock Type

Rock Type	**Phyllite**			
Weatheing	None	Slight	**Moderate**	**Highly**

Rock Strength

>250 MPa	100-250 MPa	50-100 MPa	24-50 MPa	5-25 MPa	1-5 MPa	<1 MPa
15	12	7	**4**	**2**	**1**	**0**

Joint Number and Spacing

Joint Set Number (Jn)		**Spacing**		**Joint Set**	**Spacing**	**1/spacing**
Massive, no or few joints	**0.5**	>2m	**20**	J1	0.16	6.25
One joint set	**2**	0.6-2m	15	J2		
One plus random	3	200-600mm	10	J3		
Two joint sets	4	60-200mm	**8**	J4		
Two plus random	6	<60mm	**5**	**Jv** = sum of the inverse spacings		6.25
Three joint sets	**9**					
Three plus random	**12**	**No of Joint Sets**	2			
Four or more	**15**					

Rock Quality (RQD)

	100-90 %	90-75 %	75-50 %	25-50 %	0-25 %
Bieniawski	**20**	17	13	8	**5**
Barton	RQD = 115 – 3.3 Jv		94.375		

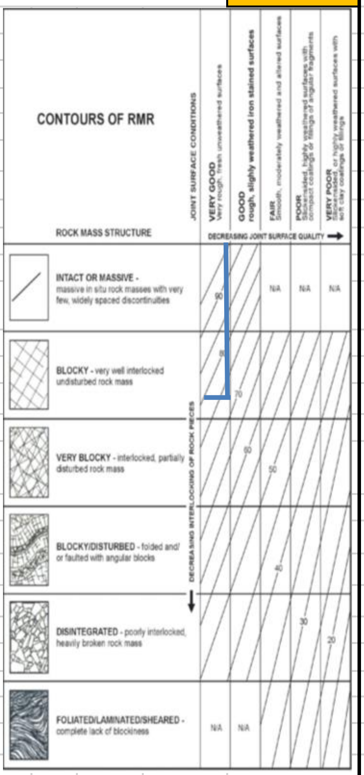

Joint Condition

Very Rough, Not continuous, No seperation, Unweathered walls	30	**Joint Roughness (Jr)**	
		Discontinuous	**4**
Slightly rough, Seperation <1mm, Slightly weathered	25	Rough, Irregular, Undulating	3
		Smooth Undulating	**2**
Slightly rough, Seperation <1mm, Highly weathered	**20**	Slickensided, Undulating	**1.5**
		Rough or irregular, planar	1.5
Slickensided or Gouge <5mm thick or Seperation 1-5mm, Continuous	**10**	Smooth, planar	**1**
		Slickensided, planar	**0.5**
Soft gouge >5mm thick or Seperation >5mm, Continuous	**0**	**Joint Alteration (Ja)**	
		Tightly healed	0.75
		Unaltered, staining only	1
		Slightly altered	2
		Hard infill material	3
		Soft infill material	4

Joint Water

	Compl. Dry	Damp	Wet	Dripping	Flowing
Bieniawski	15	10	**7**	**4**	**0**
Jw	1	0.88	**0.66**	**0.5**	**0.33**

Stress Reduction Factor

Description	***UCS /σ₁***	***σ_t/ σ₁***	***SRF* Value**
Low stress, near-surface	>200	>13	2.5
Medium stress	200-10	13-0.66	1.0
High stress, very tight structure (usually favourable to stability, may be unfavourable for wall stability)	10-5	0.66-0.33	0.5-2
Mild rock burst (massive rock)	5-2.5	0.33-0.16	5-10
Heavy rock burst (massive rock)	<2.5	<0.16	10-20

Orientation Adjustment	**0**
Favourable	-5
Fair	-25
Unfavourable	**-50**
Q Value	16.61
RMR	72
GSI	70 - 75

Appendix E – Core logs for borehole KALGT0027 for UCS and hydraulic conductivity computation


START
14.76m
KALGT0027
BOX#05
18.46m
END
START
18.46m
KALGT0027
BOX#06
22.20m
END
KALGT0027
22.20m
BOX# 07
25.90m
START
25.90m
BOX# 08
29.50m
29.75


KALGT0027 29.75m
G6
KALGT0027 33.20m
BOX#10
35.50
G7
WB
37.20m
KALGT0027 37.20m
BOX#11
38.50
41.20m
KALGT0027 41.20m
BOX#12
41.50
44.50
LC
44.75m


KALGT0027 44.75m
BOX#13
47.50
48.40m
KALGT0027 48.40m
14
50.50
G8
G9
52.35m
KALGT0027 52.35m
BOX#15
53.50
56.50
G10
56.94m
KALGT0027 56.94m
BOX# 16
WB
LC
60.80m


60.80m
Box#17
62.50
64.50m
KALGT0027 64.50m
Box # 18
65.50
↑65,50m
68.10m
START KALGT0027 68.10m
Box # 19
180° OUT
68.50
71.50
71.90m
START KALGT0027 71.90m
Box # 20
75.80m

-

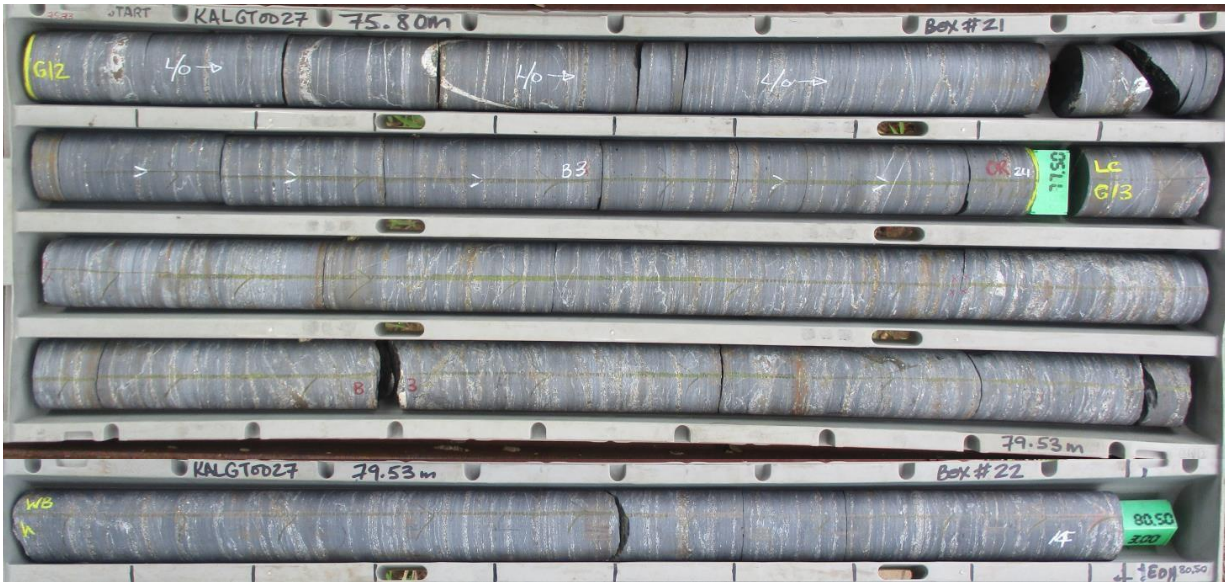
START
KALGT0027
75.80m
Box #21
G12
77.50
LC
G13
79.53m
KALGT0027
79.53m
Box #22
WB
80.50
EOH

-

Appendix F: Blast induced ground vibrations measurement

Figure F-1: Set up of the seismograph at the power substation above the western wall

-

Appendix G: Blastability Index (BI) tables

Table G-1: Specific gravity influence (SGI) (Christaras and Chatziangelou, 2014)

SGI	**specific gravity of rock (t/m^3)**
25*specific gravity of rock (t/m^3)-50	
-22,5	1,1
-20	1,2
-17,5	1,3
-15	1,4
-12,5	1,5
-10	1,6
-7,5	1,7
-5	1,8
-2,5	1,9
0	2
2,5	2,1
5	2,2
7,5	2,3
10	2,4
12,5	2,5
15	2,6
17,5	2,7
20	2,8
22,5	2,9
25	3

Table G-2: Classification standards of rock mass blastability (Christaras and Chatziangelou, 2014)

Blastability Index Value	Ease of blasting description
<8	Very Difficult
8 - 13	Difficult
13 - 20	Moderate
20 - 40	Easy
>40	Very Easy

Appendix H: Presplit audit Findings

Blaster with a tape dipping the pre split holes and marking

Holes being charged with megamite and splitex

Pre split tied up for the blast.

Holes marked for redrilling were not redrilled. They were blasted without any corrective measures

The presplit was drilled about 1.8m from the highwall

Figure H-1: Pre-blast photographs for audit 1

Table H-1: Individual hole findings for audit 1

HOLE ID	Planned Depth	Actual Depth	Spacing	Length Catridge(m)	Uncharged Collar	Depth Variance	Flag +/-	Spacing Variance	Flag +/-
PS1	13.1	14.2	1.7	0.60	2.40	1.1	BAD	-0.1	
PS2	13	7.8	1.7	0.60	2.40	-5.2	BAD	-0.1	
PS3	13	14.4	1.6	0.60	2.40	1.4	BAD	0	
PS4	13	14.3	1.7	0.60	2.40	1.3	BAD	-0.1	
PS5	13.3	15	1.3	0.60	2.40	1.7	BAD	0.3	BAD
PS6	13.1	9.7	1.8	0.60	2.40	-3.4	BAD	-0.2	
PS7	13.1	13.5	2	0.60	2.40	0.4		-0.4	BAD
PS8	13.3	6.8	1.7	0.60	2.40	-6.5	BAD	-0.1	
PS9	13.2	9.2	2.5	0.60	2.40	-4	BAD	-0.9	BAD
PS10	13.3	11.8	1.7	0.60	2.40	-1.5	BAD	-0.1	
PS11	13.2	13.3	2.5	0.60	2.40	0.1		-0.9	BAD
PS12	13	5.8	2.1	0.60	2.40	-7.2	BAD	-0.5	BAD
PS13	13	13	1.8	0.60	2.40	0		-0.2	
PS14	13	13	2.3	0.60	2.40	0		-0.7	BAD
PS15	13.6	15	1.8	0.60	2.40	1.4	BAD	-0.2	
PS16	13.4	5.4	2.2	0.60	2.40	-8	BAD	-0.6	BAD
PS17	13.3	12.6	2.3	0.60	2.40	-0.7	BAD	-0.7	BAD
PS18	13.2	12.3	1.8	0.60	2.40	-0.9	BAD	-0.2	
PS19	13.1	14.2	1.6	0.60	2.40	1.1	BAD	0	
PS20	13	11.6	1.3	0.60	2.40	-1.4	BAD	0.3	BAD
PS21	13.1	13.2	1.7	0.60	2.40	0.1		-0.1	
PS22	13.3	11.8	2.2	0.60	2.40	-1.5	BAD	-0.6	BAD
PS23	13.6	15	1.7	0.60	2.40	1.4	BAD	-0.1	
PS24	13.2	12.6	1.6	0.60	2.40	-0.6	BAD	0	
PS25	13.3	13.6	1.8	0.60	2.40	0.3		-0.2	
PS26	13	13.6	1.8	0.60	2.40	0.6	BAD	-0.2	
PS27	13.1	13	1.7	0.60	2.40	-0.1		-0.1	
PS28	13	13.1	1.7	0.60	2.40	0.1		-0.1	
PS29	13	13.6	1.8	0.60	2.40	0.6	BAD	-0.2	
PS30	13.3	13.9	1.7	0.60	2.40	0.6	BAD	-0.1	
PS31	13	13.6	1.6	0.60	2.40	0.6	BAD	0	
PS32	13.4	13.2	1.6	0.60	2.40	-0.2		0	
PS33	13.1	13.1	2.2	0.60	2.40	0		-0.6	BAD
PS34	13.2	13.3	1.3	0.60	2.40	0.1		0.3	BAD
PS36	13	13.7	1.2	0.60	2.40	0.7	BAD	0.4	BAD
PS37	13	12	1.6	0.60	2.40	-1	BAD	0	
PS38	13.4	14.3	1.9	0.60	2.40	0.9	BAD	-0.3	BAD
PS39	13	15	1.5	0.60	2.40	2	BAD	0.1	
PS40	13.6	14.8	1.5	0.60	2.40	1.2	BAD	0.1	
PS41	13	14.4	1.9	0.60	2.40	1.4	BAD	-0.3	BAD
PS42	13	12.8	1.6	0.60	2.40	-0.2		0	
PS43	13.1	14.1	1.7	0.60	2.40	1	BAD	-0.1	
PS44	13	7.8	1.6	0.60	2.40	-5.2	BAD	0	
PS45	13	14.8	1.6	0.60	2.40	1.8	BAD	0	
PS46	13.2	14	1.9	0.60	2.40	0.8	BAD	-0.3	BAD
PS47	13	15	1.3	0.60	2.40	2	BAD	0.3	BAD
PS48	13	15.5	1.2	0.60	2.40	2.5	BAD	0.4	BAD
PS49	13	5.3	1.5	0.60	2.40	-7.7	BAD	0.1	
PS50	13.3	14	1.8	0.60	2.40	0.7	BAD	-0.2	
PS51	13	14	1.6	0.60	2.40	1	BAD	0	
PS52	13	13	1.6	0.60	2.40	0		0	
PS53	13	14	1.5	0.60	2.40	1	BAD	0.1	
PS56	13.6	13.7	1.5	0.60	2.40	0.1		0.1	
PS57	13.2	13.6	1.6	0.60	2.40	0.4		0	
PS100	13.1	14.2	1.6	0.60	2.40	1.1	BAD	0	
PS58	13.2	12.6	1.5	0.60	2.40	-0.6	BAD	0.1	
PS59	13.4	11.8	1.6	0.60	2.40	-1.6	BAD	0	
PS60	13.5	11.4	1.4	0.60	2.40	-2.1	BAD	0.2	

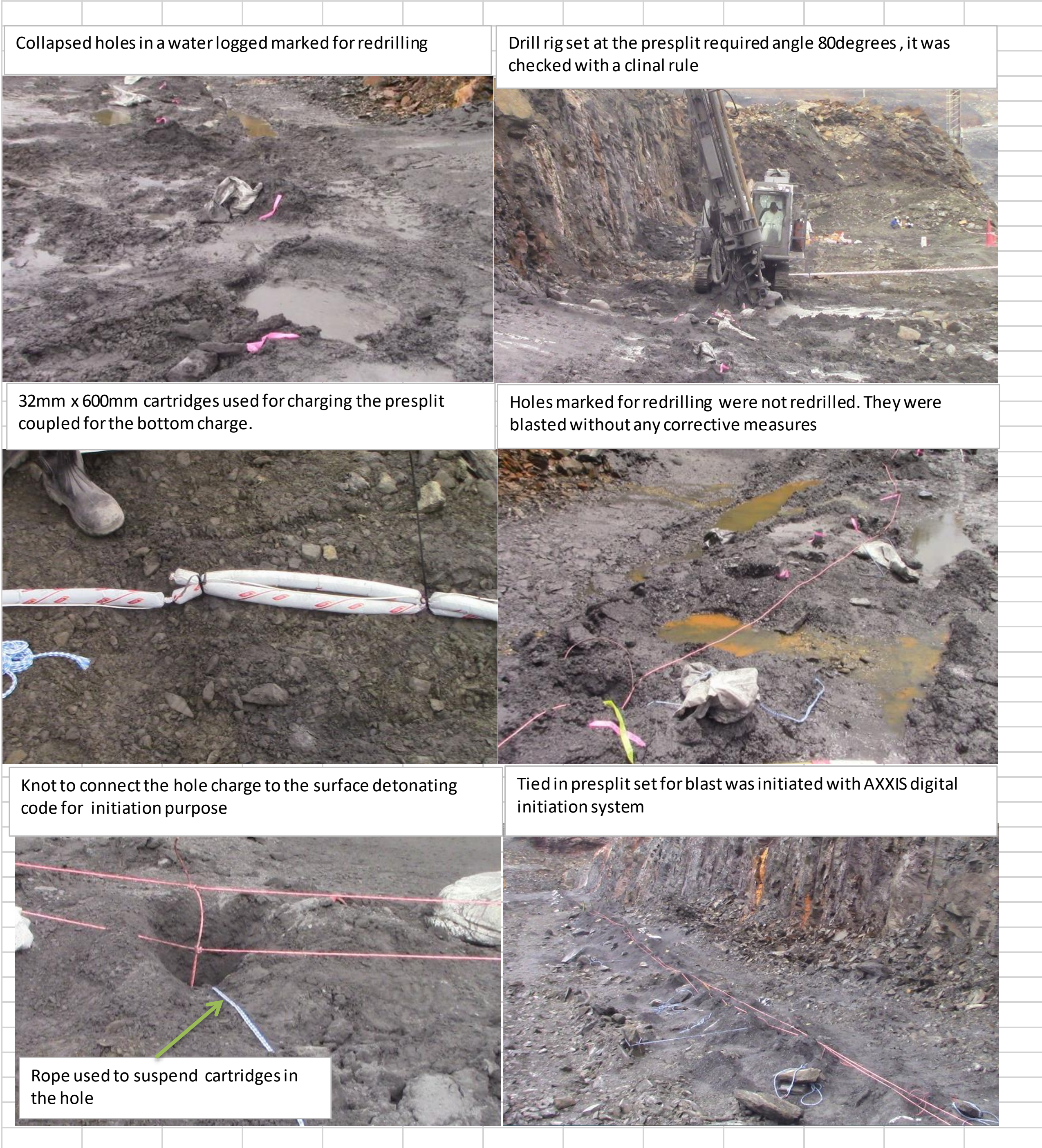

Figure H2: Pre-blast photographs for audit 3

Table H-2: Individual hole findings for audit 3

HOLE ID	Planned Depth	Actual Depth	Spacing	Length Catridge(m)	Uncharged Collar	Depth Variance	Flag +/-	Spacing Variance	Flag +/-
PS8	13.4	14.2	1	0.60	2.40	0.8	BAD	0.6	BAD
PS9	13.4	13.7	1.1	0.60	2.40	0.3		0.5	BAD
P10	13.4	14.4	1	0.60	2.40	1	BAD	0.6	BAD
PS11	13.5	14.3	1.3	0.60	2.40	0.8	BAD	0.3	BAD
PS12	13.2	15	1.4	0.60	2.40	1.8	BAD	0.2	
PS14	14	13.3	1.7	0.60	2.40	-0.7	BAD	-0.1	
PS15	13.4	14.1	1.8	0.60	2.40	0.7	BAD	-0.2	
PS16	13.6	13.5	1.7	0.60	2.40	-0.1		-0.1	
PS17	13.5	13.7	1.5	0.60	2.40	0.2		0.1	
PS18	13.5	13.8	1.6	0.60	2.40	0.3		0	
PS19	13.5	13.6	1.4	0.60	2.40	0.1		0.2	
PS20	13	14.7	1.5	0.60	2.40	1.7	BAD	0.1	
PS21	13.1	11.8	1.5	0.60	2.40	-1.3	BAD	0.1	
PS22	13	13.3	1.7	0.60	2.40	0.3		-0.1	
PS23	13.1	12	0.8	0.60	2.40	-1.1	BAD	0.8	BAD
PS24	13	13	0.8	0.60	2.40	0		0.8	BAD
PS26	13.2	13	1.7	0.60	2.40	-0.2		-0.1	
PS27	13.2	15	1.8	0.60	2.40	1.8	BAD	-0.2	
PS28	13.3	14.4	1	0.60	2.40	1.1	BAD	0.6	BAD
PS29	13.3	14.8	0.9	0.60	2.40	1.5	BAD	0.7	BAD
PS30	13.3	15	1.5	0.60	2.40	1.7	BAD	0.1	
PS31	13.7	14.2	1.3	0.60	2.40	0.5	BAD	0.3	BAD
PS33	13.9	14.3	1.3	0.60	2.40	0.4		0.3	BAD
PS34	14	15	0.9	0.60	2.40	1	BAD	0.7	BAD
PS35	14.1	14.3	2.2	0.60	2.40	0.2		-0.6	BAD
PS36	14.2	15	1	0.60	2.40	0.8	BAD	0.6	BAD
PS37	14.3	14.8	1.6	0.60	2.40	0.5	BAD	0	
PS38	14.3	13.6	1.8	0.60	2.40	-0.7	BAD	-0.2	
PS39	14.4	15.2	1.8	0.60	2.40	0.8	BAD	-0.2	
PS40	14.4	15.1	1.7	0.60	2.40	0.7	BAD	-0.1	
PS41	14.5	15.6	1.7	0.60	2.40	1.1	BAD	-0.1	
PS42	14.6	13.2	1.8	0.60	2.40	-1.4	BAD	-0.2	
PS43	13.3	15	1.7	0.60	2.40	1.7	BAD	-0.1	
PS44	14.3	15.5	1.6	0.60	2.40	1.2	BAD	0	
PS46	14.2	13.2	1.6	0.60	2.40	-1	BAD	0	
PS47	14.2	13.1	2.2	0.60	2.40	-1.1	BAD	-0.6	BAD
PS48	14.2	13	1.3	0.60	2.40	-1.2	BAD	0.3	BAD
PS49	14.2	13.7	1.2	0.60	2.40	-0.5	BAD	0.4	BAD
PS50	14.2	13.7	1.6	0.60	2.40	-0.5	BAD	0	
PS53	14.1	12.5	1.9	0.60	2.40	-1.6	BAD	-0.3	BAD
PS54	14.2	13.7	1.5	0.60	2.40	-0.5	BAD	0.1	
PS55	14.2	11.8	1.5	0.60	2.40	-2.4	BAD	0.1	
PS56	14.3	13.7	1.3	0.60	2.40	-0.6	BAD	0.3	BAD
PS80	15	12.8	1.6	0.60	2.40	-2.2	BAD	0	
PS87	15.8	14.5	1.7	0.60	2.40	-1.3	BAD	-0.1	
PS86	15.8	15	1.6	0.60	2.40	-0.8	BAD	0	
PS85	15.7	16	1.6	0.60	2.40	0.3		0	
PS83	15.4	14	1.9	0.60	2.40	-1.4	BAD	-0.3	BAD
PS82	15.3	15	1.3	0.60	2.40	-0.3		0.3	BAD
PS81	15.1	15.5	1.2	0.60	2.40	0.4		0.4	BAD
PS80	15	14.5	1.5	0.60	2.40	-0.5	BAD	0.1	
PS93	15.8	14	1.8	0.60	2.40	-1.8	BAD	-0.2	
PS94	15.4	14	1.6	0.60	2.40	-1.4	BAD	0	
PS95	15.4	13	1.6	0.60	2.40	-2.4	BAD	0	
PS96	13.4	14	1.5	0.60	2.40	0.6	BAD	0.1	
PS97	13.6	13.7	1.5	0.60	2.40	0.1		0.1	
PS100	14.2	14.9	2.2	0.60	2.40	0.7	BAD	-0.6	BAD
PS102	14.2	15.8	1.6	0.60	2.40	1.6	BAD	0	
PS103	14.2	14	1.6	0.60	2.40	-0.2		0	
PS116	14.8	9	1.5	0.60	2.40	-5.8	BAD	0.1	
PS117	14.8	10.7	1.6	0.60	2.40	-4.1	BAD	0	
PS118	14.9	15.5	1.4	0.60	2.40	0.6	BAD	0.2	
PS119	15	14.8	1.5	0.60	2.40	-0.2		0.1	
PS120	14.4	14.9	1.5	0.60	2.40	0.5	BAD		
PS121	14.3	14.1		0.60	2.40	-0.2			
PS122	15.2	13.6		0.60	2.40	-1.6	BAD		
		13.99		0.60	2.40				